City, University of London Institutional Repository

Neural Networks and Monte Carlo Simulation to Determine Structural System Reliability: Application to Static and Blast Loadings

By VU Thuy Dung

November 2020

A dissertation submitted in partial fulfilment for

the degree of Doctor of Philosophy

in

Department of Engineering

School of Mathematics Computer Science and Engineering

City, University of London, United Kingdom

2

Table of Contents

5

List of Figures

9

List of Tables

Acknowledgement

First, I offer my sincerest gratitude to my supervisor, Dr. Feng Fu, who has supported me throughout my study with his patience and knowledge whilst allowing me the room to work in my own way. I also would like to express my special appreciation and thanks to Ms Nathalie Chatelain, my course officer and other staffs of London City University for their supports in various ways during my course of studies.

Very special thanks to my beloved husband Manh Chu for his assistance and encouragement in every step of this PhD thesis. I also would like to thank to my daughter – Sophia Chu, who joined us during my study, for giving me unlimited happiness and pleasure. Last but not least, I own so much thanks to my mother Thi-Cuong Do, who were continuously supporting me throughout my life and leaving me free in all my decision. Without my family, I would not have been able to complete this research.

Declaration

I, Thuy Dung VU, Department of Engineering, School of Mathematics Computer Science and Engineering, being a candidate for Doctor of Philosophy in Civil Engineering, hereby declare that to the best of my knowledge, the content of this thesis is my own work. This thesis has not been submitted for any degree or other purposes.

I certify that the intellectual content of this thesis is the product of my own work and that all the assistance received in preparing this thesis and sources have been acknowledged.

Signed

Thuy Dung VU

Date 14 November 2020

Abstract

In assessment of the structure-based reliability, there are two levels of reliability required to consider including (1) structural member reliability and (2) system reliability. The former is originated through the failure of a particular component that partial local reliability in a structural system might possibly cause loss of serviceability. However, it is argued by many researchers that structural system is often designed to possess a high level of redundancy making its collapse to occur most likely because of the combined effect of several different failure modes rather than only one particular member. For this reason, it is important to consider both structural member and system reliability in forming any problems related to the structural failure.

Regardless of this statement, literature in the field of structural reliability are focused on the structural member reliability leaving the system reliability to received very little attentions. Although recently, some researches devoted to considering system reliability, the accuracy of this assessment has been considered as a serious issue, which is driven from the fact that these models developed to assess reliability are often assumed to be in linear or weakly nonlinear performance functions. For this reason, the objective of this paper is to propose the approach employed Monte Carlo Simulation and Neural Network to effectively calculate the system reliability of the structural system.

In order to determine the structural system reliability, the proposed method contains the two main stage. In the first stage, the β-unzipping method is employed to determine reliability analysis of structural systems at different level such as Level 0 (on the basic of a single structural element), Level 1 (considering the structural system as a series system), Level 2 (on the basic of a series system where the elements are parallel systems each - with critical pairs of failure elements), and Level 3 (on the basic of a series system where the elements are parallel

systems each - with critical triples of failure elements). In the second stage, the Monte Carlo Simulation with Importance Sampling is first employed to general the sample population, which will be then used to trained, test and predict the system reliability of the structure by Back-Propagation Neural Network Algorithm.

The proposed method was validated against the conventical β-unzipping method to estimate the structural system reliability. The results indicate the closed and yet more accurate reliability index and failure probability of the structural system in consideration of its system reliability analysis. This study is thus moving further by demonstrating the whole process of application of Monte Carlo Simulation with the Importance Sampling Techniques and Neural Network with Back-Propagation Algorithm towards the case study of a 10-bar truss structure. The promising results indicate the potential of employing the proposed method to solve the complex problem of the structural system reliability.

The proposed was then applied to assess the structure system reliability employed for a CFTA girder under blast loading and the obtained results were compared against current Eurocodes guidelines for the structure in the event of extreme loading like explosion. The results prove the possibility of employing the proposed method to solve the complex problem of the structural system reliability assessment under explosion in consideration of the loading uncertainties that the application of the proposed method.

This thesis work is dedicated to a future PhD – my daughter Sophia,

who was born during my study

1 Introduction

1.1 Research Background

In assessment of the structure-based reliability, there are two levels of reliability required to consider including (1) structural member reliability and (2) system reliability. The former is originated through the failure of a particular component that partial local reliability in a structural system might possibly cause loss of serviceability. However, it is argued by many researchers that structural system is often designed to possess a high level of redundancy making its collapse to occur most likely because of the combined effect of several different failure modes rather than only one particular member. For this reason, it is important to consider both structural member and system reliability in forming any problems related to the structural failure. Regardless of this statement, almost all contributions of literature in the field of structural reliability are focused on the structural member reliability leaving the system reliability to received very little attentions (Chun, Song and Paulino, 2015; Okasha, 2016).

System reliability is defined as the probability that a system remains available or functional despite the likelihood of component failures, considerable work has been conducted in this area (Der Kiureghian 2006). Specifically, since Moses (1982); Fu and Moses (1988) highlighted two major limitations occurred in structural design code developments utilizing reliability theory; firstly upon the significant difference of the notional system reliabilities and calibrated component reliabilities, and secondly upon the fact that actual failures are are not reflected in most code formats at that time. However, the probabilistic analysis of structural system requires the evaluation of the probability of union of several events. Here, it is assumed that the probability $P(E_i)$ of each event E_i, the bi-section probability $P(E_i \cap E_j)$ between the events P_i and P_j and the tri-section probability $P(E_i \cap E_j \cap E_k)$ are available. For simplicity and convenience, $P(E_i)$, $P(E_i \cap E_j)$ and $P(E_i \cap E_j \cap E_k)$ will be termed P_i, P_{ij} and P_{ijk}, respectively.

17

As the evaluation of the exact probability of a system is a formidable task, if not an impractical one (Ramachandran, 2004). Accordingly, system reliability analysis of structures is a rather complex subject and so far it has been mostly developed for idealized structures, and still there is a need for research in this area.

With the development of the structural reliability theory, many approaches for the structural system reliability analysis have appeared in the literature, e.g. branch and bound method, β-unzipping method and load incremental method. All of these methods place emphasis on modelling the structural system with the combination of different failure paths, and then calculating the system failure probability. The difficulty encountered in these studies lies mainly in the lack of knowledge of identifying the critical failure paths. The critical failure paths are those which give a remarkable contribution to the system failure probability. Lack of this kind of knowledge will cause the combination explosion phenomenon of the failure path which then makes the system reliability analysis impractical.

For the last four decades, there have been active research efforts to overcome the challenges in structural system reliability analysis. Der Kiureghian (2006) revisited the topic in early 20002 and built the critical pathways to next-generation structural system reliability methods, in which, this paper provides a new insight and perspective towards the structural system reliability and demonstrated it as a crucial research topic, especially, in consideration of system reliability formulation, system reliability updating, component importance measure along with other field such as parameter sensitivity of structural system reliability as well as system reliability itself as a complex combination of components that their failures are seen as stochastic process or at significant level of statistical dependence. With reflect to this review, there have been a wide range of researches took a deeper look into different aspects of structural system reliability and accordingly, there have been a wide range of SSR methods developed in purpose bridging the gaps in application of computational resources.

18

Byun and Song (2017) followed up this report and provided a critical review on a variety of new research activities, which eventually reloaded the research community with new SSR technologies reflected the recent growth of computational capabilities to address challenges and needs in risk management of real-world systems. In order to evaluate the different methods existing in literature, this study identified a list of essential needs for structural system reliability method namely: (1) Generality: there is a desire towards the application of SSR methods in general systems; (2) Flexibility: there is need to improve the current capability of SSR methods in analysing the complex system of components with special regards to the issues of incorporating inequality or incomplete information; (3) Inference: the conditional probabilities and the identification of importance components in an entire system should be also taken into account through SSR analysis; (4) Sensitivity: there is an open field of facilitating decision-making process with results from system reliability analysis, which might possibly requires a parameter sensitivity analysis of system reliability through one may wish to compute parameter sensitivities of system reliability through an SSR analysis; (5) Efficiency: there is a desire to increase the computational efficiency level of current SSR methods in order to perform better result of system reliability analysis; and (6) Scalability: in order to reflect the real structural system (which often seen as large scale of structures), there is a need to develop SSR methods that can handle a large number of components, in which, the application of big data techniques should be well consideration.

Up to recent, there have been four most used and influenced structural system reliability methods namely Bounds on System Reliability by Linear Programming (LP Bounds) proposed by Song and Der Kiureghian (2003); Matrix-Based System Reliability (MSR) Method proposed by Kang, Song and Gardoni (2008); Sequential Compounding Method (SCM) proposed by Kang and Song (2010); and Cross-Entropy-Based Adaptive Importance Sampling (CE-AIS) proposed by Rubinstein and Kroese (2013). In critical of its strengths and limitation,

19

Table below indicated a considerable development in terms of computational capability of current SSR methods that is expected to produce a closer and more efficient system reliability analysis. However, practical systems are often too large and far complex with requirement of taking into account a relative huge number of data that needs a higher power of computational system to be analytically examined. Under consideration of limited information on hand, there is a must for SSR methods to propose suitable strategies to overcome these challenges in order to employ efficient analysis scheme and introduce proper approximation scheme in analysing structural reliability as a system of complex components.

Table 1-1 Evaluation of SSR methods

	Generality	*Flexibility*	*Inference*	*Sensitivity*	*Efficiency*	*Scalability*
LP Bounds	F	F	F	F	F	NF
MSR	F	NF	F	F	F	NF
SCM	F	NF	IF	F	F	F
CE-AIS	F	NF	IF	NF	F	F

Note: F represents for fulfilment, IF stands for indirect fulfilment and NF means non fulfilment

At higher efficiency level of computing structural system performance – system level performance, it is much depended on the determination of the complex relationship of its own components as well as their arrangement in the whole system, in which the interaction between the states of components in turn will decide the patterns of system failures or survivals. While it is relative hard to observe the patterns of the entire structural system failure or even the patterns of the combination of several component events for a redundant system, it is thus crucial to identify a small number of critical components, which would possibly cause the prompt system failure. In this sense, Byun and Song (2017) identified three essential needs for effective structural system reliability analysis of complex systems: (1) handling cascading

failure in system-level performance with special reflect the sequential failure or progressive collapse of multiple component failure events that cause the failure of the entire system; (2) focusing on identifying critical failure modes through cutting and linking sets with dominant contribution to the failure of structural system; and (3) obtain updated or conditional probabilities for inference. To satisfy these demands in structural analysis is not only to provide a better estimation of structural system reliability, a closer investigation into the real complexity of the structure but also give a deeper look into the structural performance of the entire system. Such information will definitely benefit both practitioners and researchers in order to design and maintain of structural systems.

In literature, there have been three most acceptable and widely used to analysis namely: Selective Recursive Decomposition Algorithm (S-RDA) proposed by Liu and Li (2009); Branch-and-Bound Method Employing System Reliability Bounds (B_3 Method) proposed by Lee and Song (2011); and Genetic-Algorithm-Based Selective Search for Dominate Failure Modes proposed by Kim et al. (2013). With their strengths and limitation indicated in the Table below, it can be seen that there is a significant computational cost relived in the current technological reload, leading to a broader application of SSR analyses in the field of structural system reliability. Such achievement has given a new insights and perspective in regards of SSR methods as well as gain better supports for the basic of decision making with matters related to structural system. On the other hand, the current literature also opens zoom for more application of modern technologies into SSR analysis by revealing the gap between what information can achieve through SSR analysis and what critically needed for risk-based assessment in practical decision making. It is not to mention the fast growing of technological demand from the society in many aspects of the structure complexity as well as safer assessment in guidance of codes and regulations. Accordingly, Adrees (2017) strongly indicated the desire in reloading SSR methods in order to take advantages of rapid growths of

computational powers, unprecedented amount of available data and statistical learning algorithms to support (near) real-time inference using monitoring and sensor data, and systematic decision-making scheme on complex systems and networks based on SSR.

Table 1-2 Evaluation of SSR methods for SSR analysis of complex systems

	Cascading failure	Critical failure modes	Updating/ Inference
S-RDA	NF	F	F
B3 method	F	F	F
GA-based selective Search	F	F	NF

Note: F represents for fulfilment and NF means non fulfilment

Despite all of the difficulties mentioned above, system reliability is an important factor in reliability evaluation of structures as the overall system reliability of a structure can be significantly different form the component reliabilities (Byun and Song, 2017). For example, due to the existing of multiple failure modes, there is need to take into account the influence of each failure mode on the structural system reliability in consideration of simplifying the system model and improving the performance of the system (Lu and Li, 2018). Even if the potential failure modes are known or can be identified, the computational assessment of system reliability of structures has remained a challenge in the field of reliability engineering, because available analytical methods require determination of the sensitivity of performance functions, information on mutual correlations among potential failure modes, and determination of design points (Zhao and Ang, 2003).

Added to this, the competition between failure modes should take failure consequences, or failure costs, into account. Considering the progressive collapse of hyper-static structures in

system reliability based-design optimization formulation often results in isostatic optimal structures. As pointed in Lee, Choi and Gorsich (2010), failure costs can be differentiated w.r.t. primary failure of hyper-static or redundant members, and ultimate failure of isostatic members. Failure cost differentiation reflects the fact that redundant member failures provide warning before final collapse, whereas isostatic member failures provide no warning. It is shown herein that when failure consequences are differentiated, optimal solutions include hyper-static structures. However, very few methods and benchmark examples involving optimal design considering system behaviour with progressive failure can be found in the literature. Among others, Beck, Tessari and Kroetz (2019) provide a simple and yet inclusive academic example of a hyper-static six-member truss and bar numbers, to demonstrate the main features of probabilistic analysis of progressive collapse. Such examples are extremely important in civil engineering, considering the current trend to incorporate robustness concepts in design standards. Results obtained herein show that, having the failure of a redundant member as a warning, before eventual collapse, leads to lower optimal system reliability, and allows the structure to be cheaper. Results presented herein were obtained for an academic benchmark example, but they are relevant within the modern trend for robust structural design considering progressive collapse.

Furthermore, the issue of system reliability can also arise when the repair optimization of a structure. The need to design and construct structural systems throughout the life of the structure with adequate levels of reliability and redundancy is widely acknowledged along with optimization to provide safer and more economical maintenance strategies (Frangopol and Estes, 1997). However, treating both system reliability and redundancy as criteria in the lifetime optimization process can be highly rewarding. The complexity of the process, however, requires the automation of solving the optimization problem, although some researchers have put in effort to solve these obstacles. Ghodoosi et al. (2018) develop a rational

method of an innovative combination of reliability analysis, nonlinear finite-element modelling, and genetic algorithms optimization that predicts the most cost-effective intervention schedule for bridges. Okasha and Frangopol (2009) introduced genetic algorithms (to obtain solutions to the multi-objective optimization problems considering system reliability, redundancy and life-cycle cost to provide the optimization program the ability to optimally select what maintenance actions are applied, when they are applied, and to which structural components they are applied. However, up to recent, an integral risk-based optimization procedure for entire structural systems is not available; existing risk-based inspection methods are limited to optimizing inspections component by component (Luque and Straub, 2019). The challenges to an integral approach lie in the large number of optimization parameters in the inspection-repair process of a structural system, and the need to perform probabilistic inference for the entire system at once to address interdependencies among all components.

For the above-mentioned reasons, there has been a pressing research need for formal and accurate treatment of system reliability as the concept and importance of safety. However, in accordance to Byun and Song (2017), there are innumerable roadblocks for effective system reliability analysis especially because systems are becoming more complex and larger as the technological demands from the societies increase rapidly. Moreover, in such complex systems, there exist significant statistical dependence between component failure events characterized in terms of physical members, failure modes, failure locations, and time points of failure occurrences. These technical challenges make system reliability analysis more and more difficult.

1.2 Research Aim and Objectives

According to the logical relationship of the failure modes of structures, structural systems can be divided into three types: series system (referred to as the weakest link or chain system

because the system failure is caused by the failure of any one component), parallel system (referred to as a redundant system because the system fails only if all components fail. The hybrid system is a mixed system comprising the series and parallel systems), and hybrid (is a mixed system comprising the series and parallel systems). Since the analytic estimation of the system probability of failure involves multi-dimensional integration over the overall failure domain, it is numerically very difficult to evaluate (Bjerager, 1990; Thoft-Christensen and Murotsu, 2012). Many efforts have been made to improve this situation but it still cannot deal efficiently with the complicated combination of external loads (Byun and Song, 2017). Added to this, Pan et al. (2019) recently highlighted the lacks of the probability background towards the process to obtain the failure paths in this method lacks the probability background.

One of the most commonly used method to overcome this problem in literature is the branch and bound method introduced by McLeavey and McLeavey (1976), which has been employed to solve the system failure probability for plane and space truss structures. For example, Lee and Song (2011) demonstrated by numerical example of a three-dimensional offshore structure. Biabani and Kalatjari (2018) performed system reliability analysis for truss structures through branch-and-bound method. It is worth to note that wide bound estimation is simple to estimate since it only considers the component probability of failures; however, the bounds can be very wide, which could yield a system probability of failure estimation that is too conservative (Zhao, Liu and Jiao, 2017). For the narrow bound method, Ditlevsen's first-order upper bound (Ditlevsen, 1979), which is the summation of component failure probabilities, can be used as the system probability of failure (Cho, 2013; Low and Tang, 2007; Ramachandran, 2004), or Ditlevsen's second-order upper bound by considering the joint probability of failure can be used (Xiao and Mahadevan, 1994; Liang Mourelatos and Nikolaidis, 2007; Haldar and Mahadevan, 2000). However, the branch and bound process, which is used to seek the failure

paths is complicated and it is difficult to use the computer program to generate the failure paths automatically (de Santana Gomes, 2019).

Another method that is considered at the same time simple to use and reasonably accurate was thus introduced by Thoft-Christensen and Murotsu (1986). The β-unzipping method is a method by which the reliability of structures can be estimated at a number of different levels. This method is quite general in the sense that it can be used for two-dimensional and three-dimensional framed and trussed structures, for those with ductile or brittle elements and also in relation to a number of different failure mode definition (Thoft-Christensen and Murotsu, 2012). The process to generate the failure paths in the β-unzipping method is very similar to that of state-space search in the problem-solving methods in artificial intelligence (Salehi and Burgueno, 2018). Thus the concept of the heuristic state-space search method mentioned by Zhang (1989) can be employed in the traditional β-unzipping method. In regards of de Santana Gomes (2019), the solving graph in the problem-solving method can then be taken as the critical failure paths. Chen, Zhang and Huang (1996) is among the first researchers put efforts on this problem by giving simple examples of a single frame and a typical transversal frame of a large oil ship. Biabani and Kalatjari (2018) employed an Artificial Intelligent agent to identify and control the repeated failure paths to avoid the use of extra computational time. Zhao et al. (2020) is the most recent publication on this field for three-dimensional jacket structures (simplified as a series-parallel system) employed the β-unzipping technique to determine critical failure components, and a trained artificial neural network (ANN) to reduce computational effort for searching failure components and failure paths.

Added to this the β-unzipping method can be combined with the response surface method (Shen, Zhang and Fan, 2018; Daghigh and Makouie, 2003; Zhao et al., 2020; Jia et al., 2016) and other reliability analysis methods, such as simulation (Shao and Murotsu, 1999; Liu and Tang, 2004; Lee, 2012) or sampling methods (Engelund and Rackwitz, 1993; Dubourg, Sudret

26

and Deheeger, 2013; Hurtado, 2007; Xu and Dang, 2019) for the actual calculation of the system probability of failure. In this regard, it is believed that the response surface method combined with simulation or sampling methods may have an accuracy problem that results in an error in the system probability of failure estimation. Accordingly, the objective of this research is: *to propose the approach employed Monte Carlo Simulation and Neural Network to effectively estimate the system reliability of the structural system.* It is considered as an attempt to bridge the existing gap in practice by combining not only β-unzipping method with the technique of problem solving in Artificial Intelligence but also other sampling techniques such as response surface method and Monte Carlo Simulation along with simulation by FE Model. The concept of critical failure probability is established and used as the path value, i.e. the heuristic information to identify the critical failure paths in the structural system. A computer program procedure is developed to generate the system reliability analysis model automatically for the space frame structures. In order to assess efficiency of the proposed method and the accuracy of the program procedure, the proposed method is employed and calculated for some typical structures and the results are compared with those in the existing literature.

The second objective of this research is to consider an application of the proposed approach considering the different parameters of the reflected blast loading into the structural system reliability that has been a very limited research in the existing literature. The selection of variables is in regards to Campidelli, Razaqpur and Foo (2013) involving three principal components: threat, vulnerability, and consequences assessment. The load factors for structural system reliability assessment are considered in accordance to Ellingwood (2006) that a partial load factor should be equal to the one that of other abnormal loads. This principle is adopted in the Eurocode 0 in respect to the UK National Annex (BSI, 2002) as well as design guidance such as Eurocode 1 (1994), CEN (1998) or BIS (2006) for accidental actions like explosions.

27

Furthermore, to determine the compliance of a structural system to a prescribed limit state, the random variables involved in the design, i.e., loads and resistances, must fall within a range determined according to the tolerable probability of failure. If the probability distribution of all random variables is known, the probability of failure p_f can be approximately related to the so-called reliability index (or safety index) β, which is a measure of the reliability of the design; the larger the $β$, the smaller the p_f . On this basic, the general format for deriving reliability-based load and resistance factors is produced. However, in the context of blast resistant design, there are insufficient data available from carefully executed blast tests or actual blast events to quantify the statistical variation of the properties of construction materials subjected to the high strain rates caused by a blast event (Campidelli, Razaqpur and Foo, 2013). Therefore, it is currently not possible to derive realistic resistance factors. For this reason, *the third objective of this study is to present such data and to demonstrate how they can be used to derive the appropriate load factors in the event of blast.* The obtained results are then compared against the current specifications, standards and guidelines for component reliability analysis.

1.3 Thesis Structure

The transfer report is structured as following:

Chapter 1: Introduction – This chapter provides an overview on the research background of related issues such as reliability analysis and structure behaviour under blast loading upon which the research problem identified to propose the research aim and objectives.

Chapter 2: Literature Review – This chapter presents an exclusive literature review on the theoretical concepts towards the research topic of structural reliability analysis and structural response under blast loading. The basic theories of structure system modelling and system reliability assessment are introduced. Moreover, learning process, transfer function and algorithm are given. In terms of the structural analysis, the basic concepts of structural

behaviour in event of explosion are also presented with special reflection to the probability of progressive collapse cause by blast loading. Added to this, the general knowledge of Neural Networks such as its architecture, learning process, transfer function and algorithm as well as Monte Carlo Simulation (in system reliability) are also given.

Chapter 3: Research State of Art – This chapter represents the current development in the field of structure system reliability and reliability assessment under explosion. The existing techniques developed in an effort of solving the complex problem of system reliability are critically reviewed with a highlight of its challenges in computing power. The limitation of Monte Carlo Simulation and Neural Network in assessing the system reliability is also pointed out in this section; along with the research gap in system reliability considered progressive collapse under blast loading.

Chapter 4: Proposed Monte Carlo Simulation – Neural Network for Structural System Reliability (MCS-NN SSR) – This chapter presents into details the proposed method of employing Monte Charlo Simulation and Neural Network in order to assess the structural system reliability. The selected model is mechanism modelling for structure system that enables to estimate the structural system reliability at different level – demonstrated in this study level 0, level 1, level 2 and level 3. The interval Monte Carlo Simulation is considered to generate the sample population with the importance sampling of the reliability indexes obtained earlier. Mean-Interactive Neural Networks proposed by the author in earlier research is used to train and test as well as eventually estimate the structural system reliability.

Chapter 5: Validation and Application – This chapter presents an application of the proposed MCS-NN SSR is to estimate the structural system reliability index for a 10-truss bar structure. The result obtained from this analysis is compared against what obtained from the conventional β-unzipping method in order to validate the proposed method.

29

Chapter 6: System Reliability for CFTA Girder – This chapter demonstrates the application of the proposed MCS-NN SSR for the real structural system under blast loading. The obtained results are compared with what has been given in the Eurocode guideline in order to provide further modification in the current code and standards with reflection to the system reliability under extreme events.

2 Theoretical Background

2.1 Structural System Reliability

2.1.1 Modelling of Structural Systems

There is no doubt that the complexity of a real structural system makes it relatively impossible to direct calculating the exact probability of structural system failure (Chassiakos and Masri, 1996). It is due to the fact that if considering all the possible different failure modes, such number would be too large to be all been taken into account and even if they could, a very powerful computational system needed to calculate the exact probability of system failure. Therefore, it is a must in idealising the structure in purpose of managing the estimation of the system reliability. Thoft-Christensen and Murotsu (2012) added the need of not only to idealise the structure itself but also the loading system employed to such structure. Bearing these idealisations in the structural system and applied loading, any estimations such as probability of system failure or structural system failure modes are related to the idealised system or model of structural system rather than the real structural system itself. However, it is expected that the modelling of the structural system will reflect most of its critical actual behaviour, there is a must to carefully select the most suitable model for structural analysis. With specific reflection on the main objective of a reliability analysis of structure system is to enable designing process to minimise the probability of failure within the requirements of the recent regulations, the most important failure modes for either consequential failure or progressive failure must be carefully chosen that is reflected the real structure behaviour. For this reason, this section will discuss about the modelling of structural system in purpose of estimating the system probability.

Current applications of modelling of structural system is based on the basic of Thoft-Christensen and Murotsu (1986) with the basic assumption that it is possible to accurately and sufficiently estimate the total reliability of the structural system through first dominating considerations of a finite number of failure modes and then combining such modes into a complex reliability systems. It is critical by Thakkar (2020) that to sufficiently model of structural system, it is critical to identifying the dominant or significant failure modes, which has become of the main problem of structural system modelling. In accordance to Graves et al. (2010), when assessing system reliability using system, subsystem and component-level data, assumptions are needed towards the form of the system structure in purpose of utilising the lower-level data. It is required to consider modelling forms that allow for assessment and modelling of possible discrepancies between reliability estimates based on different levels of data. Of which, the two most fundamental types of systems are series system and parallel system, which will be presented in this section. It is believed by many researchers that such fundamental systems play a dominant role in respect to how structural system is modelled and in turn, how its reliability is estimated (Yalaoui et al., 2005; Suykens et al., 2012; Kim et al., 2013; Gaspar et al., 2011; Gao and Li, 2017; Li et al., 2018).

The series system is symbolised and shown in Figure 2-1. In consideration of a statically determinant (non-redundant) structure with total structural elements of n with an assumption of only one failure element for each structural element. The total number of failures is thus determined as equal to n. Accordingly, the failure of the entire structural system is occurred as soon as there is a failure of any structural element.
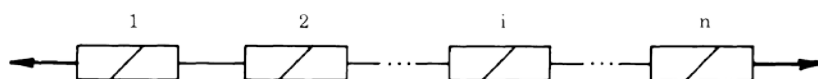
Figure 2-1 Series system

The series system is seen by Thoft-Christensen and Murotsu (1986) as a weakest-link system and no difference is made when the failure of single element is either ductile or brittle. It is noted that the series system demonstrated in Figure 2-1 is employed only for the purpose of showing relation to failure interaction intending to show an idea of how the failure interacts between the component elements.

The parallel system is symbolised and shown in Figure 2-2, of which the main difference towards the series system is that failure in a single structural element for a statically indeterminant (redundant) structure not always cause the failure of the entire system. It is due to the fact that in an event of one single element failure, there might cause a redistribution of the load on the remaining structural elements that enable the system in sustaining the external loading. Accordingly, a failure of a parallel system occurs only in an event that all of its elements fail. For the entire statically indeterminant structure to fail, there is often required for not just only one structural element to fail but more elements' failures take place. In this sense, Wei et al. (2018) acknowledged the importance of understanding what is defined as total failure of a structural system.

In consideration of forming towards a mechanism, a failure mode is understood as failure in a set of failure elements formed a mechanism. In this respect, there is a need to simultaneously generate failures in a number of elements' failures in forming a failure mode of the entire structural system. However, it is a matter of fact that in reality, there is relatively high number of failure models generated from a practical redundant structure making it quite difficult to generate the exact number of system reliability. Rather, Thoft-Christensen and Murotsu (1986) proposed a method to model each failure mode as a parallel system and such parallel systems

33

(represented different failure modes) are combined in a series system. In this sense, the failure of the entire structure is determined in case the weakest failure mode (parallel system) fails as shown in Figure 2-3. Accordingly, it is suggested that the structural system reliability should be generated by estimating on a model defined through a series system, in which, its elements are parallel system. Failure modes are thus considered as the single parallel systems and a failure mode of the entire system is defined as a mechanism.
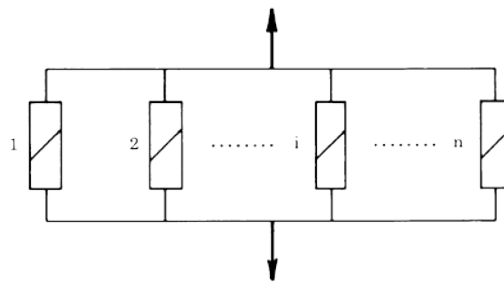
Figure 2-2 Parallel system
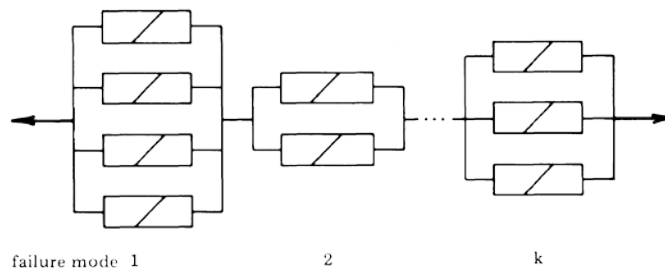
Figure 2-3 Failure mode

2.1.1.2 System Modelling at Level N

At a basic level, for some structures, the system failure can be appropriately defined as failure of any failures of its elements. Accordingly, the structural system reliability can then be generated on the basic of failure of any single failure of any structural element by defining the highest probability of failure amongst the probabilities of failure of all elements. Although such estimation is not actually based on a modelling of the system as a complexity of its elements

34

(or not in fact being a system reliability modelling) but rather an element reliability modelling, at a system modelling, such generation is considered based on the system modelling at level 0 and the reliability generated is called the structural system reliability at level 0. It is noted that this level of system modelling does not take into account the failure interaction between the failures of the different elements to estimate the system reliability. In other words, each element of the entire structural system is individually considered.

On the other hand, a system modelling at level 1 is viewed as a better estimation of the structural system reliability as it obtains the correlation between the probabilities of failures of any failure elements. As shown in Figure 2-4, the system is modelled with series system where its elements are failure elements, such modelling is considered as a more natural and more satisfactory generation to model the system reliability. Similar to the probability of failure of the structural system at level 0, at level 1, this probability is also estimated on the basic of the probability of failure of each failure of the individual element; however, it also takes into account the correlation between the safety margins of the failure elements. Although the estimation is done by simply finding the highest probability amongst those of failure elements, such performance is seen as satisfactory and accuracy enough for some structures (Gao and Li, 2017). Each dominant failure elements modelled in the system modelling at level 1 is called critical failure elements in purpose of indicating that their significances and importance are included in terms of performing an estimation towards the system probability failure.
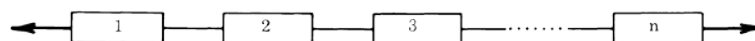
Figure 2-4 System modelling at Level 1

At a higher level of system modelling – level 2, it is relatively not acceptable for some structures to assume its system failure taken place in only one failure but rather in two failure elements. In other words, the failure of such structures is considered in a state of failure, as thus, it should be estimated through an assumption that its failure mode is a parallel system. Accordingly, the reliability modelling is seen as Figure 2-5, of which, it contains a series system where each element is parallel system of two failure elements. In principle, there is must to include all combinations of two random failure elements as failure modes (parallel system) in the series system to generate the structural system reliability. However, considering the relatively large number of failure elements in a real structure, there would be an extreme large number of possible combinations required a high computational power. To solve such problem, Thoft-Christensen and Murotsu (1986) propose to include failure modes with high probabilities of failure to estimate the system probability of failure at level 2. Gao and Li, (2017) believed such performance is satisfactory and accuracy enough for some structures. Similar to system modelling at level 1, each dominant failure modes at level 2 is called critical pair of failure elements in purpose of indicating that their significances and importance are included in terms of performing an estimation towards the system probability failure. It is also noted that a selection of critical pair of failure elements has a significant influence on the accuracy of probability of failure generated for a structure at level. For this reason, what method used to identify such critical pair will be discuss later in the next section – Method of system reliability computing.
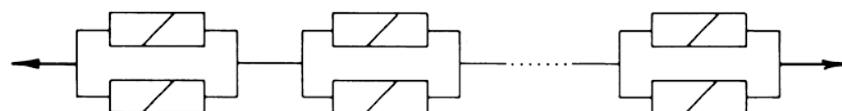
Figure 2-5 System modelling at Level 2

Similar to what approaches for system modelling at level 2, the system reliability at level 3 is generated on the basic of a series system where each of its element (failure mode) is critical triples of failure elements (as shown in Figure 2.5). By continuing in this approach, the system modelling at level N, where $N = 4, 5, 6$ ...can be developed by finding the critical group of four, five elements, respectively, amongst failure elements. In this sense, it is also noted that a selection of critical pair of failure elements has a significant influence on the accuracy of probability of failure generated for a structure at level. For this reason, what method used to identify such critical pair will be discuss later in the next section – Method of system reliability computing.
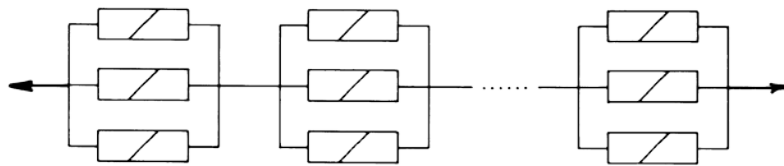
Figure 2-6 System modelling at Level 3

2.1.1.3   System Modelling at Mechanism Level

The most frequently used definition of systems failure for elasto-plastic structures is formation of a mechanism. In the line with this definition, a mechanism is seen as a failure mode that is modelled by a parallel system where each of its elements are the yield hinges in correspondence to the mechanism. These failure modes are then combined in a series system to define the system modelling at mechanism level as shown in Figure 2-3. It is noted that for a real structural system, considering the large number of mechanisms, including all possible mechanisms in the series system possible cause too much effort in computation in order to generate the system reliability. It is therefore recommended by Thoft-Christensen and Murotsu (1986) to only employ only the most dominant mechanisms (depending on its probability of occurrences) (to be called as significant mechanisms), what applied in the system modelling at different levels

37

presented earlier. As other mechanisms have a relatively small probability of occurrence, such performance is satisfactory and accuracy enough (Gao and Li, 2017).

2.1.2 System Reliability Assessment

Consider a structural system for which several failure modes may be defined, and assume that each failure mode is represented by a safety margin,

$$M_i = G_i(X_1, ..., X_n)$$

<div align="right">**Equation 2-1**</div>

With

- G_i, i= 1, 2, … m, the limit state function that defines the safety margin

- M_i as a function of a vector X = $[X_1,..., X_n]^T$ of n basic random variables.

It is noted by Gaspar et al. (2014) that the limit state function G_i can be a rather complicated function of the random vector X. In some cases, a closed-form equation is not known and the evaluation of G_i requires computationally demanding numerical models, e.g., non- linear finite element structural models.

Failure in the mode i of the system is assumed to occur when $M_i = G_i(X) \leq 0$. For a basic system of m failure modes in series the system failure probability is defined by,

$$p_f = P\left[\bigcup_{i=1}^{m} (M_i \leq 0)\right]$$

<div align="right">**Equation 2-2**</div>

while for the parallel case it is,

38

$$p_f = P\left[\bigcap_{i=1}^{m}(M_i \leq 0)\right]$$

These are the elementary cases considered in structural systems reliability analysis (Thoft-Christensen and Murotsu, 2012), which are here introduced as an example. In general, any system can be formulated as a series combination of parallel subsystems. To overcome the computational cost typically involved in the estimation of the failure probability of a system of failure modes, the method proposed in Naess et al. (2009) formulates the system safety margins in the following way:

$$M_i(\lambda) = M_i - \mu_i(1 - \lambda)$$

where M_i is a system safety margin, given by Equation 2-4, and $\mu_i = E[M_i]$ is the mean value of M_i. μ_i is generally unknown a priori, but it is estimated with high accuracy as part of the method. The parameter λ assumes values in the interval $0 \leq \lambda \leq 1$ and its effect on the system failure probability may be interpreted as a scale factor. The original system is obtained for $\lambda = 1$, and for $\lambda = 0$ the system is highly prone to failure, as the mean value of the system safety margins is $E[M_i(0)] = 0$.

The system failure probability as a function of the λ parameter is obtained substituting Equation 2-4 in Equation 2-2 and Equation 2-3 above. Analysing the behaviour of $p_f(\lambda)$ we may conclude that this function decreases monotonically from a high value at k $\lambda = 0$ to a typically small target value at $\lambda = 1$. It was shown in Thoft-Christensen and Murotsu (2012) that this function can be approximated by,

$$p_f(\lambda) \underset{\lambda \to 1}{\approx} q(\lambda) \exp\{-a(\lambda - b)^c\}$$

where $q(\lambda)$ is a slowly varying function compared with the exponential function $\exp\{-a(\lambda - b)^c\}$. For practical applications it can be implemented in the following form (Thoft-Christensen and Murotsu, 2012)

$$p_f(\lambda) \approx q \exp\{-a(\lambda - b)^c\} \quad \text{for} \quad \lambda_0 \leq \lambda \leq 1$$

for a suitable value of λ_0, with the function $q(\lambda)$ replaced by a constant q. An important part of the method is therefore to identify a suitable λ_0 so that the right hand size of Equation 2-5 represents a good approximation of $p_f(\lambda)$ for $\lambda \in [\lambda_0, 1]$.

The functional form assumed in Equation 2-5 is strictly speaking based on an underlying assumption that the reliability problem has been transferred to normalized Gaussian space where a FORM/SORM or similar type of approximation would work for the transformed limit state functions. However, when the basic random variables have "exponential" type of distributions (e.g., Weibull, normal, lognormal, and Gumbel) there is no need to make a transformation to normalized Gaussian space. One can instead work in the original space and adopt Equation 2-5 there. This is the procedure adopted in this paper.

The practical importance of the approximation provided by Equation 2-5 is that the target failure probability $p_f = p_f(1)$ can be obtained from values of $p_f(\lambda)$ for $\lambda < 1$. This is the main concept of the estimation method proposed in Thoft-Christensen and Murotsu (2012), as it is easier to estimate the failure probabilities $p_f(\lambda)$ for $\lambda < 1$ accurately than the target value, since they are larger and, hence, require less simulations and therefore less computational cost.

Fitting the approximating function for $p_f(\lambda)$ given by Equation 2-6 to the estimated values of failure probability obtained by Monte Carlo simulation with $\lambda < 1$, will then allow to provide an estimate of the target failure probability by extrapolation.

2.2 Probability of Progressive Collapse

2.2.1 Measure of Structure Redundancy

Ellingwood (2006); Ellingwood et al. (2009) suggested that the probability of structural collapse, P(C), due to different damage scenarios, L, caused by multiple hazards, E, be expressed as:

$$P(C) = \sum_E \sum_L P(C|LE)P(L|E)P(E)$$

Equation 2-7

wn which, $P(E)$ stands for the probability of occurrence of hazard E; $P(L|E)$ stands for probability of local failure, L, given the occurrence of E, and $P(C|LE)$ stands for the probability of structural collapse given the occurrence of a damage scenario L resulting from hazard, E. The probability of collapse will be obtained by summing over all possible hazards and all possible load failure scenarios. The conditional probability of collapse term $P(C|LE)$ is related to the analysis of the response of the structure to a given damage scenario independently of what hazards have led to the damage. Equation 2-17 assumes independence between the conditional probabilities of failure $P(C|LE)$ calculated for different local failures. This assumption is not strictly speaking correct since we are dealing with the same structure even if it is subjected to different local damage scenarios following the occurrence of multiple hazards and collapse may be due to different failure modes.

The probability of structural collapse must be limited to an acceptable level of risk expressed in terms of a target probability level $P_{threshold}$ which can be determined based on a cost-benefit analysis or based on previous experience with successful designs. This can be represented as

$$P(C) \leq P_{threshold}$$

<div align="right">**Equation 2-8**</div>

In some cases, the data may be insufficient to define $P(E)$. In such cases, **Equation 2-8** can be replaced by

$$P(C|E) = \sum_E \sum_L P(C|L)P(L|E)$$

<div align="right">**Equation 2-9**</div>

To this date, the only known studies that provided non-subjective and quantifiable definitions of bridge redundancy along with specific criteria for assessing bridge redundancy are those of Ghosn and Moses (1998) in The National Cooperative Highway Research Program (NCHRP) NCHRP 406 which based their criteria on the performance of typical bridge configurations that have shown in the past adequate levels of redundancy. In which, the reliability index $\beta_{member}=3.5$ as the basic member safety criterion as established during the calibration of the AASHTO LRFD specifications (AASHTO 2002). The redundancy is defined in terms of the difference between the reliability index of the bridge system and the reliability index of the weakest components. The approach includes checking the redundancy of intact bridges under the effect of overloads as well as evaluating the risks to damaged bridges that have been subjected to local failures but have survived these failures.

According to NCHRP 406, four limit states are defined to ensure adequate bridge redundancy and system safety as well as functionality. These four limit states include: a) Member failure; b) Ultimate limit state; c) Functionality limit state; and d) Damaged condition limit state. Figure 2-7 gives a conceptual representation of the behaviour of a structure and the different levels that should be considered when evaluating member safety, system safety and system redundancy. For example, the solid line labelled "Intact system" may represent the applied load versus maximum vertical displacement of a ductile multi-girder bridge superstructure or the lateral load versus lateral displacement of a bridge bent or combined superstructure-substructure system. In this case, the load is incremented to study the behaviour of an "intact system" that was not previously subjected to any damaging load or event.
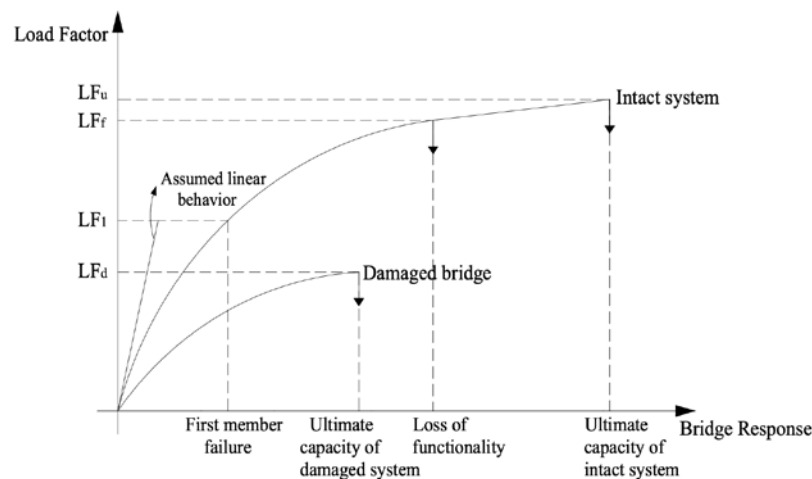
Figure 2-7 Representation of typical behavior of bridge systems

As an example, for the analysis of superstructures under vertical loads, assuming that the vertical live load applied has the configuration of the AASHTO HS-20 vehicle. The bridge is first loaded by the dead load and then the HS-20 load is applied. Usually, due to the presence of safety factors, no failure occurs after the application of the dead load plus the HS-20 load. The first structural member will fail when the HS-20 truck weight is multiplied by a factor *LF1*. *LF1* would then be related to member safety. Note that if the bridge is under-designed or has

major deficiencies, it is possible to have *LF1* less than 1.0. Generally, the ultimate capacity of the whole bridge is not reached until the HS-20 truck weight is multiplied by a factor *LFu*. *LFu* would give an evaluation of system safety. Large vertical deformations rendering the bridge unfit for use are reached when the HS-20 truck weight is multiplied by a factor *LFf*. *LFf* gives a measure of system functionality. A bridge that has been loaded up to this point is said to have lost its functionality.

If the bridge has sustained major damage due to the brittle failure of one or more of its members, its behaviour is represented by the curve labelled "damaged system". A damaged bridge may be a bridge that has lost one of its members due to a collision by a truck or due to major degradation of the member capacity due to corrosion. Other damage scenarios may include the failure of a member due to a fatigue fracture or if some extreme event led to shearing off of the member. In this case, the ultimate capacity of the damaged bridge is reached when the weight of the HS-20 truck is multiplied by a factor LFd. LFd would give a measure of the remaining safety of a damaged system. As noted earlier, the ability of a damaged system to continue to carry load has been defined by some researchers as structural robustness. According to that definition, LFd would provide a measure of bridge robustness.

The comparisons between the load multipliers *LFu*, *LFf*, *LFd* and *LF1* would provide non-subjective and quantifiable measures of system redundancy. Thus, NCHRP 406 defines three deterministic measures of the system's capacity as compared to the most critical member's capacity:

$$R_u = \frac{LF_U}{LF_1} \quad R_f = \frac{LF_f}{LF_1} \quad R_d = \frac{LF_d}{LF_1}$$

Equation 2-10

Where Ru =system reserve ratio for the ultimate limit state, Rf=system reserve ratio for the functionality limit state, Rd= system reserve ratio for the damage condition.

The load multipliers, LF_i, provide deterministic estimates of critical limit states that describe the safety of a structural system. These load multipliers are usually obtained by performing an incremental nonlinear Finite Element Analysis of the structure. Because of the presence of large uncertainties in estimating the parameters that control member properties, the bridge response, and the applied loads, the safety of the bridge members or system may be represented by the probability of failure, P_f, or the reliability index, β.

Both P_f and β can be evaluated for each of the four critical limit states identified in Figure 4-2. Assuming that the structural system or member capacity beyond the ability to carry the dead load expressed in terms of R', as well as the applied load, P, follow lognormal probability distributions, the relationship between the reliability index and the load multipliers, LF, for a bridge superstructure subjected to HS-20 truck loading can be approximated by:

$$\beta = \frac{\ln\left(\dfrac{\overline{R'}}{\overline{P}}\right)}{\sqrt{V_{R'}^2 + V_P^2}} = \frac{\ln\left(\dfrac{\overline{LF} \times HS20}{\overline{LL} \times HS20}\right)}{\sqrt{V_{LF}^2 + V_{LL}^2}} = \frac{\ln\left(\dfrac{\overline{LF}}{\overline{LL}}\right)}{\sqrt{V_{LF}^2 + V_{LL}^2}}$$

Equation 2-11

where LF is the load multiplier obtained from the incremental analysis, LL×HS20 is the expected maximum live load that will be applied on the superstructure within the appropriate return period. *HS20* is the load effect of the nominal HS-20 design truck. V_{LF} is the coefficient of variation of the bridge resistance defined as the standard deviation divided by the mean value. V_{LL} is the coefficient of variation of the applied live load. Both the resistance and the

applied live load are expressed as a function of the HS-20 truck load effect which can then be factored out.

Equation 2-11 lumps all the random variables that control the load carrying capacity of a bridge structure into the load multipliers, LF. Advanced methods for evaluating the system reliability are available and have been implemented as described by Miao and Ghosn (2016).

Equation 2-11 or similar models for other probability distributions can be used to determine the reliability index, β, for any member or system limit state. The reliability indices corresponding to the load multipliers LF_l, LF_f, LF_u or LF_d of Figure 4-2 may be expressed respectively as β_{member}, $\beta_{functionality}$, $\beta_{ultimate}$, and $\beta_{damaged}$. The relationship between these four reliability indices can be investigated by studying the differences between them represented by $\Delta\beta_u$, $\Delta\beta_f$, $\Delta\beta_d$ which are respectively the relative reliability indices for the system's ultimate, functionality and damaged limit states and are defined as:

$$\Delta\beta_u = \beta_{ultimate} - \beta_{member}$$

$$\Delta\beta_f = \beta_{functionality} - \beta_{member}$$

$$\Delta\beta_d = \beta_{damaged} - \beta_{member}$$

Equation 2-12

According to these criteria, a bridge will have an adequate level of redundancy and robustness when the differences between the system reliability index and the member reliability index under four critical limit states (member capacity, ultimate system capacity, system functionality, damaged condition) are higher than a set of target values that were determined

based on bridge configurations which are known to provide adequate levels of safety and redundancy.

Bridges that do not satisfy the set criteria will have to be strengthened to increase their system reliability levels or else the bridge topology may be changed to meet the proposed criteria. It is noted that increasing member strength will not lead to higher redundancy level but will ensure higher overall member and system safety.

Following the criteria set by Ghosn and Moses (1998), the evaluation of the redundancy of a bridge system requires the calculation of the reliability index under the previously listed four limit states if probability of failure P(F) can be accurately calculated. However, the criteria proposed were based on current practice in the safety evaluation of bridge structures established using simplified analyses models that considered pre-identified single modes of failure. The simplified methods were used in the recent past due to the difficulties encountered in using existing reliability methods to analyse realistic models of structural systems.

2.2.2 Progressive Collapse

Progressive collapse occurs if a local structural damage causes a chain reaction of structural elements failures, disproportionate to the initial damage. According to ASCE 7-05 (ASCE 2005), Progressive Collapse is defined as the spread of an initial local failure from element to element resulting, eventually, in the collapse of an entire structure or a disproportionately large part of it.

The Ronan Point collapse in England in 1968, initiated the interest of building engineers in the subject of progressive collapse. The Eurocode has also provided general comments about designing structures to prevent damage to an extent disproportionate to the original abnormal loading event (Eurocode8 1994). More recently, both the General Services Administration (GSA) (GSA, 2000) and the Department Of Defence (DOD) (Stevens et al., 2011) have issued

47

guidelines which provide general information about the approach and method for performing a progressive collapse analysis. In addition, non-mandatory commentary of the American ASCE 7-10/ANSI A58 standard recommends several general approaches to design against progressive collapse (ASCE, 2010).

Progressive Collapse includes two types of loadings (Marjanishvili, 2004): The primary load which causes a structural element to fail, and the secondary loads which are generated due to the structural motions caused by the sudden brittle failure of the element. External abnormal loads, such as blast pressures due to explosive attacks, could cause primary loads, while secondary loads result from the internal static and dynamic forces that are caused by sudden changes in the load path through the structure's geometry. Although estimation of the primary loads is important, most analyses of progressive collapse have focused on the effects of the secondary loads. Focusing on the secondary loads makes the progressive collapse analysis process independent of the hazards that cause the sudden loss of the identified damage initiating elements.

Starossek and Haberland (2009) gave a good illustration of this formula together with assigned appropriate terms (see Figure 2-8). Considering the above Equation 2-7 and Figure 2-8, the probability of progressive collapse can be minimised in three ways, namely by: controlling abnormal events, controlling local element behaviour and/or controlling global system behaviour. Controlling abnormal events by structural engineers is normally very difficult. However, engineers can influence the local and global system behaviour e.i. $P(D|H)$ and $P(C|DH)$.

Figure 2-8 Terms in the context of progressive collapse

2.3 Neural Network

A Neural Network has two main advantages: (1) its massively parallel distributed structure; and (2) its ability to learn and therefore generalize (Rojas, 2013). Karayiannis and Venetsanopoulos (2013) considered a trained Neural Network as an "expert" in categorising information that is given to be analysed. This expert can then generally be employed in providing projections given new situations of interest and answer "what if" questions. In general, the following properties and capabilities of Neural Network have been employed in many fields of researches as presented by Müller, Reinhardt and Strickland (2012):

- *Nonlinearity*

A Neural Network itself is non-linear as it made up of an interconnection of non-linear neurons. This is viewed as a highly important property, particularly if the underlying physical mechanism responsible for generation of the input signal is inherently nonlinear.

- *Input-output mapping*

A Neural Network involves a modification of the synaptic weights through employing a set of labelled training examples or task examples that each of these examples consists of a unique input signal and a corresponding desired response. This mapping process starts by randomly picking up an example from the given set and then it modifies the synaptic weight (free parameters) of the network in purpose of minimizing the difference between the actual output

49

produced by the network (for the input signal in regard to an appropriate statistical criterion) and the desired response. This process is repeated until no further significant changes observed in the synaptic weights, in other words, the network achieves a steady state. By doing so, the network learns from the examples given in the data set to construct an input-output mapping to solve the assigned task. Such input-output mapping is seen as a popular paradigm of learning namely supervised learning or learning with a teacher.

- *Adaptively*

A Neural Network does not only have a capability to map input-output through a given date set of examples or initial experiences, adaptability is also another important property of a Neural Network as their synaptic weights can be changed in accordance to the surrounding environment. Accordingly, a Neural Network trained for operation in one specific environment can easily be retrained to adapt minor changes in other environmental conditions of operations. Moreover, in practices, it is possible to design a Neural Network to adapt its synaptic 8 weights.

- *Self-Organisation*

A NN can create its own organisation or representation of the information it receives during learning time.

- *Real Time Operation*

 NN computations may be carried out in parallel, and special hardware devices are being designed and manufactured which take advantage of this capability.

- *Fault Tolerance via Redundant Information Coding*

Partial destruction of a network leads to the corresponding degradation of performance. However, some network capabilities may be retained even with major network damage.

50

2.3.1   Architecture of Neural Networks computing

In accordance to Rojas (2013), the architecture of Neural Network is classified into three fundamental categories as following:

1) Singer-Layer Feed-forward Networks demonstrated in Figure 2-9

With only one hidden layer, such network allows signals to travel only one way - from input to output. As there is no feedback (loop) existed in this network, there is no corresponding influences of one to another output layer. In other words, this type of Neural Network architecture tends to observed as straight forward networks that the inputs are directly in association with the outputs without any other influences. Accordingly, it is extensively useful in terms of pattern recognition.
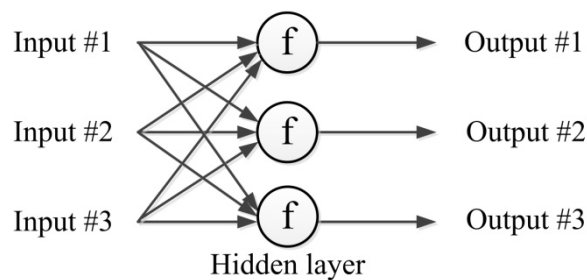
Figure 2-9 A single layer of neurons

2) Multilayer Feed-forward Networks demonstrated in Figure 2-10

With two or more hidden layers, this system allows signals to travel in both directions through the application of loops. Multilayer Feed-forward is considered as dynamic networks, as their "state" is continuously changed until an achievement of an equilibrium point that is remained while inputs are changing until a new equilibrium reached. Although such architecture of Neural Network is considered to be very powerful, it can sometimes get extremely complicated that required to be carefully designed in practices.

51
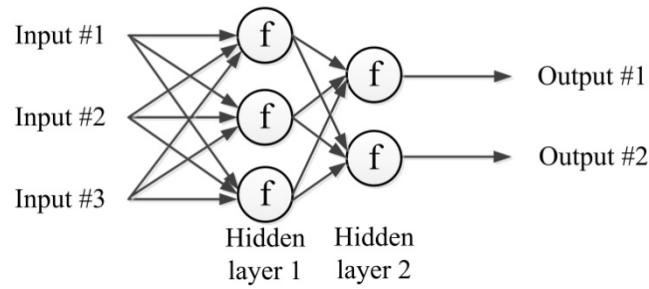
Figure 2-10 Fully connected feed-forward

3) Recurrent Neural Networks demonstrated in Figure 2-11

Not only allow the signals to travel in both directions as multilayer feed-forward, a recurrent Neural Network also comprise of at least one feedback that involves the use of particular branches composed of unit-delay element resulted in a nonlinear dynamical behaviour. Moreover, unlike other architectures that assumed all inputs and outputs are independent of each other, the idea behind recurrent neural networks is to make use of sequential information that it perform the same task for every element of a sequence, with the output being depended on the previous computations – so called "*recurrent*".
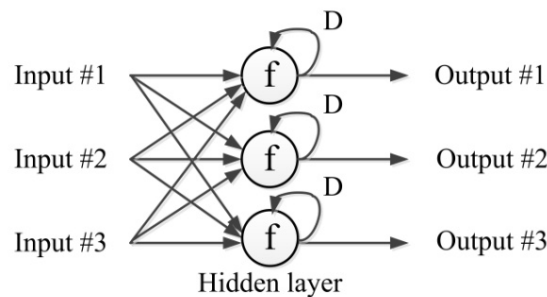
Figure 2-11 A simple recurrent network

2.3.2   Learning Processes

Learning is considered as one of fundamental components of an intelligent system; however, literature has not given a precise definition of learning process. Anthony and Bartlett (2009) defined the learning process of a Neural Network as the process to adjust the weighted

52

connection found between neurons in the network that effectively emulates the strengthening and weakening of the synaptic connections found in our brain, which enables the network to learn. In other words, learning typically happens in a Neural Network in a specific training phrase under a combination of learning paradigms, learning rules, and learning algorithms. Learning algorithms are extremely useful when it comes to certain problems, as the learning process within artificial neural networks is a result of altering the network's weights, with some kind of learning algorithm. The objective is to find a set of weight matrices which when applied to the network should map any input to a correct output. In accordance to Anthony and Bartlett (2009), there are many different algorithms that can be used when training artificial neural networks, each with their own separate advantages and disadvantages; however, they can be categorised into three major learning paradigms:

1) Supervised learning

This is a learning process that the majority of practical machine learning uses recently. In the supervised learning, there are input variables (x), an output variable (Y) and an algorithm to learn the mapping function from the input to the output. The goal is to approximate the mapping function to predict the output variables (Y) for the new input data (x).

$$Y = f(X)$$

Supervise learning incorporates an external teacher, so that each output unit is told what its desired response to input signals ought to be that the algorithm iteratively makes predictions on the training data and is corrected by the teacher. Learning stops when the algorithm achieves an acceptable level of performance. In supervised learning, error-correction learning, reinforcement learning and stochastic learning are considered paradigms to solve an important problem of error convergence, i.e. the minimization of error between the desired and computed unit values. Some popular examples of supervised machine learning algorithms are: Linear

regression for regression problems, random forest for classification and regression problems, and support vector machines for classification problems.

2) Reinforcement Learning

Reinforcement learning is similar to supervised learning in that some feedback is given, however instead of providing a target output a reward is given based on how well the system performed. The aim of reinforcement learning is to maximize the reward the system receives through trial-and-error. This paradigm relates strongly with how learning works in nature, for example an animal might remember the actions it's previously taken which helped it to find food (the reward).

3) Unsupervised learning

Unlike supervised learning, this type of learning process does not use external teacher rather it only bases upon local information that is generally referred as self-organisation by mean that it self-organises data presented to the network and detects their emergent collective properties. In other words, there is only input data (x) in unsupervised learning leaving no corresponding output variables. As there is no correct answer and there is no teacher, the gold for unsupervised learning is to model the underlying structure or distribution in the date in purpose of learning more about the date. Some popular examples of unsupervised learning algorithms are k-means for clustering problems and Apriori algorithm for association rule learning problems that are left to their own devises to discover and present the interesting structure in the data. There are two. In unsupervised learning, a Neural Network learns off-line if the learning phase and the operation phase are distinct; while it learns on-line if it learns and operates at the same time. Usually, supervised learning is performed off-line, whereas unsupervised learning is performed on-line.

54

2.3.3   Transfer Function

In determining the behaviour of a Neural Network, apart from the weights, the input-output function or transfer function specified for the units is also considered as an essential factor. Transfer functions should provide maximum flexibility of their contours with small number of adaptive parameters. Large networks with simple neurons may have the same power as small networks with more complex neurons. According to Müller, Reinhardt and Strickland (2012), activations transfer function are needed for hidden layer of the Neural Network to introduce nonlinearity. Without them NN would be same as plain perceptions. If linear function were used, NN would not be as powerful as they are.

Activations transfer function is generally categorised into three main groups: (1) linear (or ramp), in which the output activity is proportional to the total weighted output; (2) threshold, in which the output is set at one of two levels, depending on whether the total input is greater than or less than some threshold value; and (3) sigmoid, in which units bear a greater resemblance to real neurones than do linear or threshold units, but all three must be considered rough approximations.

2.3.4   Learning Algorithm

In purpose of training a Neural Network to perform an assigned task, it is a must of adjusting the weights of each unit in the way to minimise the error between the desired response and the actual output produced by the learning process. This process requires that through the learning algorithm, the neural network compute the error derivative of the weights (EW) that are the error changes as each weight is increased or decreased slightly. Literature has indicated back-propagation (Figure 2-12) as the most popular Neural Network algorithms (Karayiannis and Venetsanopoulos, 2013) that is broken by Rojas (2013) into four main steps: (1) Feed-forward computation; (2) Back propagation to the output layer; (3) Back propagation to the hidden layer; and (4) Weight updates. After choosing the weights of the network randomly, the back-

55

propagation algorithm is used to compute the necessary corrections. The algorithm is stopped when the value of the error function has become sufficiently small. This is very rough and basic formula for back-propagation algorithm. There is some variation proposed by other scientist but Rojas definition seem to be quite accurate and easy to follow. The last step, weight updates is happening throughout the algorithm.

The back-propagation algorithm could be easily expressed in case all the units in the network are linear. In this regard, the four steps of back-propagation learning algorithm can be demonstrated as following:

- Step 1: It calculate the rate at which the error changes as the activity level of a unit is changed (EA).

- Step 2: For the output layer, the EA is simply calculated as the difference between the actual output produced by the learning process and the desired response.

- Step 3: For the hidden layer, it is first identified all the weights between that hidden and the output units to which it is connected; then it is to multiply those weights by the EAs of those output units and add the products. This sum equals the EA for the chosen hidden unit. After calculating all the EAs in the hidden layer just before the output layer, we can compute in like fashion the EAs for other layers, moving from layer to layer in a direction opposite to the way activities propagate through the network. This is what gives back propagation its name.

- Step 4: Once the EA has been computed for a unit, it is straight forward to compute the EW for each incoming connection of the unit. The EW is the product of the EA and the activity through the incoming connection.
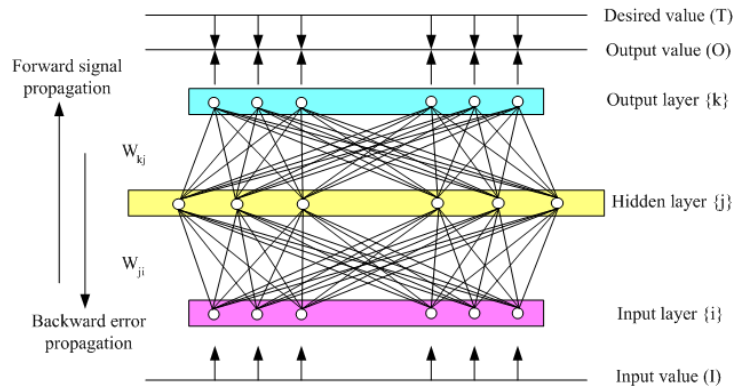
Figure 2-12 Structure of back-propagation NNs

2.4   Monte Carlo Simulation

2.4.1   Basic concept

The Monte Carlo simulation (MCS) method is a powerful modelling tool for the analysis of complex systems, due to its capability of achieving a closer adherence to reality. It may be generally defined as a methodology for obtaining estimates of the solution of mathematical problems by means of random numbers. By random numbers, we mean numbers obtained through a roulette-like machine of the kind utilized in the gambling Casinos of the Monte Carlo Principate: then, the name of the method. The random sampling of numbers was used in the past, well before the development of the present computers, by skillful scientists. The first example of what we would now call a MCS method seems to date back to the French naturalist Buffon (1707–88) who considered a set of parallel straight lines a distance D apart onto a plane and computed the probability P that a segment of length $L\backslash D$ randomly positioned on the plane would intersect one of these lines (Zio, 2013). The theoretical expression he obtained was:

$$P = \frac{L/D}{\pi/2}$$

Equation 2-13

57

Nowadays, MCS seems to be emerging unchallenged as the only method that can yield solutions to complex multi-dimensional problems. For about three decades it was used almost exclusively, yet extensively, in nuclear technology. Presumably, the main reason for this limited use was the lack of suitable computing power as the method is computer memory and time intensive for practical applications. Yet, with the increasing availability of fast computers the application of the method becomes more and more feasible in the practice of various fields. Indeed, the present power of computers allows uses of MCS otherways unimaginable. The underlying tasks common to the various applications are:

- Simulation of random walks in a naturally stochastic environment or for the solution of equations, both differential and integral;

- Adoption of variance reduction methods for improving the efficiency of MCS calculations.

The advantage of the MCS approach comes from the fact that it allows taking into account, in a realistic manner, the many phenomena that can occur, without additional complications in the modelling and in the solution procedure. The principal disadvantage in the use of MCS in practice is the use of relevant calculation times, which diverge with the required accuracy. This disadvantage is decreasing thanks to the rapid development of computing power and to the availability of a number of techniques for efficient simulation, some of which will be illustrated in details in this book. Also, parallel computers are particularly useful for MCS because the various histories that contribute to the estimate of the solution are independent of each other and can thus be processed in parallel. On this account, in the future it can be foreseen that in many disciplines MCS will take the place of the more traditional numerical methods.

2.4.2 System Reliability Analysis by Monte Carlo Based Method

The solution of realistic structural system reliability problems is generally difficult to obtain through conventional reliability methods as the first-order reliability method (FORM) or the second-order reliability method (SORM). The main reason is the high number of limit state functions and basic random variables that may be required to define the problem. The system failure event in a realistic case may be defined by a complex combination of failure modes, in general as a combination of series and parallel systems. The failure criteria are very often associated with nonlinear structural behavior, requiring computationally demanding numerical approaches such as the nonlinear finite element analysis to accurately assess the structural capacity.

At least in principle, the reliability of complex structural systems can be accurately predicted through Monte Carlo simulation. With this method the system failure criterion is relatively easy to check, almost irrespective of the complexity of the system and the number of basic random variables. However, the system failure probabilities are typically of rather small magnitude and therefore the computational cost involved in the Monte Carlo simulation may be prohibitive. If numerical approaches such as the one above mentioned are used to assess the structural capacity, the problem may be intractable if efficient. In regards to Gaspar et al. (2014) and Naess, Leira and Batsevych (2009) this section explains further concept approached for system reliability estimation and this system based Monte Carlo Simulation.

2.4.2.1 *System Reliability Estimation*

Consider a structural system for which several failure modes may be defined, and assume that each failure mode is represented by a safety margin,

$$M_i = G_i(X_1, \ldots, X_n)$$

Equation 2-14

59

with G_i, $i = 1,\ldots,$ m, the limit state function that defines the safety margin M_i as a function of a vector $X = [X_1,\ldots, X_n]^T$ of n basic random variables. The limit state function G_i can be a rather complicated function of the random vector X. In some cases a closed-form equation is not known and the evaluation of G_i requires computationally demanding numerical models, e.g., nonlinear finite element structural models. Failure in the mode i of the system is assumed to occur when $M_i = G_i(X) \leq 0$. For a basic system of m failure modes in series the system failure probability is defined by,

$$p_f = P\left[\bigcup_{i=1}^{m}(M_i \leq 0)\right]$$

Equation 2-15

These are the elementary cases considered in structural systems reliability analysis (Thoft-Christensen and Murotsu, 2012), which are here introduced as an example. In general, any system can be formulated as a series combination of parallel subsystems. To overcome the computational cost typically involved in the estimation of the failure probability of a system of failure modes, the method proposed in Naess, Leira and Batsevych (2009) formulates the system safety margins in the following way:

$$M_i(\lambda) = M_i - \mu_i(1 - \lambda)$$

Equation 2-16

where M_i is a system safety margin, given by Equation 2-14, and $\mu_i = E[M_i]$ is the mean value of M_i. μ_i is generally unknown a priori, but it is estimated with high accuracy as part of the method. The parameter λ assumes values in the interval $0 \leq \lambda \geq 1$ and its effect on the system failure probability may be interpreted as a scale factor. The original system is obtained for $\lambda =$

1, and for $\lambda = 0$ the system is highly prone to failure, as the mean value of the system safety margins is $\mu_i = E[M_i]$. For small to intermediate values of k the increase in the system failure probability is sufficiently high to get accurate estimates of the failure probability by Monte Carlo simulation with moderate computational cost.

The system failure probability as a function of the λ parameter is obtained substituting Equation 2-16 in Equation 2-14 and Equation 2-15 above. Analyzing the behavior of $p_f(\lambda)$ we may conclude that this function decreases monotonically from a high value at $\lambda = 0$ to a typically small target value at $\lambda = 1$. This function can be approximated by,

$$p_f(\lambda) \underset{\lambda \to 1}{\approx} q(\lambda) \exp\{-a(\lambda - b)^c\}$$

Equation 2-17

where $q(\lambda)$ is a slowly varying function compared with the exponential function $\exp\{-a(\lambda - b)^c\}$. For practical applications it can be implemented in the following form:

$$p_f(\lambda) \approx q \exp\{-a(\lambda - b)^c\} \quad \text{for} \quad \lambda_0 \leq \lambda \leq 1$$

Equation 2-18

for a suitable value of λ_0, with the function $q(\lambda)$ replaced by a constant q. An important part of the method is therefore to identify a suitable λ_0 so that the right hand size of Equation 2-17 represents a good approximation of $p_f(\lambda)$ for $\lambda \in [\lambda_0, 1]$. The functional form assumed in Equation 2-17 is strictly speaking based on an underlying assumption that the reliability problem has been transferred to normalized Gaussian space where a FORM/SORM or similar type of approximation would work for the transformed limit state functions. However, when the basic random variables have "exponential" type of distributions (e.g., Weibull, normal,

lognormal, and Gumbel) there is no need to make a transformation to normalized Gaussian space. One can instead work in the original space and adopt Equation 2-17 there. This is the procedure adopted in this paper.

The practical importance of the approximation provided by Equation 2-17 is that the target failure probability $p_f = p_f(1)$ can be obtained from values of $p_f(\lambda)$ for $\lambda < 1$. This is the main concept of the estimation method proposed in Ref. [1], as it is easier to estimate the failure probabilities $p_f(\lambda)$ for $\lambda < 1$ accurately than the target value, since they are larger and, hence, require less simulations and therefore less computational cost. Fitting the approximating function for $p_f(\lambda)$ given by Equation 2-18 to the estimated values of failure probability obtained by Monte Carlo simulation with $\lambda < 1$, will then allow us to provide an estimate of the target failure probability by extrapolation.

2.4.2.2 *System Reliability Based Monte Carlo Simulation*

To find the four parameters *q, a, b,* and *c* in Equation 2-18 that define the optimal fit between these function and the estimated values of failure probability obtained by Monte Carlo simulation, an optimized fitting procedure was suggested in Naess, Leira and Batsevych (2009).

For a sample of size *N* of the vector of basic random variables $X = [X_1, \ldots, X_n]^T$, let $N_f(\lambda)$ denote the number of samples for which failure of the system is verified. An empirical estimate of the failure probability is then given by,

$$\hat{p}_f(\lambda) = \frac{N_f(\lambda)}{N}$$

Equation 2-19

The coefficient of variation of this estimator is,

$$C_v\big(\hat{p}_f(\lambda)\big) = \sqrt{\frac{1 - p_f(\lambda)}{p_f(\lambda)N}}$$

which for small failure probabilities can be approximated by,

$$C_v\big(\hat{p}_f(\lambda)\big) \approx \frac{1}{\sqrt{p_f(\lambda)N}}$$

A fair approximation of the 95% confidence interval for the value $p_f(\lambda)$ can be obtained as:

$$\text{CI}_{0.95}(\lambda) = [C^-(\lambda),\, C^+(\lambda)]$$

where

$$C^{\pm}(\lambda) = \hat{p}_f(\lambda)\big[1 \pm 1.96 C_v\big(\hat{p}_f(\lambda)\big)\big]$$

Considering now that we have obtained empirical estimates of the failure probability using Equation 2-19 for a suitable set of λ values, the problem then becomes one of finding the optimal fit between the proposed approximating function for the failure probability given by Equation 2-18 and the empirical estimates obtained. This optimal fit can be carried out by minimizing the following mean square error function with respect to the four parameters q, a, b, and c in Equation 2-18 at the log level:

$$F(q, a, b, c) = \sum_{j=1}^{M} w_j\big[\log \hat{p}_f(\lambda_j) - \log q + a(\lambda_j - b)^c\big]^2$$

Equation 2-23

where $\lambda_0 \leq \lambda_1 \leq \lambda_2 \leq \ldots\lambda_M < 1$ denotes the set of λ values where the failure probability is empirically estimated and w_j denotes a weight factor that puts more emphasis on the more reliable data points. The choice of the weight factors is to some extent arbitrary. The following definition was suggested:

$$w_j = \left[\log C^+ (\lambda_j) - \log C^- (\lambda_j)\right]^{-\theta}$$

Equation 2-24

with $\theta = 1$ or 2, combined with a Levenberg-Marquardt least squares optimization method. This has proved to work well provided that a reasonable choice of the initial values for the parameters is made. In this study $\theta = 2$ is adopted for the optimized fitting. Note that the definition adopted for w_j puts some restriction on the use of the data. Usually, there is a level λ_j beyond which wj is no longer defined. Hence, the summation in the mean square error function given by Equation 2-24 has to stop before that happens. Also, the data should be preconditioned by establishing the tail marker λ_0 in a sensible way.

Although the Levenberg-Marquardt least squares method as described above generally works well, it may be simplified by exploiting the structure of the mean square error function F. It is realized by scrutinizing Equation 2-23 that if b and c are fixed, the optimization problem reduces to a standard weighted linear regression problem. That is, with both b and c fixed, the optimum values of a and log q are found using closed-form weighted linear regression formulas in terms of

$$w_j, y_j = \log \hat{p}_f (\lambda_j) \text{ and } x_j = (\lambda_j - b)^c$$

It is obtained that the optimal values of a and q are given by the relations:

$$a^*(b,c) = -\frac{\sum_{j=1}^{M} w_j(x_j - \bar{x})(y_j - \bar{y})}{\sum_{j=1}^{M} w_j(x_j - \bar{x})^2}$$

<div align="right">**Equation 2-25**</div>

and

$$\log q^*(b,c) = \bar{y} + a^*(b,c)\bar{x}$$

<div align="right">**Equation 2-26**</div>

where

$$\bar{x} = \sum_{j=1}^{M} w_j x_j \Big/ \sum_{j=1}^{M} w_j$$

$$\bar{y} = \sum_{j=1}^{M} w_j y_j \Big/ \sum_{j=1}^{M} w_j$$

The Levenberg-Marquardt method may now be used on the function

$$\tilde{F}(b,c) = F(q^*(b,c), a^*(b,c), b, c)$$

to find the optimal values b^* and c^*, and then the corresponding a^* and q^* can be calculated from Equation 2-25 and Equation 2-26. For estimation of the confidence interval for a predicted value of the failure probability provided by the optimal curve (i.e., for the probability given by Equation 2-18 with optimal parameters q^*, a^*, b^*, and c^* evaluated at $\lambda = 1$), the empirical confidence band given by Equation 2-22 is reanchored to the optimal curve. The range of fitted curves that stay within the reanchored confidence band will determine an optimized confidence interval of the predicted value. This is obtained by constrained nonlinear optimization. As a

65

final point, it was verified that the predicted value is not very sensitive to the choice of the tail marker λ_0 provided that it is chosen with some care. A suitable initial value for the tail marker is $\lambda_0 = 0.3$, however slightly different values can be considered.

3 Research State of Art

3.1 Technical Challenges in System Reliability Analysis

Over the last four decades, structural system reliability (SSR) has been an active research topic as engineering systems including structures and infrastructure networks become more complex, and the computational power has been remarkably advanced (Zio, 2013; Hu and Mahadevan, 2016; Coit and Zio, 2019). Although researchers desire to evaluate system reliability accurately and efficiently over the years, Youn and Wang (2009) provided an exclusive literature review and concluded that little progress has been made on system reliability analysis. Up to now, bound and β-unzipping method methods for system reliability prediction have been dominant (Stern, et al., 2017). However, two primary challenges are as follows: (1) Most numerical methods cannot effectively evaluate the probabilities of the second (or higher)–order joint failure events with high efficiency and accuracy, which are needed for system reliability evaluation and (2) there is no unique system reliability approximation formula, which can be evaluated efficiently with commonly used reliability methods. Moreover, in such complex systems, there exist significant statistical dependence between component failure events characterized in terms of physical members, failure modes, failure locations, and time points of failure occurrences (Zang et al., 2018). Truong and Kim (2017) indicated that main problem of advanced techniques has generated the complex challenges for structural system reliability that is far more difficult comparing to a component event. In purpose of overcoming such these challenges, there is a need for SSR methods to be developed on a basic of suitable strategies that can consider limited information on hand, employ efficient analysis schemes, and introduce proper approximation schemes (Zhang et al., 2019). In Chapter 2, there was an introduced of two most commonly used theoretical approach for system reliability analysis namely β-unzipping method and the branch-and-bound methods. This

section aims to review the current state of art towards the efforts to solve the complexity of the problem in the structural system reliability including:

- *Bound on system reliability*: The failure of a structural system is usually governed by multiple failure criteria, all of which are to be taken into consideration for reliability estimation. If all the uncertain parameters are defined as random variables, then the system reliability can be estimated accurately by using existing techniques. However, when modelling variables with limited information as intervals with upper and lower bounds, the entire range of these bounds should be explored while estimating the system reliability. The computational cost involved in estimating reliability bounds increases tremendously because a single reliability analysis, which is a computationally expensive procedure, is needed for each configuration of the interval variables. To reduce the computational cost involved, high quality function approximations for individual failure functions and the joint failure surface are in need to consider in regard to their accuracy and efficiency. For this reason, the first technical challenges reviewed in this section is towards bounds on system reliability and its most common approach of linear programming.

- *Framework to facilitate analytical evaluation:* The methods of structural reliability analysis provide a systematic framework that introduces simplifying assumptions in the evaluation of failure probability with an aim to treat the difficulties outlined above. The present review covers topics that include reliability index-based techniques, simulation based methods that include variance reduction strategies, system reliability analysis, time variant reliability analysis, probabilistic model reduction and importance measures, random field modelling and stochastic finite element methods, critical load models, convex models of uncertainty and robust reliability, and nonlinear structural behaviour.

- *Computational cost:* A system reliability analysis is that there often exist innumerable failure modes, i.e. possible combinations or sequences of component failures, because real structures are highly redundant and the failure of a member redefines the limit-states of the remaining members (e.g. stress re-distribution caused by a member failure). Therefore, it is infeasible in most cases to enumerate all the possible failure modes for system reliability analysis. This challenge becomes even greater for complex structures with a large number of structural elements. In order to overcome this difficulty, there is a need to focus on the possibility of using only dominant failure modes with significant likelihood, instead of using all possible failure modes, specifically, to identify dominant failure modes by evaluating their probabilities in an event tree. The system failure probability is then computed based on the probabilities and statistical dependence of the identified failure modes. While evaluating the contributions of individual failure modes to the system failure probability during the search process, component and system reliability analyses need to be performed repeatedly, which may entail huge computation time cost especially for large structures with a high level of redundancy.

3.1.1   Bounds on System Reliability

The probabilistic analysis of any system (structural, geo-technical, water networks) requires the evaluation of the probability of union of several events. Here, it is assumed that the probability $P(E_i)$ of each event E_i, the bi-section probability $P(E_i \cap E_j)$ between the events P_i and P_j and the tri-section probability $P(E_i \cap E_j \cap E_k)$ are available. For simplicity and convenience. $P(E_i)$. $P(E_i \cap E_j)$ and $P(E_i \cap E_j \cap E_k)$ will be termed P_i, P_{ij} and P_{ijk}, respectively. As the evaluation of the exact probability of a system is a formidable task, if not an impractical one, bounds on this probability are usually sought.

Ding et al. (2017) pointed out the two issues in the current investiment and development of probability bounds. First, we have to get a set of upper and lower bounds for the union of events for a given ordering of events. Second, re-order the events or re-formulate these bounds, so that optimal or near-optimal bounds could be obtained. Note that separate re-ordering or re-formulation is necessary for upper and lower bounds. Kounias (1968) tried to achieve an optimal bound in a single operation using optimisation techniques (linear programming) but failed to make much progress owing to the exponential increase in computational effort with the number of events. Since then much improved elegant methods have been produced by Ditlevsen (1979), Ramachandran (1990; 2004) and Greig (1992) to obtain better bounds. This article gives a simple method of deriving first-, second- and third-order bounds, so that direct formulations of optimal bounds can be made. Methods are given to obtain higher-order bounds; however, fourth- and higher-order bounds have very little use in structural reliability problems. Among later efforts on solving this problem, it is worth to mention Song and Der Kiureghian (2003), who propose Bounds on System Reliability by Linear Programming (LP Bounds) as presented in Figure 3-1.
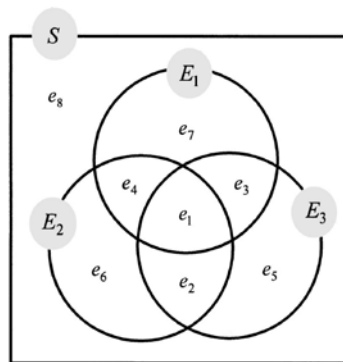
Figure 3-1 Illustration of LP bounds method

Table 3-1 Coefficients c_i of the object functions for three-component Systems

	Baisc MECE Events							
	$e_1=E_1E_2E_3$	$e_2=\bar{E}_1E_2E_3$	$e_3=E_1\bar{E}_2E_3$	$e_4=E_1E_2\bar{E}_3$	$e_5=\bar{E}_1\bar{E}_2E_3$	$e_6=\bar{E}_1E_2\bar{E}_3$	$e_7=E_1\bar{E}_2\bar{E}_3$	$e_8=\bar{E}_1\bar{E}_2\bar{E}_3$
	Design Variables							
System event	p_1	p_2	p_3	p_4	p_5	p_6	p_7	p_8
$E_1\cup E_2\cup E_3$	1	1	1	1	1	1	1	0
$E_1E_2E_3$	1	0	0	0	0	0	0	0
$E_1E_2\cup E_3$	1	1	1	1	1	0	0	0
$(E_1\cup E_2)(\bar{E}_2\cup E_3)$	1	1	1	0	0	0	1	0

The probability of any intersection of the component events is given as the sum of the probabilities of the basic MECE events that constitute the intersection event.

$$P(E_i)=P_i=\sum_{r:e_r\subseteq E_i} p_r$$

$$P(E_iE_j)=P_{ij}=\sum_{r:e_r\subseteq E_iE_j} p_r$$

$$P(E_iE_jE_k)=P_{ijk}=\sum_{r:e_r\subseteq E_iE_jE_k} p_r$$

Equation 3-1

In most system reliability problems, the uni-, bi- and sometimes tri-component probabilities are known or can be computed. In that case, the above expressions provide linear equality constraints on the variables p in the form of

$$\begin{aligned}\text{minimize (maximize)} \quad & \mathbf{c}^T\mathbf{p} \\ \text{subject to} \quad & \mathbf{a}_1\mathbf{p}=\mathbf{b}_1 \\ & \mathbf{a}_2\mathbf{p}\geqslant\mathbf{b}_2\end{aligned}$$

Equation 3-2

Any Boolean function of the component events can also be considered as being composed of a subset of the basic MECE events. It follows that the probability of the system event E_{system} can be written in the form $P(E_{\text{system}})= c^T p$, where c = a vector whose elements are either 0 or 1.

71

Table 3-1lists the elements of the vector *c* for example systems with *n = 3* components. Included are series, parallel, and general systems, the latter represented by both cut-set and link-set formulations. It is seen that in all cases the system probability is a linear function of *p*. It is clear from the above analysis that the system reliability problem can be cast in the form of an LP problem.

Although LP has previously been used in the context of structural system reliability by Nafday (1987) and Corotis and Nafday (1989). However, they used LP for the purpose of identifying the most critical failure mode for a structural system, not for computing the system probability. The LP bounds developed by Song and Der Kiureghian are applicable for any type of system and any level of information regarding the component probabilities (Jimenez-Rodriguez and Sitar, 2007). Equally important, these bounds are the narrowest possible bounds that one can obtain for a system for any specified information regarding the component probabilities. Using the LP bounds method, the bounds on various quantities such as component importance measures (Song and Der Kiureghian 2005), conditional probabilities given observed events and parameter sensitivities of the system failure probability (Der Kiureghian and Song 2008) can be calculated as well.

In the same line with this research achievement, many other researchers have put their efforts in overcoming the scalability issue of the LP bounds method, of which, a multi-scale analysis approach was combined with the LP bounds method to reduce the size of LP problems in Der Kiureghian and Song (2008); Kang et al. (2012). Furthermore, Chang and Mori (2013; 2014) employed a relaxed linear programming (RLP) bounds method through an introduction of a universal generating function. Added to this, Wei et al. (2013) proposed a small-scale linear programming (SSLP) based boundary theory which can sufficiently reduce the scale of the linear programming model involved. This approach was applied to a structural system with

multiple failure modes where both random and fuzzy inputs are present as what presented in Wei et al. (2018).

3.1.2 Framework to facilitate analytical evaluation

3.1.2.1 *Matrix-Based System Reliability (MSR) Method*

Another approach to solve the problem towards estimating the structural system reliability is called Matrix-Based System Reliability (MSR) Method that provides a systematic framework to facilitate analytical evaluation of general system reliability (Kang et al. 2008) and their series of Kang and Song (2009); Kang et al. (2012) as shown inFigure 3-2.

Consider a system whose *ith* component has s_i distinct states, *i=1,...,n*. The sample space can be divided into $m=\Pi_{i=1}^{n}s_i$ mutually exclusive and collectively exhaustive events named as the "basic" MECE events and denote them by e_j, *j=1,...,m*. One can describe any event by identifying the basic MECE events that belong to it. Therefore, a general system event can be represented by an "event" vector c whose *jth* element is *1* if e_j belongs to the system event and *0* otherwise. Let $p_j=P(e_j)$, *j=1,...,m*, denote the probability of e_j. Due to the mutual exclusiveness of e_j's, the probability of a system event, E_{sys}, i.e., $P(E_{sys})$ is simply the sum of the probabilities of e_j's that belong to the system event. Where *p* is the "probability" vector that contains p_j's, the system failure probability is computed by a simple vector calculation

$$P(E_{sys}) = \sum_{j:e_j \subseteq E_{sys}} p_j = \mathbf{c}^{T}\mathbf{p}$$

Equation 3-3

That can be generalized to compute the probabilities of multiple system events under multiple conditions of component failures by a single matrix multiplication

73

$$\mathbf{P}_{\text{sys}} = \mathbf{C}^{\mathrm{T}}\mathbf{P}$$

$$\mathbf{C} = \begin{bmatrix} \mathbf{c}_1 & \mathbf{c}_2 & \cdots & \mathbf{c}_{N_{sys}} \end{bmatrix}$$

$$\mathbf{P} = \begin{bmatrix} \mathbf{p}_1 & \mathbf{p}_2 & \cdots & \mathbf{p}_{N_{\text{cond}}} \end{bmatrix}$$

Equation 3-4

where c_i, $i=1,...,N_{sys}$, is the event vector of the ith system event; p_j, $i=1,...,N_{cond}$, denotes the probability vector for the jth condition; and P_{sys} is the matrix whose element at the ith row and the jth column is the probability of the jth system event under the jth condition.
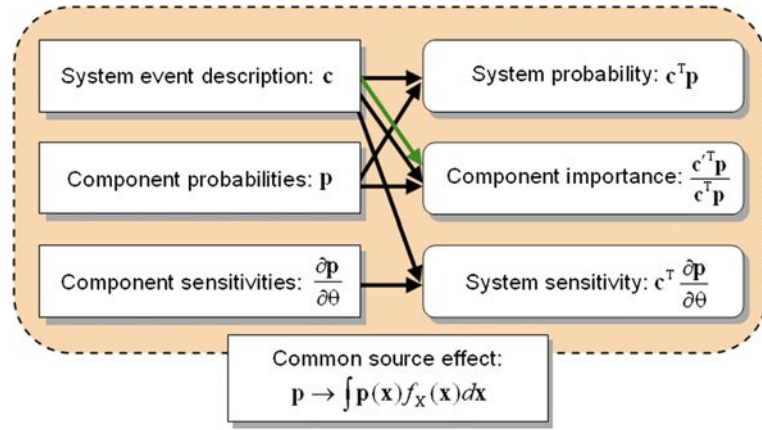
Figure 3-2 Main calculation procedures and outputs of the MSR method

In regard of Nale et al. (2019); Song and Kang (2009), comparing to the LP method, the MSR method has the following merits over existing system reliability methods.

- The complexity of the system reliability computations is not affected by that of the system event definition because the reliability of a system event is calculated by a single matrix multiplication regardless of the system definition.

- The matrix-based formulation allows us to identify/handle the system events conveniently and compute the corresponding probabilities efficiently.

- If one has incomplete information on the component failure probabilities or their statistical dependence, the matrix-based framework enables us to obtain the narrowest possible bounds on any general system event. This is equivalent to the LP bounds method (Song and Der Kiureghian, 2003)

- One can calculate the conditional probabilities and various importance measures (Song and Der Kiureghian, 2005) using the MSR method without introducing further complexity.

- The recent developments of matrix-based computer languages and software including MATLAB® and Octave rendered matrix calculations more efficient and easier to implement.

- The MSR method can be extended for evaluating various system reliability metrics such as average connectivity loss or service flow reduction (Dueňas-Osorio et al., 2006) by describing the average or exceedance probability of such a metric in terms of C and P.

The MSR method is applicable to a wide range of system types, i.e. series, parallel, cut set, and link set systems, which satisfies the needs for Generality. This general applicability has been demonstrated by many examples of not only structural systems, e.g. truss systems, a bridge pylon system, a combustion engine, a hardware system of train and Daniels systems but also, infrastructure networks, e.g. bridge networks, a gas distribution system, complex slopes.

In this line, other researchers have put efforts to extend the usage of the MSR methods to system, whose performance is evaluated in terms of a continuous measure. Song and Kang (2009) presents a further develop on the MSR method it in terms of statistical dependence and parameter sensitivity of system reliability that uses the MSR method for systems with statistically dependent components; and the correlation coefficients between the basic random variables or the component safety margins are represented by a Dunnett–Sobel

class correlation matrix to identify the source of the statistical dependence and to make use of the matrix-based procedure developed for independent components. This study provided two numerical examples of structural systems: (1) the system fragility of a bridge structure; and (2) the collapse of a statistically indeterminate structure subjected to an abnormal load. Kang et al. (2012) introduced two further developments of the MSR method: (1) for efficient evaluation, the integral in the CSRV space is performed using the first- or second-order reliability methods; (2) a new matrix-based procedure to compute the sensitivity of the system failure probability with respect to the parameters that affect the correlation coefficients between the components. This study also demonstrated two examples for a three-storey Daniels system structure, and a bridge pylon system. Nguyen et al. (2010) proposed a single-loop system reliability-based design optimization (SRBDO) approach using the recently developed matrix-based system reliability (MSR) method to eliminate the inner-loop of SRBDO that evaluates probabilistic constraints that can apply to general systems including series, parallel, cut-set, and link-set system events. Currently, Byun et al. (2017) extended the MSR method to *k-out-of-N* systems by modifying the formulations of event and probability vectors that can incorporate statistical dependence between component failures for both homogeneous and non-homogeneous k-out-of-N systems; and compute measures related to parameter sensitivity and relative importance of component. This study also provided two numerical examples: (1) hypothetical systems each consisting of series, parallel and k-out-of-N subsystems, and (2) a simplified high-speed train system modelled by multiple k-out-of-N subsystems.

3.1.2.2 *Sequential Compounding Method (SCM)*

System reliability analysis often requires efficient and accurate evaluation of a multivariate normal integral. Despite recent advances in system reliability analysis methods, it is still a challenging task especially when the definition of the system event is complex; the system has a large number of components; and/or the component events have significant statistical

dependence. Kang and Song (2010) presented a sequential compounding method (SCM) as a new method developed for evaluating multivariate normal integrals defined for general system events including series, parallel, cut-set and link-set systems. The method compounds two components coupled by union or intersection sequentially until the system becomes a single compound event. Efficient numerical procedures are developed for obtaining the reliability index of the new compound event, and the correlation coefficients between the compound event and the remaining component events, at each step of the sequential compounding. The SCM sequentially compounds a pair of component events in the system until the system is merged into one super-component as illustrated by an example in Figure 3-3.
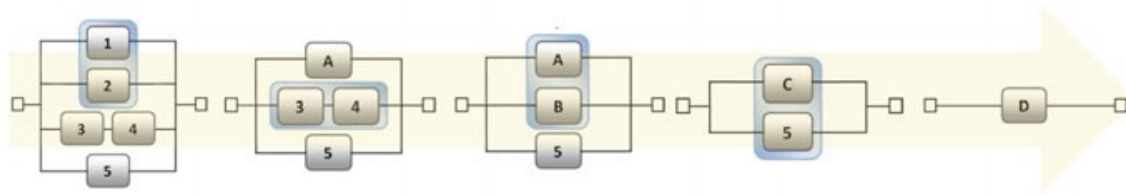
Figure 3-3 Example of sequential compounding by SCM

For a parallel or series system, the procedures introduced in Figure 3-3 can be applied to adjacent components sequentially until it becomes a single compound event. For a cut-set or link-set system, one can first compound components in each cut-set or link-set until the system becomes an equivalent series or parallel system, respectively. Then, the compound components in the series or parallel system are compounded sequentially again. One can follow alternative orders of compounding as long as it is compatible with event operation rules (e.g. associative rule and commutative rule). Although each compounding process requires solving the nonlinear equation of compounding two components coupled by intersection or by union as followed:

If coupled by intersection

77

$$\Phi_2\left(-\beta_{1|k}, -\beta_{2|k}; \rho_{1,2|k}\right) = \Phi\left(-\beta_{(1\text{and}2)|k}\right)$$

<div align="right">**Equation 3-5**</div>

$$\beta_{1|k} = (\beta_1 - \rho_{1,k}A) / \sqrt{1 - \rho_{1,k}^2 B}$$

$$\beta_{2|k} = (\beta_2 - \rho_{2,k}A) / \sqrt{1 - \rho_{2,k}^2 B}$$

$$\rho_{1,2|k} = (\rho_{1,2} - \rho_{1,k}\rho_{2,k}B) / \left(\sqrt{1 - \rho_{1,k}^2 B}\sqrt{1 - \rho_{2,k}^2 B}\right)$$

$$\beta_{(1\text{and}2)|k} = (\beta_{1\text{and}2} - \rho_{(1\text{and}2),k}A) / \sqrt{1 - \rho_{(1\text{and}2),k}^2 B}$$

<div align="right">**Equation 3-6**</div>

$$A = \varphi(-\beta_k) / \Phi(-\beta_k)$$

$$B = A(-\beta_k + A)$$

<div align="right">**Equation 3-7**</div>

in which, φ denotes for the PDF of the standard normal distribution

If coupled by union

$$1 - \Phi_2\left(\beta_{1|k}, \beta_{2|k}; \rho_{1,2|k}\right) = \Phi\left(-\beta_{(1\text{or}2)|k}\right)$$

<div align="right">**Equation 3-8**</div>

$$\beta_{(1\text{or}2)|k} = (\beta_{1\text{or}2} - \rho_{(1\text{or}2),k}A) / \sqrt{1 - \rho_{(1\text{or}2),k}^2 B}$$

<div align="right">**Equation 3-9**</div>

numerically for all remaining components, the proposed procedure is efficient because it does

not involve sampling or expensive multi-fold numerical integrations. It is also noteworthy that

the proposed approach can be used to quantify the statistical dependence between sub-systems, e.g., cut-sets or link-sets by the equivalent correlation coefficients between the compound events.

An important merit of the SCM method is that one can quantify the statistical dependence between sub-systems by the equivalent correlation coefficients between compound events. Its accuracy and efficiency for series, parallel, cut-set and link-set systems are demonstrated through comparison with other existing methods such as the PCM method and MSR method. For example, Johari and Lari (2016) predicted the system reliability indices and corresponding probabilities of failure from the SCM method and compared against those of the Monte Carlo simulation (MCs). The results of sensitivity and parametric analyses show that the water pressure parameters are the most effective parameters in rock wedge stability. It is also confirmed by Johari and Rahmati (2019) that the accuracy of the method is not significantly affected by the large number of components in a system.

An alternative approach to the SCM method was later developed by Kang and Kliese (2014) that proposed a rapid reliability estimation method for node-pair connectivity analysis of lifeline networks especially when the network components are statistically correlated. Recursive procedures are presented to compound all network nodes until they become a single super node representing the connectivity between the origin and destination nodes. The proposed method was applied to numerical network examples and benchmark interconnected power and water networks in Memphis, Shelby County. The connectivity analysis results show the proposed method is reasonable accuracy and remarkable efficiency as compared to the Monte Carlo simulations. It is noted by Byun and Song (2017) that the SCM also satisfies the criteria of Efficiency and Scalability since the proposed sequential compounding processes are straightforward and computationally efficient even for large-scale systems. Recently, Chun et al. (2019) proposed a new SCM method to incorporate constraints on the first-passage

79

probability into reliability-based optimization of structural design or topology. For efficient evaluations of first-passage probability during the optimization, the failure event is described as a series system event consisting of instantaneous failure events defined at discrete time points. The probability of the series system event is then computed by use of a system reliability analysis method termed as the sequential compounding method. The adjoint sensitivity formulation is derived for calculating the parameter sensitivity of the first-passage probability to facilitate the use of efficient gradient-based optimization algorithms.

3.1.2.3 B^3 method

In risk-informed design, maintenance and retrofit for such structural systems, it is essential to quantify the risk of fatigue-induced sequential failures and identify critical sequences of local failures. When a series of component failures are observed, their sequence is generally an important factor that characterizes the system failure. Particularly for an indeterminate structure, the failures of certain members cause re-distribution of forces in the structural system, which affects the likelihood and sequence of the cascading failures. Different contributions of preceding failed members affect whether the structure would be able to withstand more external impacts or would collapse. There is a need for a reliability analysis method to reflect the importance of the sequence of events.

There have been many research efforts for quantifying such system-level risk in consideration of sequential failures. Monte Carlo simulation (i.e., repeating computational simulations for many scenarios based on randomly-generated values of uncertain parameters) is the most straightforward and widely-used method; however, when structural analysis demands time-consuming computational simulations or when the failure probabilities are low, the computational and time costs required for converged results can be exceedingly large. For such a reliability analysis concerning fatigue-induced cascading failures, a branch-and-bound method employing system reliability bounds, termed B^3 method was developed (Lee and Song

80

2011). Based on a recursive formulation of the limit-state functions of fatigue- induced failures, a system failure event is formulated as a *disjoint* cut-set system event. A new search scheme identifies critical fatigue-induced failure sequences in the decreasing order of their probabilities while it systematically updates both lower and upper bounds on the system failure probability without additional system reliability analyses. As a result, the method can provide reasonable criteria for terminating the branch-and-bound search without missing critical failure sequences and reduce the number of computational simulations required to obtain reliable estimates on the system risk. **Error! Reference source not found.** illustrates the search scheme of the B^3 method and how the system reliability bounds are narrowed as the search process proceeds.
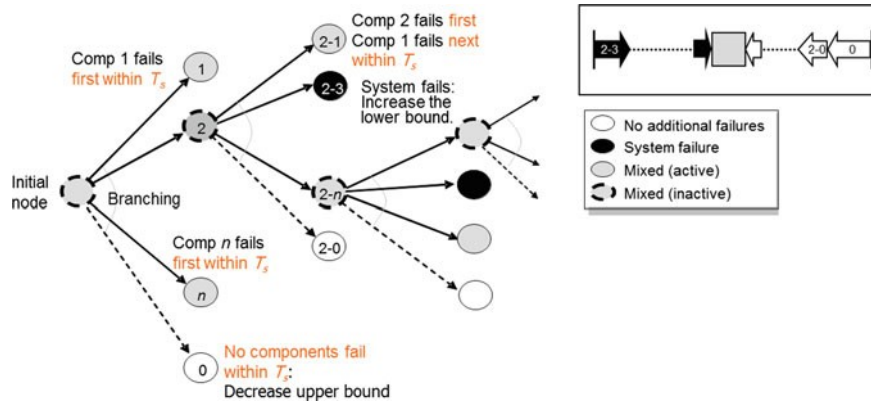
Figure 3-4 Procedure in B³ method

The main difference between the B^3 method and existing branch-and- bound-based methods is that the proposed method describes a system event by use of mutually exclusive (or disjoint) failure sequences. By contrast, when a branch-and-bound method uses a non-disjoint cut-set formulation, the probability of a failure sequence is computed without considering the likelihoods of specific orders. For example, the probability of a sequence {1 → 2 → .. → N} would be computed as:

$$P_i^{1,\dots,i-1} = P\left\{\left(T_1^0 < T_s\right) \cap \left(T_1^0 + T_2^1 < T_s\right) \cap \cdots \cap \left(T_1^0 + T_2^1 + \cdots + T_i^{1,\dots,i-1} < T_s\right)\right\}$$

81

Equation 3-10

This is simplified as

$$P_i^{1,...,i-1} = P\left\{\left(T_1^0 + T_2^1 + \cdots + T_i^{1,...,i-1} < T_s\right)\right\}$$

Equation 3-11

Compared to the corresponding formulation of the B^3 method, this probability is easier to obtain because one can compute this probability by a component reliability analysis rather than a system reliability analysis. However, the identified failure paths are non-disjoint and correlated, so the lower bound on the system failure probability should be computed by a system reliability analysis for the union of all identified failure paths, i.e.,

$$P_{low} = P\left(\cup_{i=1}^{N_{id}} E_i\right)$$

Equation 3-12

where E_i is the occurrence of the i-th identified system failure sequence *(i = 1,..., N_{id})* that appears in Eq. (19), and N_{id} is the total number of system failure sequences identified by the branch-and- bound search. By contrast, the B^3 method updates the lower bound just by adding the probability of newly identified system failure sequences to the current bound. Moreover, the B^3 method can provide the upper bound as well, which helps provide reasonable termination criteria for the search process.

The B3 method was later combined with finite-element-based reliability analysis for applications to continuum structures, in which, the limit-state formulations are modified to incorporate crack-growth analysis using an external software package, and an additional search-termination criterion is introduced. Lee and Song (2013) also proposed an inspection-

based reliability updating scheme using B3 method for both discrete and continuum structures. Quintana et al. (2014) employed the B3 method to combine system reliability analysis, and "failure mode effects and criticality analysis" (FMECA) for quantitative classification of structural hot spots. The method is considered to have inference capability as well since the updating method can compute conditional probabilities given information obtained from the inspections, both equality and inequality-type events.

In the existing methods, even though a branch-and-bound method can identify critical failure sequences in the decreasing order of their probabilities (unless heuristic or problem-dependent truncation rule is introduced), the changes in the lower bound caused by newly identified system failure sequences are not decreasing monotonically. This is due to the statistical dependence between the failure sequences. However, in the B^3 method, the increments of the lower bound are the same as the probabilities of the identified system failure cases, which are found in the decreasing order. Therefore, the increments on the lower bound diminish monotonically, which helps terminate the search process without performing more searches than necessary. To achieve the aforementioned merits of the disjoint cut-set formulation, the B3 method needs to perform more component and system reliability analyses than conventional branch-and-bound methods. Considering the efficiency in the search process and accuracy in system failure probability calculations, this additional task is worthwhile especially when the computational cost of the structural or finite element analysis is dominant. The component reliability analysis method used in the B^3 method should be able to identify the statistical dependence between the component events such that a system reliability analysis can be later performed with the dependence fully considered. The system reliability analysis method should be able to compute the probability of parallel systems accurately. In particular, the method should be able to handle parallel systems with a large number of component events because the number of component events quickly increases as the search process proceeds.

Although the B3 method was originally developed for fatigue-induced failures in a system, the search scheme can be extended to other types of cascading failure phenomena by re-formulating the reliability calculations of the failure sequences.

3.1.3 Computational effort

3.1.3.1 *Importance Sampling*

Structural reliability analysis frequently requires the use of sampling-based methods, particularly for the situation where the failure domain in the random variable space is complex. Although the Monte Carlo Simulation (MCS) is the most straightforward approach applicable to all system problem, the computational cost is sometimes overwhelming, especially, when the probability of the event is low. Typically, MCS focuses on finding the failure probability estimate and the variability associated with that estimate, but not on identifying the design point or important areas in the failure domain. One of the most efficient and widely utilized methods to remedy these issues is to use in such a situation is importance sampling (Melchers and Beck, 2018). Importance sampling (IS) has been developed to alleviate the computational cost of simulation by using a more efficient sampling density located at relatively important regions, which are usually identified by additional reliability analysis.

When implementing IS, one must specify an alternative sampling density that is expected to reduce the variability of the sampled estimates and thus the associated computational cost. One example of such alternative densities is a Gaussian density whose mean vector is located at the design point found from a First-Order Reliability Method (FORM) analysis (Engelund and Rackwitz, 1993); nevertheless, this approach does not completely address the aforementioned issues for structural reliability problems with (1) multiple design points (Der Kiureghian and Dakessian, T.), which might result in significant errors, or (2) numerical issues that make a non-sampling-based analysis difficult, including numerical noises in the limit-state function.

84

For series system reliability problems, there have been some attempts to combine multiple sampling densities cantered at the design points identified from FORM analyses of the component limit-state functions. However, it is difficult to optimally determine the relative weights of those densities (Fu et al., 1988) or filter non-critical ones (Tomasson and Söder, 2016). For parallel systems, it is desirable to sample around the joint design point, which can be found by mathematical programming (Xia et al., 2020). However, the approach may introduce significant computational cost in addition to that required for FORM analysis. For general system reliability problems, i.e. neither series nor parallel, no general procedure is available to find an effective importance sampling density based on the results of FORM analysis.

To identify an effective IS density, various adaptive IS procedures have been suggested, which are categorized into two major approaches. One approach focuses on updating the sampling density function based on intermediate results or pre-sampling while the other focuses more on updating a surrogate representation of the limit-state function. Many have made hybrids of these two approaches. Bucher (1988) proposed an adaptive IS approach in which the sampling density is updated based on statistical moments estimated by pre-samples. Ang et al. (1991) used an IS density found by constructing kernel models based on samples generated in the failure domain. Ching and Hsieh (2007) used subset simulations coupled with a maximum entrophy optimization to find a local approximation of the limit state for given design values. The maximum entropy approach selects a probability density function (PDF) that maximizes its entropy subject to moment constraints from sample data. Dubourg and Deheeger (2011) used a variance minimizing IS with a surrogate meta-model based off of a Kriging procedure. Grooteman (2011) used an adaptive directional IS approach to improve the efficiency of directional IS approaches by finding the most important directions and sampling the rest using

a response surface. This method is most recently updated by Zhang et al. (2020) with an adaptive Kriging oriented importance sampling (AKOIS) approach

Several other methods have been suggested, but most of these falls within similar veins of the aforementioned methods. Another notable adaptive IS approach is to find a near-optimal IS density by minimizing the Kullback–Leibler cross entropy (CE) (Rubinstein and Kroese, 2013) through a few rounds of small-size pre-sampling. In this methodology, CE is used as a measure of the "distance" between the absolute best sampling density function (Binder et al., 2012) and the current IS density model; however, the suggested probability density function distributions in this work are based on unimodal distribution models of statistically independent random variables. This unfortunately limits the breadth of structural reliability problems the methodology can address; nevertheless, such a CE-based IS approach is largely absent from general use in the field of structural reliability, although various approaches do perform entropy maximization, as discussed previously.

Recently, in Rubinstein and Kroese (2013), the adaptive importance sampling approach is further developed by incorporating a nonparametric multimodal probability density function model called the Gaussian mixture as the importance sampling density. This model is used to fit the complex shape of the absolute best sampling density functions including those with multiple important regions. An efficient procedure is developed to update the Gaussian mixture model toward a near-optimal density using a small size of pre-samples. The proposed cross-entropy-based adaptive importance sampling (CE-AIS) needs only a few steps to achieve a near-optimal sampling density and shows significant improvement in efficiency and accuracy for a variety of component and system reliability problems. The method requires far less samples than both crude Monte Carlo simulation and the cross-entropy-based adaptive importance sampling method employing a unimodal density function; thus achieving relatively small values of the coefficient of variation efficiently. The computational efficiency and

86

accuracy of the proposed method are not hampered by the probability level, dimension of random variable space, and curvatures of limit-state function. Moreover, the distribution model parameters of the Gaussian densities in the obtained near-optimal density help identify important areas in the random variable space and their relative importance.

Kurtz and Song (2013) proposed to adopt a Gaussian mixture as a sampling density model in the CE-AIS approach and developed closed-form updating rules to find the near-optimal sampling density by a few rounds of small pre-sampling. Figure 3-5 demonstrates how Gaussian mixture models converge to near-optimal sampling densities by the CE-AIS-GM algorithm. The black lines in the figures represent the limit-state surface of a series system problem. The contours in the far-left figures represent the initial GM sampling densities, and after few rounds of pre-sampling, the sampling densities converge into critical regions as noted in the far-right figures in Figure 3-5. Although CE-AIS-GM is not able to directly estimate conditional probabilities, the criterion of Inference is considered to have been partially fulfilled in a sense that the GM model parameters obtained during pre-sampling process are helpful in identifying important areas in random variable space. As strongly stated by Barkhori et al. (2019), CE-AIS employing a Gaussian mixture (CE-AIS-GM) has proved to be efficient and accurate by numerical examples including a parabola limit-state function and reliability analyses of systems such as parallel, series and general systems, i.e. requiring far less samples to achieve the target coefficient of variation than crude MCS or CE-AIS using a unimodal distribution model for seismic reliability analysis (Choi and Song, 2017) and time-dependent reliability of structural system (Yang et al., 2015). It is noted that the method is yet able to incorporate available information in a flexible manner or evaluate parameter sensitivities. While CE-AIS-GM shows good performance for systems including up to about 50 random variables, the method does not work well in the random variable spaces with higher

dimensions. This is because most of the probability volume is highly concentrated around the surface of the hypersphere with a certain radius in a high dimension random variable space.

To be able to sample in the so-called "important ring" region, later on, Wang and Song (2016) developed a cross-entropy-based adaptive importance sampling technique that employs a von Mises-Fisher mixture (CE-AIS-vMFM) as the sampling density model. By small-size pre-samplings, the proposed approach first finds a near-optimal sampling density by minimizing the Kullback–Leibler cross entropy between a von Mises-Fisher mixture model and the absolute best importance sampling density. Three numerical examples are investigated in this study to test and demonstrate the proposed importance sampling method; and their obtained results show that the proposed approach, applicable to both component and system reliability problems, has superior performance for high dimensional reliability analysis problems with low failure probabilities. The performance of CE-AIS-vMFM was successfully demonstrated by reliability analyses of both component and system events which included up to 300 random variables.

There has been another effort to resolve the difficulty in high-dimensional systems by integrating CE-AIS with Markov chain Monte Carlo methods (Wang, 2017) nesting a specially optimized partially collapsed Gibbs sampler to help in avoidance of locally trapped Markov chain samples which may be encountered by traditional cross-entropy methods. RTS-79 is utilized for illustrating the superiority of the proposed method, termed E-MICEM, against its parent method, i.e., the Markov chain Monte Carlo-integrated cross-entropy method. Two traditional indices including loss of load probability and expected demand not supplied are comparatively evaluated and the simulation results suggest that the E-MICEM is superior in the efficiency of estimating the two indices.

Recently, Geyer et al. (2019) investigated the suitability of the multivariate normal distribution and the Gaussian mixture model as importance sampling densities within the cross entropy method; and compared the performance of the cross entropy method to sequential importance sampling, another recently proposed adaptive sampling approach, which uses the Gaussian mixture distribution as a proposal distribution within a Markov Chain Monte Carlo algorithm. Accordingly, this study prosed a modified version of the expectation-maximization algorithm that works with weighted samples. To estimate the number of distributions in the mixture, the density-based spatial clustering of applications with noise (DBSCAN) algorithm is adapted to the use of weighted samples. The performance of the different methods was compared in several examples, including component reliability problems, system reliability problems and reliability in varying dimensions. The obtained results show that the cross-entropy method using a single Gaussian outperforms the cross-entropy method using Gaussian mixture and that both distribution types are not suitable for high dimensional reliability problems. It is noteworthy that even when an excessive number of sampling densities are originally employed in the Gaussian mixture model, densities tend to merge to form a Gaussian mixture model concentrating only on the important areas.
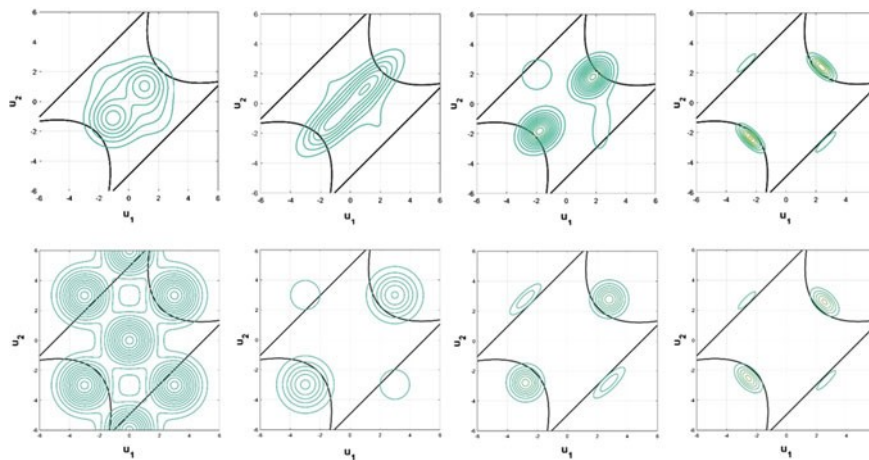
Figure 3-5 Illustration of Cross-Entropy-Based Adaptive Importance Sampling (CE-AIS)

3.1.3.2   Genetic-Algorithm-Based Selective Search

The B^3 method presented earlier analytically tracks down dominant failure modes in an event-tree setting. Therefore, the approach may become computationally intractable as the number of failure sequences increases exponentially as the number of components increases. By contrast, Kim et al. (2013) proposed a new simulation-based selective searching technique namely a multi-scale matrix-based system reliability (MSR) method to identify dominant failure modes in the space of random variables, and then perform system reliability analysis to compute the system failure probability. Lower-scale MSR analyses evaluate the probabilities of the identified failure modes and their statistical dependence. A higher-scale MSR analysis evaluates the system failure probability based on the results of the lower-scale analyses. The advantages of this approach are: (1) the separation of the failure mode identification and probability evaluation processes can prevent the computational cost of the repeated structural reliability from increasing exceedingly with the complexity of a structure. Therefore, this approach can be applied effectively to a large structure with a high-level of redundancy such as cable-supported bridges.; (2) the modified simulation-based searching technique can capture multiple failure modes, which enables identifying all modes observed in Monte Carlo simulations, while the β-unzipping method may miss some dominant failure modes and the branch-and-bound method possibly requires excessive number of component and system reliability analyses for a large structure. Moreover, its searching performance is significantly improved through genetic-algorithm-based selective search compared to Monte Carlo simulations; (3) The multi-scale MSR method can skilfully account for the statistical dependence among components as well as among dominant failure modes; (4) The multi-scale MSR method estimates the failure probabilities of the dominant failure modes and the system

90

reliability efficiently. Figure 3-6 shows the domain of a failure mode in the two-dimensional standard normal space. The dotted lines show the limit-state surfaces of component events while the solid lines represent that of the failure mode. Note that the term "component" in this paper does not mean a physical member, but a failure *event* that can occur to members under a given load distribution.

In literature, the GA-based selective searching scheme has been applied to several practical problems. For example, Kurtz (2011) proposed method uses a multi-objective genetic algorithm, called Non-dominated based Sorting Genetic Algorithm II (NSGA II) to perform many FORM analyses simultaneously to generate a Pareto Surface of design points. The applicability of this approach is shown through two numerical examples. The first example is a general situation with few random variables. The second example analyses a statically indeterminate truss subjected to cyclic loading. Both numerical examples are validated with crude-MCS results and show that the method can find a full Pareto Surface, which provides reliability analysis results at a range of performance levels along with the probability distribution of the performance quantity. Moreover, Coccon et al. (2017) provided an extensive application of this method to the offshore structural systems. Following to this study, the main advantage of the proposed method is that the identification process of dominant failure modes is decoupled from the evaluation process of the probabilities of failure modes and the system failure event. The identification phase consists of a multi-point parallel search employing a genetic algorithm, and it is followed by the evaluation phase, which performs a multi-scale matrix-based system reliability analysis where the statistical dependence among both components and failure modes is fully considered.
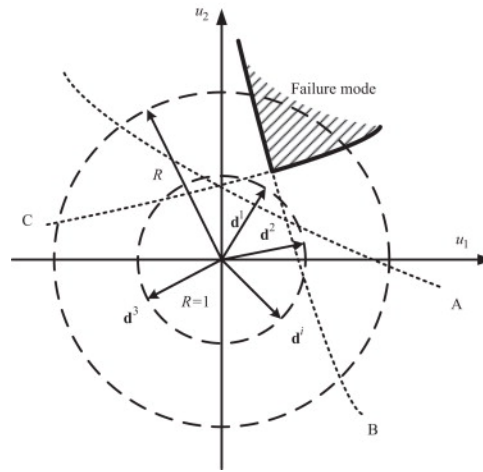
Figure 3-6 Failure mode in standard normal random variable space.

Since the events generated by GA-based selective search represent the potential failure modes and the probability of each of them is identified during the analysis, criteria related to cascading failures and critical failure modes are dealt with by this methodology. Since the method is a sampling-based approach, it is applicable to a wide class of structures and failure phenomena as long as a proper computational simulation is feasible for the cascading failure of interest. Compared to event-tree-based search approaches such as the B3 method, the GA-based search method is more scalable to systems with a large number of components.

3.2 Limitation of MCS and NNs Application in System Reliability Analysis

The feasibility towards application of Monte Carlo Simulation in the reliability analysis of complex structural systems have been well documented in literature as an accurate method (Zhang, Mullen and Muhanna, 2010; Xu, Zhang and Sun, 2016). Researchers have highlighted many attractive features of Monte Carlo Simulation in analysing structural system reliability that the most important one is its capability to check almost irrespective of the complexity of the system through the system failure criterion. However, the burden in cost and time of computation involved in the simulation may be prohibitive for highly reliable structural systems. For this reason, up-to-date, there are not many researches that have been employed

the system reliability based Monte Carlo Simulation. Among others, there are three main researches worth to mention to demonstrate the feasibility of employing Monte Carlo Simulation to accurately predicted the system reliability of complex structures through four test cases namely Naess, Leira and Batsevych (2009; 2012) and Gaspar et al. (2014).

The two important examples (a portal frame and 13-member truss structure) were presented in Naess, Leira and Batsevych (2009) that all basic random variables are concerned with simple explicit limit state functions. For this reason, there was only minor or even no efforts in terms of the computational time and cost during the process of investigating the structural system reliability that is expressed in Equation 3-13 as the failure probability of the targeted systems:

$$p_f(\lambda) = \text{Prob}\left(\bigcup_{j=1}^{m}\{M_j(\lambda) \leqslant 0\}\right),$$

Equation 3-13

in which, $M_j = G_j(X_1,...,X_n)$, $j = 1,...,m$ denotes for a set of m given safety margins expressed in terms of n basic variables. The extended class of safety margins then become $M_j(\lambda) = M_j - \mu_j(1 - \lambda)$, where $\mu_j = E[M_j]$.

Naess, Leira and Batsevych (2012) provided another example on a 3D beam system (grillage) with a grid of 40×40 equidistant and intersecting main beams. The random variables are included (1) a set of loading system – vertical load at each of the intersections; (2) a set of cross-section property – dimension and length of bean, yield stress. In particular, because initial yield is considered, there are three critical stresses considered as random variables namely vertical shear stress, torsion share stress and yield stress that all of them are fully correlated for a given cross section. It is noted that all the selected random variables are lognormal distribution.

93

In general, it is observed from the study of Naess, Leira and Batsevych (2009; 2012) that the proposed method provides good estimates for the reliability of large structural systems with a moderate computational effort. On the basic of such results, Gaspar et al. (2014) applied Monte Carlo Simulation into system reliability analysis for the estimation of the buckling collapse strength reliability of a ship hull girder stiffened panel represented by a nonlinear finite element structural model. In this study, the buckling collapse strength reliability assessment of the stiffened panel using the Monte Carlo based reliability estimation method were performed through two analyses: (1) reliability analysis for each individual component; and (2) reliability assessment for the entire system as a whole. In the former case, it was considered only one stiffener with attached plating, the probability of failure in this case was thus estimated as the probability of buckling collapse failure of that component. In the latter case, it was considered all the stiffeners with attached plating in the stiffened panel in formulating the system reliability problem. It is noted that the failure of the structure system – the stiffened panel – in case any of its stiffeners with attached plating fails due to buckling collapse. This failure criterion corresponds to a local failure of the stiffened panel and was modelled as a system of failure modes in series. Accordingly, the author first defined the buckling collapse strength limit state of each stiffener with attached plating in Equation 3-14

$$G_i\left(X_R^s, X_{Ri}^c, X_S\right) = \sigma_{xu,i}\left(X_R^s, X_{Ri}^c\right) - \sigma_{x,hg}\left(X_S\right)$$

Equation 3-14

with m is the number of the structural components, i= [1,m] is an index that identifies each stiffener with attached plating or system's component; $\sigma_{xu,i}$ denotes for the ultimate compressive strength and $\sigma_{x,hg}$ denotes for the axial compressive load induced by the hull girder vertical bending.

It is noted that the failure of each component of the structural system due to buckling collapse is defined in terms of its ultimate compressive strength that is either equal or lower than the applied axial compressive load. These conditions are identified by a negative or zero value of the limit state function or safety margin given by Equation 3-14, respectively. Of which, the ultimate compressive strength of each component of the system is defined by the maximum value of the corresponding average stress-strain curve for axial compression as shown in Equation 3-15 functioned by four main conditions: (1) the welding-induced initial imperfections such as residual stresses and initial distortions; (2) the boundary conditions; (3) the loading system; and (4) the geometry and material properties of the stiffener and attached plating.

$$\sigma_{xu,i}\left(X_R^s, X_{Ri}^c\right) = \max_{\varepsilon_x}\left[\sigma_{x,i}\left(X_R^s, X_{Ri}^c; \varepsilon_x\right)\right]$$

Equation 3-15

The predicted failure probabilities and corresponding reliability through application of Monte Carlo Simulation is shown good estimates of the reliability of structural systems by the application of Monte Carlo Simulation with low to moderate computational effort. Moreover, it is observed that the failure probability of each individual component in terms of buckling collapse is always smaller than that of the systematic probability. Such observation was in the line with the general assumption towards the failure criterion in the system reliability analysis.

In the structural design in regard to reliability analysis and index, it is a must for the structural designer in verifying the serviceability and ultimate conditions of the structure within a prescribed safety level (Markova and Holicky, 2017). This statement is generally expressed by $S_d < R_d$, where S_d stands for the action effect and R_d stands for the resistance. Under the guidance of the Eurocode 1 (1994), Eurocode 3 (1992), the available methods to deal with the

intrinsic random nature of material properties and actions can be classified into three main levels as following:

- Level 1 methods or Semi-probabilistic: This is considered as the most common used method in practice, in which the failure probability of the structure is indirectly considered trough the definition of characteristic values and the applications of partial safety indexes;

- Level 2 methods or Approximate probabilistic: These methods are generally formed as the first order or second order reliability methods (FORM/SORM), in which the probability of failure is based on the reliability index β (Hasofer and Lind,1974);

- Level 3 methods or Exact probabilistic: This is in regards to current developments of computational models to compute the probability of failure from the joint probability distribution of the random variables associated with the actions and resistances.

The simulation method employed Monte Carlo Simulation falls within the Level 3 – Exact probability that offers the following features in regards of reliability analysis for structures: (1) it is possible to apply in cases of many different problems in practices; (2) it allows the direct considerations of any distribution type for the random variables considered in probability; (4) it enables the capability in computing the failure probability in regards to the desired precisions; and (4) it is relatively easy in simple in implementation (Zio, 2013; Rubinstein and Kroese, 2016). However, up to recent, the application of Monte Carlo Simulation has not yet widespread in the field of structural system reliability comparing to Level 2 method - Approximate probabilistic- due to the fact it requires a great number of structural analyses, one for each sample of the set of random variables (Cardoso et al., 2008). A simple expression of this burden in computational cost was demonstrated by Shooman (1968) that: with the normal values of failure probability in association with the ultimate limit states between 10^{-4} and 10^{-6},

there is a general need of at least 1.6×10^7 to 1.6×10^9 numbers of analyses performed to ensure a 95% likelihood, which accounted for 5% of the computed one in analysing the actual probability. The finite elements codes are generally employed in order to perform such analyses making the relatively high computational time, particularly, in cases of non-linear structural behaviour or the complex numerical model. In purpose of eliminating such drawback, Papadrakakis, Papadopoulos and Lagaros (1996) was first to propose the use of Neural Networks by means for performing function approximation to reduce the computational efforts in estimating structural response for system reliability analysis. With the help of Neural Networks learning and training process, it is possible to fasten the computing progress to approximate the structural responses. As strongly indicated by Chojaczyk et al. (2015), one it is trained properly, such technique enables to determine the structural responses with a relatively very small number of operations leading to a very little efforts in the corresponding structural analyses. Such feature is essential for the process to analyse the structural system reliability-based Monte Carlo Simulation as it enables the feasibility of such method for great complexity systems that would not be possible without.

Nevertheless, due to the complexity of the proposed methods that combines the developments of systematic reliability analysis, Monte Carlo Simulation and Neural Network, up to recent, there are only three papers that have discussed the related issues. This section aims to preview the results obtained from these three main researches of Papadrakakis, Papadopoulos and Lagaros (1996); Hurtado and Alvarez (2001); Cardoso et al., (2008).

Papadrakakis, Papadopoulos and Lagaros (1996) proposed a new method employing both Monte Carlo Simulation and Neural Network to approximate the 'exact' prediction of the critical load factor and thus the exact probability of system failure (p_f). It is noted by Papadrakakis, Papadopoulos and Lagaros (2002) that the prediction of p_f is depended not only on the accuracy of the predicted critical load factor but also on the sensitivity of p_f in respect

97

to a slightly modified sample space of resistances. As shown in Figure 3-7 as the shaded area, the sensitivity is refined through the probability density distribution and the failure function on the unsafe side. In other expression, it is the ratio of the shaded area over the total area. It is noted that influencing by this sensitivity, there is always an error occurred in the analysing process, which is more pronounced in terms of low probability estimations. In this case, the low probability of failure is represented through the higher ratio of the shaded area in comparison to the total area. For this reason, it is often considered Importance Sampling techniques to decrease such ratio or to substantially reduce the error in the sensitivity making sure that the sampling is performed in an area with high probability.
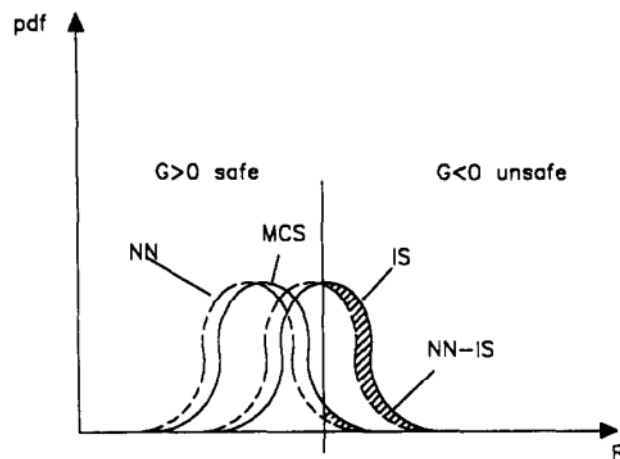
Source: Papadrakakis, Papadopoulos and Lagaros (1996)

Figure 3-7 Sensitivity of ρ_f prediction to different sample space of resistance

The proposed methodology includes the following features:

- The probability of failure is estimated using the Monte Carlo Simulation upon the data set produced with Importance Sampling technique

- The Neural Network model employed owns the back-propagation learning algorithm.

98

- The random variables are the loads act on the structure followed a Log-normal probability density function as well as yield stresses and plastic moduli associated with material and section properties followed a normal probability density function.

- The failure condition is when the entire structure collapses because of the successive formation of plastic nodes.

- Limit state analyses are considered 'exact' and are employ in producing the training pairs required for the Neural Network simulation.

In order to illustrate the feasibility of this methods in reliability analysis, there were three simple numerical case studies employed in this study – one plane frame and two space frames. All of these examples were investigated under the following limit state function expressing the limit state function as G(X), where $X = (X_1, X_2 \ldots X_n,)$ is the vector of the basic random variables:

$$p_f = \int_{G(x) \leq 0} f_x(X)\, \mathrm{d}X$$

Equation 3-16

in which $f_x(X)$ is the joint probability and G(X) is an irregular domain with highly non-linear boundaries. Following the law of large numbers, an unbiased estimator of the probability of failure is given by:

$$\bar{p}_f = \frac{1}{N} \sum_{i=1}^{N} I(X_i)$$

Equation 3-17

in which $I(X_i)$ is an indicator defined as:

$$I(X_i) = \begin{cases} 1 & \text{if } G(X_i) \leqslant 0 \\ 0 & \text{if } G(X_i) > 0 \end{cases}$$

Equation 3-18

In this regard, if considering N as independent random samples of a specific probability density function of the vector X, the failure function is computed for each sample X_i. In case, $G(X_i) \leq 0$, a successful simulation is counted and thus, Monte Carlo Simulation is performed in estimating the failure probability P_f in terms of sample mean in Equation 3-19, in which N_H is the number of successful simulations and N is the total number of simulations

$$\bar{p}_f = \frac{N_H}{N}$$

Equation 3-19

Papadrakakis, Papadopoulos and Lagaros (1996) gave three examples to express his ideas. The first test example is the five-storey plane frame with a unit load applied at the top and the load-displacement curve. The basic random variables are including external load (*Load*), yield stress of steel (σ_y) represented for the properties of the frame, and the plastic moduli of beams (Z_b,) and columns (Z_c,) are considered to be independent random variables. The second test example is the six-storey space frame Similar to the test case 1, the basic random variables are included external load (*Load*), yield stress of steel (σ_y), and the plastic moduli of five different types of beams and column (Z_1 to Z_5). The results for various number of simulations of Neural Network approximation under different neutrons of hidden layer are is measured against the difference between the predicted value and "exact" value, the smaller the error the better the architecture of training and learning networks. According, it is once again evidenced that the performance of the reliability analysis is much better in case of employing Importance Sampling. The third test example is the twenty-story space frame showing a more realistic problem in order to

100

validate the efficiency of the proposed approach of Monte Carlo Simulation and Neural Network in structural reliability analysis in regards of its accuracy and computing effort. Similar to the two previous examples, the results obtained from the analysis used Monte Carlo Simulation and Neural Network that indicates a remarkable agreement or minor errors between 'predicted values of critical load factor produced by learning and training process and "exact" value. In other word, the probability of failure of the twenty-storey space frame is relatively calculate with a very good agreement to the "exact" values. Such results evidence the earlier claim that the application of Monte Carlo Simulation based Neural Network to predict the structure failure probability is feasible regardless of the type and the scale of the structure as well as on the smoothness of the load displacement curve. This methodology thus can be implemented to accurately predict the probability of failure for even large and complex structural systems at a fraction of computing time.

Citing the work of Papadrakakis, Papadopoulos and Lagaros (1996) as the main reference to prove the feasibility of employing the Monte Carlo Simulation and Neural Network in structural reliability analysis, Hurtado and Alvarez (2001) provided further evidence on the application of this methodology in practice towards scomparisons with respect to the following issues: *Network types*: (1) multi-layer perceptrons (MLP) and (2) radial basis functions classifiers (RBF); *Learning algorithm*: (1) back-propagation with variable learning rate and momentum (BPX), (2) Gauss-Newton-Levenberg-Marquardt (GNLM), (3) Newton-Raphson-Levenberg-Marquardt (NRLM) with employment of (1) exact algebraic (EA) and (2) least squares (LS); *Cost functions*: (1) sum of square errors (SSE) and cross-entropy (CE); *Sampling procedure*: (1) random number generation from the actual distribution functions of the basic variables (CDF) and (2) from uniform distributions of the basic variables with k standard deviation about the mean (UN); *Purpose of NN use*: (1) functional approximation (FA) and data classification (DC). The comparative study was performed over four examples as: a single

101

and explicit nonlinear limit state function; a multiple, linear and explicit limit state function; an implicit, nonlinear limit state function for an elastic frame; and an implicit, nonlinear limit state function for a plastic plane structure under dynamic load. It can be observed that the use of Neural Network for data classification (DC) is more prone to error than the functional approximation (FA) option. It can be seen that the networks based on the former are not as accurate as those using the SSE error function. Accordingly, it can be concluded that the use of Neural Network for functional approximation (FA) seems to be better in performance rather than the approach inspired by pattern recognition tasks. The performance of radial basic function (RBF) network is clearly superior to multi-layer perceptions (MLPs) network on the basic of not only their accuracy but also their stability. In fact, the errors of the RBF algorithm are several orders of magnitude lower than those of the MLPs. The RBF network with the last-squares (LS) approach requires much more computation time in comparison to that with the exact algebraic (EA) algorithm. Moreover, the superiority of the GNLM method for training over the BPX is also confirmed. For all network models, the sum of training and production times is much less than the time required by standard Monte Carlo Simulation to calculate the failure probability. This support the proposal of Papadrakakis, Papadopoulos and Lagaros (1996) about the possibility of remaining several networks for applying the procedure sketched above without serious increase of the total computation time. Moreover, if this is not desired and a single network were to be used, the relative advantage over standard Monte Carlo would be much higher in this respect. Moreover, this study also supported the claim of Papadrakakis, Papadopoulos and Lagaros (1996) towards the application of Importance Sampling Technique as an effective variance reduction method, not only as an independent technique, but also in combination with other strategies, such as DC and as a basic for building more sophisticated ones intended to cope with multiple limit states. In accordance to Hurtado and Alvarez (2001), The difference between the IS and RBF methods lies in that, while the former is aimed at

102

sampling with a localized density, whose position and parameters require an exploratory sampling, the RBF technique privileges the points located near each centre, which can be located anywhere. This suggests that a good combination for further reducing the number of finite element solver calls is to combine these two methods by establishing a further privilege to those RBF centres having a high probability content in the failure region, as the IS method does.

Further developed the work of Papadrakakis, Papadopoulos and Lagaros (1996) and Hurtado and Alvarez (2001), Cardoso et al. (2008) provide a verification towards the case study of the single bay steel frame in regards of the systematic reliability analysis. Applied actions (dead load, live load and wind) are defined according to the Eurocode 1 (1994), and the steel structure is designed according to the Eurocode 3 (1992). The Neural Network used in this study is multi-layer perceptron's (MLPs) with the structure of input, hidden and output layers namely s^0, s^1 and s^2 respectively. The number of input neurons is equal to the number of random variables that influence structural response. For each limit state function considered, the corresponding probability of failure was compared to that obtained using conventional MCS (without NN), with computation of internal forces by finite elements for each sample of the set of random variables. These probabilities were also evaluated using FORM and SORM methods, built in the program COMREL-TI (1992). The results for all alternative techniques show a very good agreement between the methodology proposed by the authors and the other procedures considered. For this example, the application of conventional MCS took 6524 seconds, which is much longer than the values when NN were adopted. However, it is important to stress that a substantial amount of time involved in a NN based procedure is spent in the training phase. Consequently, a comparison based uniquely in the time consumed during the simulation phase can be misleading.

103

These three papers present the evidences towards the feasibility of applying Monte Carlo based Neural Networks to the reliability analysis of large and complex structural systems at a fraction of computing time. In summary, the entire concept has the following features as reported by Papadrakakis et al. (1996).:

- The use of Neural Networks can practically eliminate any limitation on the scale of the problem and the sample size used for Monte Carlo Simulation provided that the predicted critical load factors, corresponding to different simulations, fall within acceptable tolerances.

- A Back Propagation Neural Network algorithm is successfully used to produce approximate estimates of the critical load factors, regardless the size or the complexity of the problem, leading to very close predictions of the probability of failure. Moreover, training samples, required to train the Neural Network, appear to be independent on the type of structure or the type of the required analysis.

- The use of Monte Carlo Simulation with Importance Sampling leads to considerable improvement in Neural Network prediction of the probability of failure. This is due to the fact that using the Importance Sampling technique the sensitivity of p^r with regard to the modified sample space of critical load factors, displayed by Neural Network predictions, is reduced leading to more accurate estimates.

It is therefore clearly stated that the methodology presented could be implemented for predicting accurately and at a fraction of computing time the probability of failure of large and complex structures. However, the examples given in the literature has been seen as relatively simple that does not reflect the real structure behaviour. Taking interests into the field, the proposed study aims to update the current work by provide a further evidence to support the

application of Monte Carlo Simulation based Neural Network with Importance Sample in the system reliability analysis

3.3   Research Gap in System Reliability Analysis under Blast Loading

Blast load due to accidents or terroristic attacks cannot be forecasted in a deterministic way. The effects of blast loading on structures can be very dangerous, damages and failures are expected with serious treats to structural safety and human life (Low and Hao, 2002; Shi and Stewart, 2015; Acito et al., 2011). Therefore, design procedures that consider explosion load must take into account the randomness of the threatening and of the load scenario. Added to this, Du and Li (2009) pointed that materials stresses and strains are often pushed to the limit and the modelling of these phenomena can be very complex. In this sense, it is not possible to assess the mechanical characteristics of materials in a deterministic way, thus, in consideration of the randomness of these parameters, the structural response assumes a probabilistic nature, making it necessary to look at reliability analysis (GuhaRay et al., 2018; Wu et al., 2020). The probabilistic approach to structural reliability in the case of a blast load is a current topic in structural engineering.

As it is difficult to predict the probability of occurring and the magnitude of extreme events, it is neither practical nor possible to design a structure against them through the traditional methods for conventional loads (Stochino, 2016; Charitha et al., 2018). Present-day design standards instead try to minimise the risk and provide a minimum level of control over progressive collapse by incorporating in the codes the design concept of robustness as the insensitivity of a structure to local damage. By contrast, the insensitivity of a structure to abnormal events is referred to as collapse resistance. According to this concept, no action is taken against the extreme event itself, as this risk cannot be eliminated, but the aim is rather to control its consequences.

Analysis methods used to evaluate the possibility of progressive collapse vary widely, ranging from the simple two-dimensional linear elastic procedure to complex three-dimensional nonlinear time history analysis (Rajkumar et al., 2020). The alternate load path method requires an assessment of the capacity of a frame to redistribute load away from damaged members. Accordingly, there is a requirement for the engineer to consider the most suitable analytical procedure, model complexity and design assumptions within the constraints of expense, computing power and time. In literature, there are five procedures used to perform such an analysis namely (1) linear static analysis using dynamic load factors; (2) non-linear static analysis using dynamic load factors; (3) non-linear static pushover analysis (energy balance procedure); (4) linear dynamic analysis; (5) non-linear dynamic analysis. In regards of Byfield et al. (2014), linear methods require the material response to remain in the elastic range and second-order (P – delta) effects and instabilities to be ignored. This limits their use to small displacements and often leads to conservative design in order to prevent invalidating the assumptions. Non-linear methods include material plasticity and are able to account for geometric non-linear effects as they become more significant; they also have the potential to allow for the development of alternative load path mechanisms, such as arching action or catenary action (Figure 3-8).
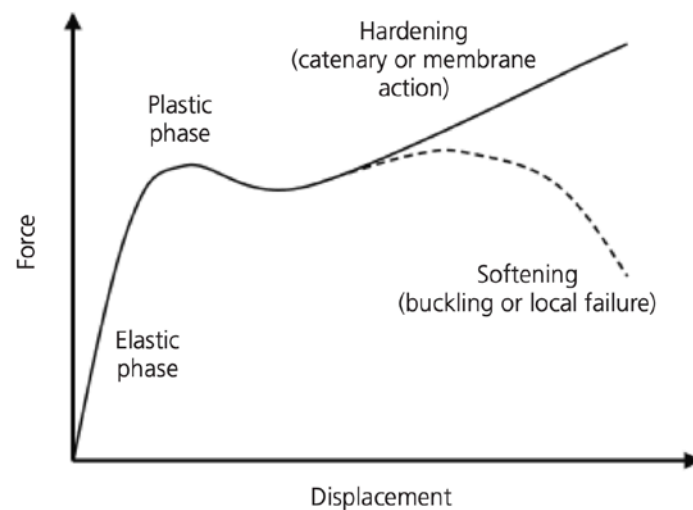
Figure 3-8 Non-linear response in beams subjected to double span loading following loss of support to a column

The US General Service Administration guidelines (GSA, 2003) advise the use of three-dimensional analytical models subject to a linear elastic or static analysis procedure, but two-dimensional models may also be used. An additional guide for preventing progressive collapse is the US Department of Defence (DoD, 2009) that incorporates flow charts to check if the structure requires progressive collapse design, the level of which is related to the occupancy category of the structure. If it is found necessary to design for progressive collapse, numerous methods are outlined which employ tying forces, alternative load paths, enhanced local resistance or a combination of all three. Both the DoD and GSA guidelines use the load and resistance factor design approach with factors obtained from the ASCE/SEI design guidance to aid designers in avoiding progressive collapse; however, the DoD guidance also provides a tie force procedure to allow large deformations through catenary action (Ellingwood et al., 2009).

In this context, Grierson et al. (2005a; 2005b) presented a progressive-failure analysis procedure to evaluate the performance of a building framework after it has been damaged by unexpected abnormal loading that its computational model allows the incremental analysis to

107

proceed beyond loading levels at which structural instabilities occur, including the formation of plastic collapse mechanisms and the disengagement of members from the building superstructure. Fu (2013) proposed a 3-D numerical model with the direct simulation of blast load to investigate the corresponding dynamic response of structure in purpose of studying the real behaviour of a 20-storey tall building under the blast loading of a typical package bomb charge of 15 kg was detonated on the 12th floor. Kim and Kim (2009) investigated the progressive collapse-resisting capacity using alternate path methods recommended in the GSA and the Department of Defense (DoD) carried out both linear static and nonlinear dynamic analysis. The obtained results show that linear procedure provided more conservative decision for progressive collapse potential of model structures. This study added as the nonlinear dynamic analysis for progressive collapse analysis does not require modelling of complicated hysteretic behaviour, it may be used as more precise and practical tool for evaluation of progressive collapse potential of building structures. Similar research was done by Marjanishvili and Agnew (2006) that compared four methods for progressive collapse analysis by analysing a nine-story steel moment-resistant frame building, employing increasingly complex analytical procedures: linear-elastic static, nonlinear static, linear-elastic dynamic, and nonlinear dynamic methodologies. This study demonstrated that dynamic analysis procedures not only yield more accurate results, however, are also easy to perform for progressive collapse determination. In addition, the results, show that current GSA performance limits for linear analysis procedures are unconservative, meaning that a structure designed with acceptable linear evaluation criteria may exceed allowable ductility and rotation limits when nonlinear dynamic analysis is performed on the same structure. Similar approach was employed by Cai et al. (2012) specifically for a case study of a cable-stayed structure. The results indicate that for static and dynamic analyses, there is large difference between the results obtained from simulations starting with either a deformed or a nondeformed configuration at

108

the time of cable loss. The static results are conservative in the vicinity of the ruptured cable, but the dynamic effect of the cable loss in the area farther away from the loss-cable cannot be considered. Moreover, the dynamic amplification factor of 2.0 is found to be a good estimate for static analysis procedures, since linear static and linear dynamic procedures yield approximately the same maximum vertical deflection. Byfield et al. (2014) provided an exclusive literature review on progressive collapse and summarised their advantages and disadvantages in Table 3-2. Abdelwahed (2019) noted that the simplest analysis methodology is static linear elastic analysis, and the most exhaustive procedure is nonlinear dynamic analysis, which yields more accurate results. Added to this, linear static and dynamic analysis cost the least time, compared to nonlinear static analysis; yet, linear elastic methods are notoriously inaccurate to describe the response of a damaged system. Instead, researchers have generally favoured the use of nonlinear static models and accounted for the dynamic effects that result from the sudden release of energy using a very conservative dynamic amplification factor applied on the total loads.

Table 3-2 Comparison of progressive collapse procedure capabilities

	Linear static DLF	Non-linear static DLF	Non-linear static pushover	Linear dynamic	Non-linear dynamic
Include material plasticity	✗	✓	✓	✗	✓
Account for strain hardening	✗	✓	✓	✗	✓
Include second-order (P–delta) effects	✗	✓	✓	✗	✓
Negates the use of dynamic load factor	✗	✗	✓	✓	✓
Explicitly account for strain-rate material effects	✗	✗	✗	✗	✓
Account for damping	✗	✗	✗	✗	✓
Allowable in GSA (2003)	✓	✓	See note[a]	✓	✓
Allowable in US DoD (2009)	✓	✓	See note[a]	✗	✓

Moreover, Adam et al. (2018) pointed out an inadequacy of current design methods for progressive collapse resistance. For example, current design codes are based on the consideration of local instead of global failure. Global structural safety against the collapse of the entire system or a major part of it is a function of the safety of all the elements against local

109

failure. The second shortcoming of current design methods is that low-probability events and unforeseeable incidents are not taken into account. And most importantly, the probabilistic concept requires the specification of acceptable failure probabilities. Up to recent, the target failure probabilities of probabilistic design codes have been derived from previous deterministic design codes. Taking into account that a potential progressive collapse can entail huge losses, it would be difficult to reach consensus from the society on acceptable value for the probability of progressive collapse.

4   Proposed System Reliability Analysis using MCS and NNs

In reliability assessment of structures, there are two levels of reliability analysis required to consider including (1) structural members reliability and (2) system reliability. The former is originated through the failure of a particular component that partial local reliability in a structural system might possibly cause loss of serviceability. However, it is argued by many researchers that structural system is often designed to possess a high level of redundancy making its collapse to occur most likely because of the combined effect of several different failure modes rather than only one particular member (Byun and Song, 2017). For this reason, it is important to consider both structural member and system reliability in reliability analysis of the structural failure.

Almost all existing literature in the field of structural reliability are focused on the structural member reliability with little attention paid to the system reliability (Chun, Song and Paulino, 2015; Okasha, 2016). Although recently, there have been some research devoted to system reliability, the accuracy of their assessment is not satisfactory, which is due to the fact that these models developed to assess reliability are often assumed to be in linear or weakly nonlinear performance functions (Chang and Kopsaftopoulos, 2015).

For this reason, the objective of this paper is to propose an approach employing Monte Carlo Simulation and Neural Network to effectively calculate the system reliability of the structural system, which is considered as the first approach ever proposed to solve the problem of structural system reliability.

In order to determine the structural system reliability, the proposed method contains the two main stage. In the first stage, the β-unzipping method (introduced by Thoft-Christensen and Murotsu, 1986) is employed to determine reliability analysis of structural systems at different level such as Level 0 (focusing on single structural element), Level 1 (considering the

111

structural system comprises of serial structural members), Level 2 (on the basic of a system where the elements are parallel to each other- with critical pairs of failure elements), and Level 3 (on the basic of a system where the elements are parallel systems each - with critical triples of failure elements). In the second stage, the Monte Carlo Simulation with Importance Sampling is first employed to general the sample population, which will be then used to train, test and predict the system reliability of the structure using machine learning approach based on Back-Propagation Neural Network Algorithm.

The proposed method was validated against the estimation using conventional β-unzipping method. The results indicate the closed and yet more accurate reliability index and failure probability of the structural system in consideration of its system reliability analysis. This study is thus moving further by demonstrating the whole process of application of Monte Carlo Simulation with the Importance Sampling Techniques and Neural Network with Back-Propagation Algorithm towards the case study of a CFTA girder. The promising results indicate the potential of employing the proposed method to solve the complex problem of the structural system reliability.

In summary, the proposed method of applying Monte Carlo Simulation into the estimation of structural system reliability has the following stages:

- Stage 1: Developing a computerised method for the system reliability analysis
- Stage 2: Estimating the structural system reliability at different level – demonstrated in this study level 0, level 1 and level 3
- Stage 3: Generating the sample population by Monte Carlo Simulation with the response surface of the reliability indexes obtained from Step 2. The probabilistic constrains check is also performed in this step.

- Stage 4: Training and testing the population formed in Step 3 using Neural Networks using Back-Forwards algorithm.

- Stage 5: Integrating data collected from Step 4 in respect to the current codes and standards
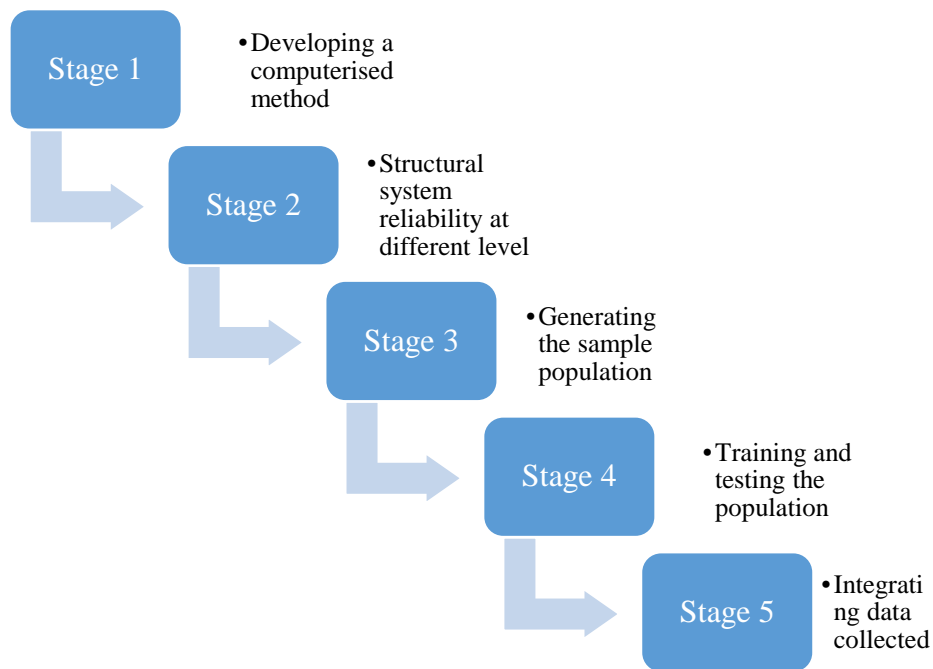
Figure 4-1 Research stage

4.1 Modelling of Structure

The modelling of structure to estimate its system reliability used in this study is based on a basic assumption that it is possible to accurately and sufficiently estimate the total reliability of the structural system through first dominating considerations of a finite number of failure modes and then combining such modes into a complex reliability systems. β-unzipping method is used as the primary method to identify the dominant (or significant) failure modes. Added to this, only truss and frame structures (two-dimensional – plane - as well as three-dimensional – space - structures) are considered, although the methods used can be extended to a broader class of structures.

Another assumption in modelling of structure system is that it contains a finite number of bars and beams those are connected to each other's by a finite number of joints. Accordingly, the structural system reliability is generated through modelling the failure elements with their connections to the structural elements (bar, beam and joint). In this respect, Figure 4-2 demonstrates the model for each of structural elements with its number of different failure modes including failures due to bending at its left end, midpoint and right end as well as failure in tension/compression caused by the axial force and failure due to large deflection at the midpoint.
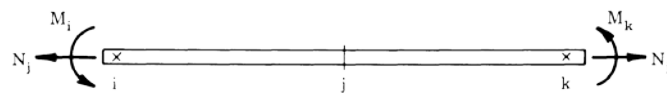
Figure 4-2 Modelling of element

Each failure mode results in element failure, but systems failure will in general only occur when a number of simultaneous element failures occur. With above-mentioned assumptions, the structural system reliability is generated through modelling the entire system as a series system, where each of its elements are critical failure modes, in which, each of the failure modes is modelled as parallel system.

The modelling used in this study for system reliability analysis is considered a certain uncertainty namely:

- Physical uncertainty such as loads, material properties, and dimensions, which is always be associated with a certain variability. In this study, due to the unexpected explosion, only blast loading with its own variables is considered as physical uncertainty.

- Statistical uncertainty mostly reflects the sample data such as distribution parameters. In this study, the statistical uncertainty is considered when employing Monte Carlo Simulation to generate the sample population from analytical data achieved through Finite Element Model.

- Model uncertainty due to difference between mathematical modelling of a structural system and the real structure as result of a number of simplifications and idealizations. In this study, the model uncertainty is not taken into account

It is well acknowledged in this study that there are several failure modes obtained for each structural element and thus, each element of the structural system possibly has several falure elements. It is also well noted that the structural system reliability depends on the fact that its elements are either brittle or ductile element (or having some third characteristic). However, this study considers the behaviour of the structure system at the mechanics level and thus, in which the mechanical behaviour e.g. the constitutive relations is the most importance in estimation of the structural system reliability is the mechanical behaviour (Thoft-Christensen and Murotsu, 2012). Accordingly, this study assumes the two main type of failure elements: perfectly brittle failure element and perfectly ductile failure element as shown in Figure below.

(a) Perfectly brittle failure element

Figure 4-3 Assumption on the failure of element

This study modelled the real structure through two fundamental types of systems, namely series systems and parallel systems. The reliability of a structural system is estimated on the basic of a modelling by a series system where the elements in the series system are parallel systems as shown in Figure 4-4.
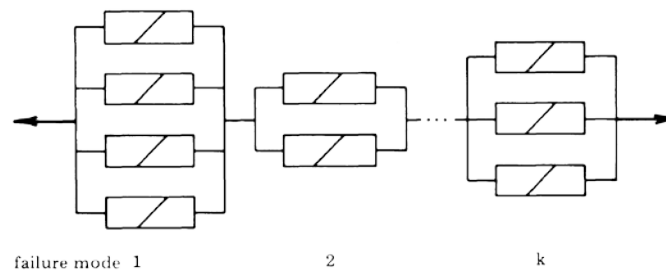
Figure 4-4 Modelling of structural system

In the first stage presented earlier for the proposed method - developing a computerised method for the system reliability analysis, there are four modules required to be developed in order to computerise the system reliability at different levels namely: the general intact structure module, damaged structure module, reliability analysis module, and system reliability analysis module. In the process of estimating the structural system reliability, these modules are actually linked to each other, in the sense that results obtained from one module will be exported to another module as its input data to be performed, as clearly demonstrated in Figure 4-5

116
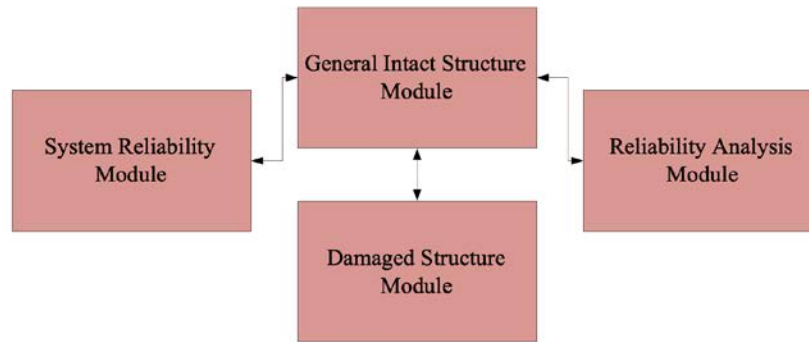
Figure 4-5 Flowchart for a computerised system reliability analysis

- *General intact structure module:* this module plays a central hub as illustrates from the Figure linking to other modules to receive and send data to/from other modules. As it is where the undamaged structure is defined, the general intact structure module includes all structural related information such as geometrical definitions, structural components and its variables (node, element, resistance, boundary condition) as well as their orientations, along with internal and external forces etc. The finite element analysis represented the structure is performed using the general intact structure module in purpose of finding the critical elements on the basic of providing unzipping criteria. Accordingly, the bounds to determine the system reliability is defined as well as the correlation matrix between the equivalent safety margins of the elements of the parallel-series system is developed.

- *Damaged structure module:* in a process of identifying the structural system reliability, there is a need to develop a modified structure by removing the most critical failure elements from the structure and replacing them with the equivalent fictious loads in consideration of its post-failure capacity. The damaged structure module is developed in order to serve this purpose to respect the damaged state of the structure. To model a certain structural damaged state, it is to insert the axial hinges as well as to replace the

117

failed element by its post-failure capacity. Accordingly, the axial hinge is modelled on the basic of the failure types and modes of the failure elements.

- *Reliability analysis module:* this module is used to estimate the reliability on the basic of those data collected either from the damaged modules or the general intact structure modules. In this study, the FORM reliability analysis method is selected to perform the reliability analysis. It is noted that the reliability analysis module is also employed to estimate the system reliability analysis at a component level.

- *System reliability module:* this module is employed in purpose of calculating the system reliability modelled as a series system that each of its elements is a parallel system. As each parallel system is formed through two (pair) or three (triple) critical elements, the data needed to collect from the general intact structure module for this system reliability module is included the reliability index values and the sensitivity coefficients. Accordingly, the results obtained from such module are expected as the reliabilities of each individual parallel system and its equivalent safety margin (equivalent sensitivity factors)

4.2 Structural System Reliability

Stage 1 in the proposed method of estimating structural system reliability analysis is to estimate the structural system reliability at different levels – demonstrated in this study level 0, level 1 and level 3. To obtain this target, the following procedure is outlined with the application of those designed modules discussed in the previous section.

- Step 1: Analysing the intact structures as well as calculating the reliability indices for each individual component (failure element) of the structures.

- Step 2: Defining a set of critical elements through a consideration of those elements with their reliability indices within the lower and upper bounds. To be specific, it should

be within the interval $[\beta_{min}, \beta_{min} + \Delta\beta_1]$ that $\Delta\beta_1$ stands for a value (arbitrarily selected) and β_{min} stands for the smallest reliability index amongst the group of the failure elements obtained through intact structures observed in earlier step.

- Step 3: Removing the most critical failure elements from the structure and replacing them with the equivalent fictious loads in consideration of its post-failure capacity. It is noted that in case of brittle elements, there is no fictitious to be added into the modified structure.

- Step 4: Performing a stochastic finite element analysis of the modified structure defined in the previous step and calculating the reliability indices for the structure at its new modified position.

- Step 5: Repeating Step 2 in defining a second set of critical failure with the reliability values within the internal $[\beta_{min}, \beta_{min} + \Delta\beta_2]$ that $\Delta\beta_1$ stands for a value (also arbitrarily selected) and β_{min} stands for the smallest reliability index amongst the group of the failure elements obtained through the modified structure..

- Step 6: Pairing the critical failure elements found in Step 5 with those obtained from Step 2 in purpose of forming a set of parallel systems

- Step 7: Repeating the process from Step 3 to Step 6 for the rest of the critical failure elements determining from Step 2 in purpose of obtaining more critical pairs of failure elements

- Step 8: Obtaining a calculation of the system probability for each of individual critical pairs of failure elements found earlier in Step 7 as well as estimating the corresponding safety margin

- Step 9: Determining the correlations between different set towards the estimated safety margins of the critical pairs of failure elements (expected outcome is the correlation matrix of coefficients for the elements of the series system)

- Step 10: Calculating the system reliability if the series system with data found in Step 8 and Step 9 to define the upper and lower bounds suggested by Ditlevsen

Calculate component

Define critical elements

Set equivalent fictious loads

Level 1

Level 2

Calculate structural reliability

Form parallel systems

Determine correlation

Estimate system reliability
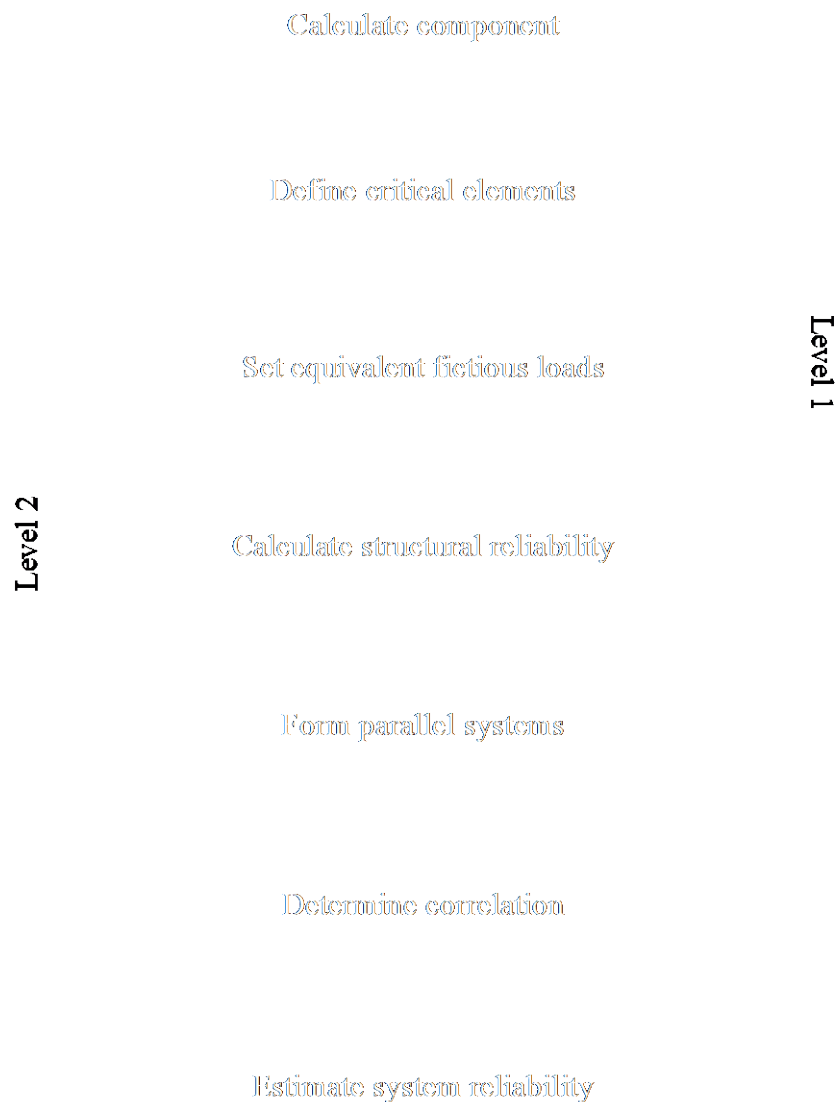
Figure 4-6 Steps taken in Stage 1

The following section will detail these 10 steps in estimating structural system reliability by the structure modelling at different levels.

4.2.1   Probability of Failure in Structural System

This research attempt to analyse the reliability of the structure using the non-linear response surface method introduced by Thoft-Christensen and Murotsu (2012), which was found efficient to obtain the probability of failure as non-probabilistic reliability theory.

To illustrate the systems reliability analysis considered a structural element or structural system with two potential failure modes defined by safety margins $M_1 = f_1(X_1, X_2)$ and $M_2 = f_2(X_1, X_2)$, where X_1 *and* X_2 are standardized basic variables. The corresponding failure surface and reliability indices β_1 and β_2 are shown in Figure below.

Realizations (x_1, x_2) in the dotted area ω_f will result in failure, and the probability of failure P_f is equal to:

$$P_f = \int_{\omega_f} \varphi_{X_1, X_2}(x_1, x_2; 0) d\bar{x}$$

Equation 4-1

where φ_{X_1, X_2} is the bivariate normal density function for the random vector $X = (X_1, X_2)$. Let $\beta_2 < \beta_1$, and assume that the reliability index β for the considered structural element or structural system is equal to the shortest distance from the origin 0 to the failure surface, i.e. $\beta = \beta_2$. Estimating the probability of failure by the formula

$$P_f \approx \Phi(-\beta) = \Phi(-\beta_2)$$

Equation 4-2

will then correspond to integrating over the hatched area (the right of the tangent t_2). Clearly the approximation will in many cases be very different from the exact P_f calculated. It is

121

therefore of great interest to find a better approximation of P_f, and then define a reliability index β by

$$\beta = - \ \Phi^{-1} (P_f)$$
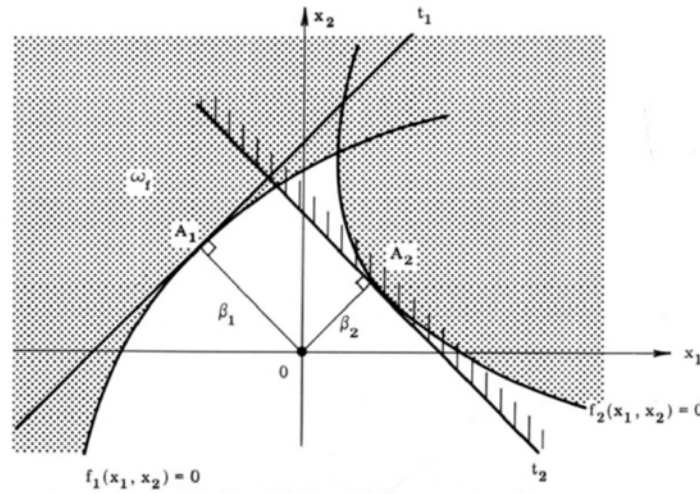
Source: Thoft-Christensen and Murotsu (2012)

Figure 4-7 Corresponding failure surface and reliability indices

Let the random variable R_i be the strength of the series system in Figure 2-1, and let R_i be a random variable describing the strength of failure element i, where $i = 1, ... , n$. Further, let a load r on the series system result in a load effect r_i in failure element i, $i = 1, ... , n$ and let F_R be the distribution function for the random variable R, $i = 1, ... , n$. Then the distribution function F_R for the random variable R is given by

$$F_R(r) = P(R \leqslant r) = 1 - P(R > r) = 1 - P((R_1 > r_1) \cap (R_2 > r_2) \cap ... \cap (R_n > r_n))$$

$$= 1 - (1 - F_{R_1}(r_1))(1 - F_{R_2}(r_2)) ... (1 - F_{R_n}(r_n)) = 1 - \prod_{i=1}^{n}(1 - F_{R_i}(r_i))$$

122

Equation 4-4

where it is assumed that the strengths R_i, $i = 1, ... , n$, are independent random variables.

Let the series system be loaded by a random load S with the density function f_s. Then the probability of failure P_f for the series system is:

$$P_f = \int_{-\infty}^{\infty} F_R(r) f_S(r) dr = 1 - \int_{-\infty}^{\infty} \prod_{i=1}^{n} (1 - F_{R_i}(r_i)) f_S(r) dr$$

Equation 4-5

where the same notation as in previous equation has been used. A formal reliability index β_s for the series system can now be calculated by:

$$\beta_S = -\Phi^{-1}(P_f)$$

Equation 4-6

If each elements of the parallel system defined in Figure 2-2 is ductile then the strength R of the fibre bundle (the parallel system) is simply determined by

$$R = \sum_{i=1}^{n} R_i$$

Equation 4-7

where the random variable R_i is the strength of fibre i, $i = 1,2, ... , n$. Note that when the random variables R_i are independent and normally distributed $N(\mu_i, \sigma_i)$ then R is also normally distributed $N(\mu_i, \sigma_i)$ with

123

$$\mu_R = \sum_{i=1}^{n} \mu_i$$

$$\sigma_R^2 = \sum_{i=1}^{n} \sigma_i^2$$

<div align="right">**Equation 4-8**</div>

However, even when R_i, $i = 1,2, \dots , n$ is non-normally distributed the distribution of R will according to the central limit theorem be close to normal, if n is not too small.

In a real structure with low degree of redundancy, it is likely that brittle failure of one structure element will result in subsequent failure of other elements. The estimate of the reliability of a structural system should consist of the following steps:

- Evaluating the probability of failure of each parallel system

- Evaluating the correlations between the parallel systems by introducing an equivalent linear safety margin for each parallel system

- Evaluating the probability of failure of the series system

Probability of Failure $P_{f,i}$ of Failure Element i

Assume that a transformation $\bar{Z} = \bar{T}(\bar{X})$ by which the basic variables $\bar{X} = (X_1,\dots,X_n)$ are transformed into independent standard normal variables $\bar{Z} = (Z_1,\dots,Z_n)$ exists so that

$$P_{f,i} = P\left(M_i \leq 0\right) = P\left(f_i\left(\bar{X}\right) \leq 0\right) = P\left(f_i\left(\bar{T}^{-1}\left(\bar{Z}\right)\right) \leq 0\right) = P\left(h_i(\bar{Z}) \leq 0\right)$$

<div align="right">**Equation 4-9**</div>

where h_i is defined by (15). An approximation of $P_{f,i}$ can then be obtained by linearization of h_i in the design point

$$P_{f,i} = P\left(h_i(\overline{Z}) \leq 0\right) \approx P\left(\overline{\alpha}_i^T \overline{Z} + \beta_i \leq 0\right)$$

<div align="right">**Equation 4-10**</div>

where $\overline{\alpha}_i$ is the unit normal vector in the design point and β_i the reliability index. The equation (16) can be written

$$P_{f,i} \approx P\left(\overline{\alpha}_i^T \overline{Z} + \beta_i \leq 0\right) = P\left(\overline{\alpha}_i^T \overline{Z} \leq -\beta_i\right) = \Phi(-\beta_i)$$

<div align="right">**Equation 4-11**</div>

where Φ is the standard normal distribution function.

Probability of Failure P_{f_s} of a Series System

Consider a series system with n elements. Then, with the same notation as above, the probability of failure of this series system can be estimated in the following way

$$P_{f_s} = P\left(\bigcup_{i=1}^{n}\{M_i \leq 0\}\right) = P\left(\bigcup_{i=1}^{n}\{f_i(\overline{X}) \leq 0\}\right) = P\left(\bigcup_{i=1}^{n}\{f_i\left(\overline{T}^{-1}(\overline{Z})\right) \leq 0\}\right)$$
$$= P\left(\bigcup_{i=1}^{n}\{h_i(\overline{Z}) \leq 0\}\right) \approx P\left(\bigcup_{i=1}^{n}\{\overline{\alpha}_i^T \overline{Z} + \beta_i \leq 0\}\right) = P\left(\bigcup_{i=1}^{n}\{\overline{\alpha}_i^T \overline{Z} \leq -\beta_i\}\right)$$
$$= 1 - P\left(\bigcap_{i=1}^{n}\{\overline{\alpha}_i^T \overline{Z} \leq -\beta_i\}\right) = 1 - P\left(\bigcap_{i=1}^{n}\{-\overline{\alpha}_i^T \overline{Z} < \beta_i\}\right) = 1 - \Phi_n(\overline{\beta}; \overline{\overline{\rho}})$$

<div align="right">**Equation 4-12**</div>

where the same transformation $\overline{T}$ as in probability of failure element is used and where $\rho_{ij} = \overline{\alpha}_i^T \overline{\alpha}_j$. Φ_n is the n-dimensional standardized normal distribution function.

Probability of Failure P_{f_p} of a Parallel System

125

Consider a parallel system with n elements. Then, with the same notation as above, the probability of failure of this parallel system can be estimated in the following way

$$
\begin{aligned}
P_{f_p} &= P\left(\bigcap_{i=1}^{n}\{M_i \le 0\}\right) = P\left(\bigcap_{i=1}^{n}\{g_i(\bar{X}) \le 0\}\right) = P\left(\bigcap_{i=1}^{n}\left\{g_i\left(\bar{T}^{-1}\left(\bar{Z}\right)\right) \le 0\right\}\right) \\
&= P\left(\bigcap_{i=1}^{n}\{h_i(\bar{Z}) \le 0\}\right) \approx P\left(\bigcap_{i=1}^{n}\{\bar{\alpha}_i^T \bar{Z} + \beta_i \le 0\}\right) = P\left(\bigcap_{i=1}^{n}\{\bar{\alpha}_i^T \bar{Z} \le -\beta_i\}\right) \\
&= \Phi_n(-\bar{\beta}; \bar{\bar{\rho}})
\end{aligned}
$$

Equation 4-13

where the same transformation $\bar{T}$ as in probability of failure element is used and where $\rho_{ij} = \bar{\alpha}_i^T \bar{\alpha}_j$.

4.2.2 System Reliability Analysis

The β-unzipping method is employed in this the study as to help to overcome the high load of computational efforts by identifying only failure elements with high element probabilities of failure or so-called critical failure elements. The *β*-unzipping method is a method by which the reliability of structures can be estimated at a number of different levels. The aim has been to develop a method which is at the same time simple to use and reasonably accurate. The *β*-unzipping method is quite general in the sense that it can be used for two-dimensional and three-dimensional framed and trussed structures, for structures with ductile or brittle elements and also in relation to a number of different failure mode definitions.

This study follows what was suggested by Ditlevsen and Kounias for upper and lower bounds of that is so-called Ditlevsen bounds. At the level of random variables, the treatment of non-Gaussianity is well known: thus, the classical Rosenblatt transformations to handle multivariate non-Gaussian random variables have been discussed in detail. Non-Gaussian random variable models for system parameters in the context of single degree of freedom (sdof)

126

dynamical systems or individual structural elements of built-up vibrating structure have been consider. Added to this, Ditlevsen has indicated the usefulness of Bayesian decision theory for treatment of mechanical model uncertainties. Ditlevsen pointed out that a best criterion is not sufficient as the basis for choosing distribution models for reliability analysis. Instead, it is argued that standardizations of distribution types need to be imposed on alternative designs if estimated reliabilities need to be compared.

It is noted that in this study, to reduce the computational effort, the estimation of the failure probability for the series system with n elements is done by only taking into account some of the failure elements, those are with the smallest reliability indices. For a structure with n failure elements, it is considered as sufficient accuracy at system modelling level 1. At level 2, the system modelling is presented with a series system, where each of its elements is presented as a parallel system of two failure elements on its own. The estimation of the system reliability analysis at this level is done by removing the most critical elements, those with the reliability indices within the unzipping interval) from the structure one at a time and then replacing such elements with a set of fictitious loads represented their post-failure capacities (in this study considered as ductile or semi-ductile failure).

Any system reliability analysis performed in this study is under a basic assumption of normal distribution for all the input basic random variables. Accordingly, to define load and resistance (yield moment, tension/compression strength), there is a need to take into account not only mean and standard deviation of all basic variables along with the correlation coefficients. Moreover, there is a must to also identify potential yield hinges and structural elements, where failures in tensions/compressions occurred as shown:
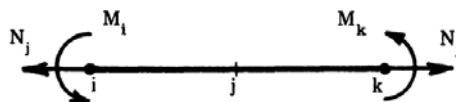
Figure 4-8 Failure elements and sign convention for axial forces and bending moments

Added to this, all geometrical quantities are presumed as deterministic in consideration that any geometrical uncertainty is negligible comparing to variables of loading and strengths. For the purpose of validating the proposed approach, only static behaviour is performed as the structures are considered as a fixed point; adding with an assumption that all elasticity coefficients are deterministic. Later in this study, the dynamic behaviour of the structure (CFTA girder) is considered. It is noted that the β-unzipping method presented in this study is applied for only truss and frame structures but can possibly be employed for other types of structures with reasonable modifications. For the statistic behaviour of structural systems, either failures of pure tensions or compressions or failures or failures of pure bending are assumed for the failure of the structural elements. The β-unzipping method employed is also to take into account the combined failure criteria. It is noted that to reduce the computational work, it is importance to keep the number of these so-called failure elements (checking points) as low as possible but still guarantee the accuracy in performing the structural system analysis.

Following Thoft-Christensen and Murotsu (1986), the structural system modelling of this study is presented at different levels – mainly level 0, level 1 and level 2. At system modelling level 0, each element is considered individually that with n failure elements and the probability of each corresponding element is P_{fi}, $i = 1, 2, …, n$. The probability of failure at level 0 is:

$$P_{f_S} = \max_{i=1}^{n} P_{f_i}$$

and the reliability of the structural system at level 0 is:

$$R = 1 - P_{fs}$$

128

At level zero the system reliability is assumed to be equal to the reliability of a component with the lowest reliability index. This means that only a component-level reliability analysis of the intact structure is required.

The structural system reliability analysis using β-unzipping method starts by determining the coefficient of influence of each individual relevant force and moment. Assuming that the structural forces are the concentrated loads presented by P_j, $j = 1, 2, ... , k$ and a stochastic variables described the load-effect (force or moment) of each individual element is presented by P_i, $i = 1, 2, ... , k$.

$$S_i = \sum_{j=1}^{k} a_{ij} P_j$$

<div align="right">**Equation 4-14**</div>

where the coefficients of influence a_{ij} are determined by a linear-elastic analysis, which in this study is performed using the finite element method. For failure element i, R and R_i stand for stochastic variables described the (yield) strength capacity in tension (used in this study indicating a tensile force or a positive moment) and compression (used in this study indicating a compressive force or a negative moment). In general, $R_i^+ = R_i^-$. With M_j stands for the safety margin of failure element i, it is calculated as:

$$M_i = \min(R_i^+ - S_i,\ R_i^- + S_i)$$

<div align="right">**Equation 4-15**</div>

Accordingly, the safety margin in connection with failures of tensions or compressions depending on what is most likely. In general, reliability indices β_{i+} and β_{i-} are in correspondence to the safety margin $M_{i+} = R_{i+} - S_j$ as well as the calculation of $M_{i-} = R_{i-} + S_j$

129

is depended on the smallest one chosen. Alternative way is when performing the reliability analysis, it is to include both safety margins M_i+ and M_i- but then double the number of safety margins. By doing so, the failure criterion for failure element i is then:

$$0 \geq M_i$$

and the corresponding reliability index β_i can be calculated as:

$$\beta_i = \min(\beta_i^+, \beta_i^-)$$

<div align="right">**Equation 4-16**</div>

The corresponding safety margin M_i is given by:

$$M_i = \begin{cases} R_i^+ - S_i & \text{if} \quad \beta_i^+ \leqslant \beta_i^- \\ R_i^- + S_i & \text{if} \quad \beta_i^+ > \beta_i^- \end{cases}$$

<div align="right">**Equation 4-17**</div>

In this case the failure criterion is $0 \geq M_i$ and

$$\beta_i = \frac{\mu_{M_i}}{\sigma_{M_i}}$$

<div align="right">**Equation 4-18**</div>

Where μ_{Mi} is the mean value of M_i and σ_{Mi} is the standard deviation of M_i

$$M_i = \min(R_i^+ - S_i, R_i^- + S_i)$$

<div align="right">**Equation 4-19**</div>

The most primitive estimate of the reliability index β_s for the structural system is then:

$$\beta_S = \min_{i=1,\,n} \beta_i$$

in which, n is the number of failure elements. β_s is not actually a system reliability estimation, though, rather it is the estimation of the reliability of the most heavily loaded failure element and therefore not a system reliability estimation. However, considering the systematically reasons expedient of the system modelling at level 0, it is called as the system reliability at level 0.

At system modelling level 1, a structure is modelled by n failure elements. The systems reliability is estimated as the reliability of a series system with n elements – the n failure elements. With F_i, $i = 1, 2, ...$, n stands for the events, where the failure occurrences take place by failure of failure element i. Then

$$P_f = P(F_1 \cup F_2 \cup ... \cup F_n)$$

Practically, F_i and F_j, $i \neq j$, often in correlation because of the fact that safety margins M_i and M_j, $i \neq j$ is correlated. The covariance $Cov[M_i, M_j]$ between the safety margins M_i and M_j, $I \neq j$, can be calculated as following:

$$Cov[M_i, M_j] = \sum_{i=1}^{m} a_i b_i \, Var[X_i] + \sum_{i,j=1,\,i\neq j}^{m} a_i b_j \, Cov[X_i, X_j]$$

in which, the safety margins are assumed by the following:

$$M_i = \sum_{i=1}^{m} a_i X_i$$

$$M_j = \sum_{i=1}^{m} b_i X_i$$

<div align="right">**Equation 4-23**</div>

This study follows what was suggested by Ditlevsen and Kounias for upper and lower bounds of P_f that is so-called Ditlevsen bounds. if $P(F_i)$, $i = 1, 2, ... , n$ stands for the probability of event F_i and $P(F_i n F_j)$ stands for the probability of the intersection of F_i and F_j, $i \neq j$. Then the Ditlevsen bounds are presented by following:

$$P_f \leq \sum_{i=1}^{n} P(F_i) - \sum_{i=2}^{n} \max_{j<i} [P(F_i \cap F_j)]$$

$$P_f \geq P(F_1) + \sum_{i=2}^{n} \max[P(F_i) - \sum_{j=1}^{i-1} P(F_i \cap F_j), 0]$$

<div align="right">**Equation 4-24**</div>

In order to calculate the Ditlevsen bounds, it is required an estimation of the probability of intersection of F_i and F_j, $i.e$, in which numerical integration is often been used to calculate $P(F_i \cap F_j)$.

It is noted that to achieve a very good approximations for P_f, the safety margins M_i, $i = 1, ... , n$, are seen as an almost perfect correlation (in other words, the correlation coefficient ρ_{jj} between any pair of safety margins is nearly one), otherwise, the very small correlation between any pair of safety margins is considered ($\rho_{jj} \sim 0$). In the former, ($\rho_{jj} \sim 1$), the probability takes the lower bound

$$P_f \geq \max_{i=1, n} P(F_i)$$

132

Equation 4-25

and in the latter case ($\sigma_{jj} \sim 0$), the probability takes the upper bound

$$P_f \leqslant 1 - \prod_{i=1}^{n} (1 - P(F_i))$$

Equation 4-26

For normally distributed and linear safety margins

$$P_f = 1 - \int_{-\infty}^{\beta_1} \int_{-\infty}^{\beta_2} \cdots \int_{-\infty}^{\beta_n} \varphi_n(\overline{x}\,;\overline{\overline{\rho}})\,dx_1\,dx_2 \cdots dx_n = 1 - \Phi_n(\overline{\beta}\,;\overline{\overline{\rho}})$$

Equation 4-27

Where φ_n and ϕ_n are the n-dimensional density and distribution function for n standardized normal variables $\overline{X} = (X_1, \ldots, X_n)$. When all correlation coefficients are equal $\rho_{jj} = \rho > 0$ then

$$P_f = 1 - \int_{-\infty}^{\infty} \varphi(t) \prod_{i=1}^{n} \Phi\left(\frac{\beta_i - \sqrt{\rho}\,t}{\sqrt{1-\rho}}\right) dt$$

Equation 4-28

When the correlation coefficients ρ_{jj} are unequal a simple approximation for P_f can be obtained from this equation by putting:

$$\overline{\rho} = \frac{1}{n(n-1)} \sum_{i,\,j\,=\,1,\,i\,\neq\,j}^{n} \rho_{ij}$$

Equation 4-29

133

Let the structure be modelled by *n* failure elements and let the number of critical failure elements at level 1 be n_1. Assuming element *e* is the critical failure element as having the lowest reliability index *β* amongst the group of critical failure elements. Accordingly, the failure occurrence is assumed for critical failure element *e*. A modification of the structure is done accordingly by a removal of the corresponding failure element as well as a pair of so-called fictitious loads F_e (normal forces or moments) are added to the modified structure. Figure 4-9 demonstrates the structure after modification, in which the left the event with failure in compression is presented on the left, while the failure in bending is presented on the right.
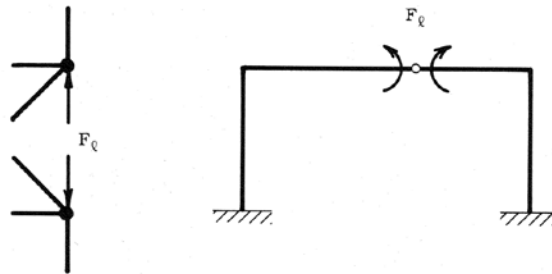

Figure 4-9 Fictitious loads

If the removed failure element is brittle, then no fictitious loads are added. However, if the removed failure element e is ductile then the fictitious load F_e is a stochastic load given by

$$F_\varrho = \gamma_\varrho R_\varrho$$

Equation 4-30

where R_e is the load-carrying capacity of failure element e and where *0 < γ$_e$ < 1*.

The modified structure with the loads P_1... P_k and the fictitious load F_e (normal force or moment) is then reanalysed and influence coefficients a$_{ij}$ with respect to P_1, ..., P_k and a_{ie} with respect to F_e are calculated. The load effect (force or moment) in the remaining failure elements

is then described by a stochastic variable. The load effect in failure element i is called S_{ie} (load effect in failure element i given failure in failure element e) and

$$S_{i|\varrho} = \sum_{j=1}^{k} a_{ij}P_j + a'_{i\varrho}F_\varrho$$

Equation 4-31

$$M_{i|\varrho} = \min(R_i^+ - S_{i|\varrho}, R_i^- + S_{i|\varrho})$$

Equation 4-32

where R_i+ and R_i- are the stochastic variables describing the (yield) strength capacity intension for failure element i. In the following M_{ie} will be approximated by either $R_i+ - S_{je}$ and $R_i- + S_{je}$ depending on the corresponding reliability indices. The reliability index for failure element I, given failure in failure element e, is

$$\beta_{i|\varrho} = \mu_{M_{i|\varrho}}/\sigma_{M_{i|\varrho}}$$

Equation 4-33

By doing so, new reliability indices are obtained for all failure elements (with exception for those elements with assumed failures) and β_{min} stands for the smallest β-value. The failure elements with β-values in the interval $[\beta min, \beta min + \Delta\beta_2]$, where $\Delta\beta_2$ stands for a prescribed positive number. A failure tree is formed by combining $\Delta\beta_2$ with failure element e and a number of parallel systems. Figure 4-10 illustrates the critical pairs of failure elements on the basic of the critical failure element, in the event that r, s, t are selected as three failure elements (the parallel system), which in turn, are included in the series system as each of its own elements.
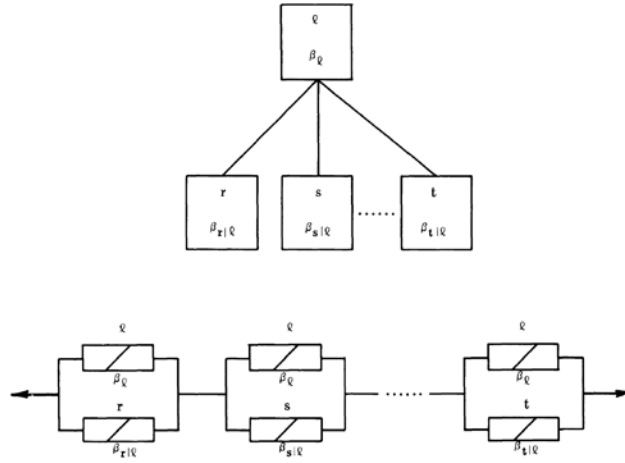
Figure 4-10 Identification of critical pairs of failure elements

After that, there is a need in evaluating the failure probability (as well as its corresponding generalised reliability index) for each critical pair of failure elements (the parallel system demonstrated in Figure 4-10). Taking into consideration the failure elements e and r amongst the parallel systems. In the process of estimating the reliability analysis at level 1, the safety margin M_e for failure element e is obtained as well as the safety margin M_{re} for failure element r has formed through Equation 4-32. From these safety margins the reliability indices $\beta_1 = \beta_e$ and $\beta_2 = \beta_{re}$ and the correlation coefficient $\rho = \rho_{r,\,re}$ can easily be calculated in accordance to Equation 4-22. Accordingly, the probability of failure for the parallel system is presented as following:

$$P_f = \Phi_2(-\beta_1, -\beta_2 ; \rho) = \Phi(-\beta_1)\Phi(-\beta_2) + \int_0^\rho \varphi_2(-\beta_1, -\beta_2 ; z)\,dz$$

Equation 4-34

Once again, Ditlevsen bounds are employed in estimating of Φ_2. It is noted that that for $\rho > 0$

$$\max(p_1, p_2) \leqslant \Phi_2(-\beta_1, -\beta_2 ; \rho) \leqslant p_1 + p_2$$

136

Equation 4-35

where

$$p_1 = \Phi(-\beta_1)\Phi(-\frac{\beta_2 - \rho\beta_1}{\sqrt{1-\rho^2}})$$

$$p_2 = \Phi(-\beta_2)\Phi(-\frac{\beta_1 - \rho\beta_2}{\sqrt{1-\rho^2}})$$

Equation 4-36

Accordingly, the average of the lower and upper values in Equation 4-35 is employed in estimating of P_f through the following calculation

$$P_f \approx \frac{1}{2}[\max(p_1, p_2) + p_1 + p_2]$$

Equation 4-37

The bounds Equation 4-35 are considered as relatively easy to be employed. In the event of the too wide gap between the lower and upper bounds, there is a need to consider another method that provides a more accurate evaluation of P_f.

It is noted that at system modelling level 1 presented earlier, the initiation of the β-unzipping is done through an assumption of failure with respect to the critical failure element e (that has the lowest β-value amongst the group of critical failure elements). Resulting from such reanalysis, a number of critical pairs of failure elements are found for the structural system as shown in Figure 4-10.

The same procedure is then in turn used for all critical failure elements and further critical pairs of failure elements are identified. In this way the total series system used in the reliability analysis at level 2 is determined. The corresponding failure tree is shown in Figure 4-11.
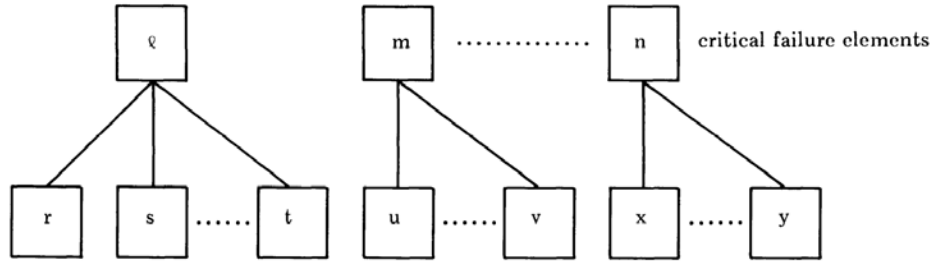
137

Figure 4-11 Failure tree at level 2

The next step is then to estimate the probability of failure for each critical pair of failure elements and also to determine a safety margin for each critical pair of failure elements. When this is done generalized reliability indices for all parallel systems and correlation coefficients between any pair of parallel systems are calculated. Finally, the probability of failure P_f for the series system is estimated.

The so-called equivalent linear safety margin introduced by Gollwitzer and Rackwitz is considered for approximating safety margins for the parallel systems. In general case with m correlated basic variables (load and strength variables) Xi, $i = 1, ... , m$, the performance in determinising equivalent linear safety margins is demonstrated as followed, in which, Mi, $i = 1, ... , k$ stands for the linear safety margin for failure element i can be calculated as:

$$M_i = \sum_{j=1}^{m} d_{ij} X_j \quad , \quad i = 1, 2, ..., k$$

Equation 4-38

With a parallel system of k elements, β_i stands for the corresponding reliability indices and P_f stands for the probability of failure of a parallel system presented in Figure 4-12. P_f is estimated as following:

$$P_f = P(M_1 \leqslant 0 \cap \ldots \cap M_k \leqslant 0) = P\left(\bigcap_{i=1}^{k} \left\{ \sum_{j=1}^{m} d_{ij}X_j \leqslant 0\right\}\right)$$

$$= P\left(\bigcap_{i=1}^{k} \left\{ \sum_{j=1}^{m} \alpha_{ij}Y_j + \beta_i \leqslant 0\right\}\right) = \Phi_k(-\bar{\beta}; \bar{\bar{\rho}})$$
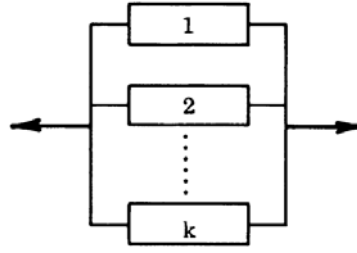
<div align="right">**Equation 4-39**</div>

Figure 4-12 Parallel system with k elements

in which, $\beta = (\beta_1, \ldots, \beta_K)$ and $Y = (Y_1, \ldots, Y_m)$ stands for a vector of uncorrelated standard normal variables. ρ stands for a correlation matrix, in which, the element ρ_{ij} is the correlation coefficient between the safety margins M_i and M_j

$$\rho_{ij} = \frac{1}{\sigma_{M_i}\sigma_{M_j}} \sum_{g=1}^{m} \sum_{h=1}^{m} d_{ig}d_{jh}C_{gh} = \sum_{s=1}^{m} \alpha_{is}\alpha_{js}$$

<div align="right">**Equation 4-40**</div>

In this equation, C_{gh} stands for an element in the covariance matrix C_X for the basic variables X; while the k-dimensional standard normal distribution function is presented by ϕ_k. With X stands for the correlated normally distributed basic variables and Y stands for the uncorrelated normally distributed variables. The transformation from $X \rightarrow Y$ is estimated as following:

$$\bar{X} = \bar{\bar{B}} \, \bar{Y} + \bar{\mu}$$

Equation 4-41

$$\bar{\mu} = (\mu_{X_1}, \ldots, \mu_{X_m})$$

Equation 4-42

$$\bar{\bar{B}}\,\bar{\bar{B}}^{T} = \bar{\bar{C}}_{\bar{X}}$$

Equation 4-43

Increasing Y by a (small) vector e is the main basic idea in determining the equivalent safety margin. Accordingly, a correspondingly generalized reliability index $e(e)$ dependent on $\beta^e(e)$ is possibly calculated as following:

$$\beta^{e}(\bar{\epsilon}) = -\Phi^{-1}\left(P\left(\bigcap_{i=1}^{k}\left\{\sum_{j=1}^{m}\alpha_{ij}(Y_j + \epsilon_j) + \beta_i \leqslant 0\right\}\right)\right) = -\Phi^{-1}\left(\Phi_k(-\bar{\beta} - \bar{\bar{\alpha}}\,\bar{\epsilon}; \bar{\bar{\rho}})\right)$$

Equation 4-44

With M^e stands for the equivalent safety margin, a vector α_e and a number β_e will define M^e in uncorrelated standard normally distributed variables Y by increasing e results in the same $\beta^e(e)$. For the equivalent safety margin - M^e one gets corresponding to the previous equation.

$$\beta^{e}(\bar{\epsilon}) = -\Phi^{-1}\left(\Phi(-\beta^{e}(\bar{0}) - \overline{\alpha^{e}}^{T}\bar{\epsilon})\right) = \beta^{e}(\bar{0}) + \overline{\alpha^{e}}^{T}\bar{\epsilon}$$

Equation 4-45

In such way, the vector α^e as well as the reliability index β_e for the equivalent safety margin M^e is calculated as following:

$$\beta^e = \beta^e(\bar{0}) = - \Phi^{-1}(\Phi_k(-\bar{\beta}; \bar{\bar{\rho}}))$$

$$\alpha_i^e = \cfrac{\left.\cfrac{\partial \beta^e}{\partial \epsilon_i}\right|_{\bar{\epsilon}=\bar{0}}}{\sqrt{\displaystyle\sum_{j=1}^{m}\left(\left.\cfrac{\partial \beta^e}{\partial \epsilon_j}\right|_{\bar{\epsilon}=\bar{0}}\right)^2}} \qquad i = 1, 2, \ldots, m$$

Figure 4-13 illustrates the case with *m = 3*, the *y* coordinate system α^e and β_e that forms a hyperplane, what is so-called the equivalent failure plane for the parallel system Figure 4-12. In approximating correlation coefficients between parallel systems, the corresponding equivalent safety margin M^e is employed as an approximation for calculating. M^e is therefore calculated through the vector α^e and the reliability index β_e as following:

$$M^e = \sum_{i=1}^{m} \alpha_i^e Y_i + \beta^e = \sum_{i=1}^{m} d_i^e X_i + \Delta\beta^e$$

$$\bar{d}^e = \bar{\bar{B}}^{-1}\bar{\alpha}^e$$

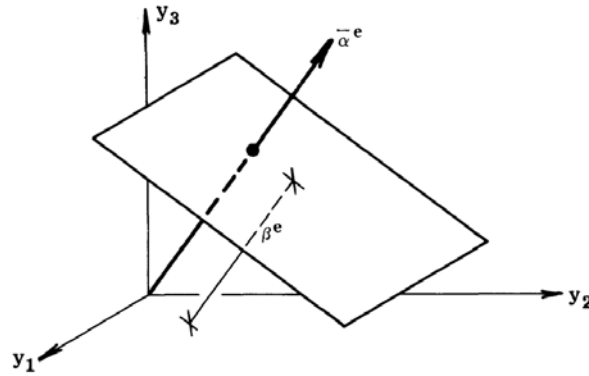$$\Delta\beta^e = \beta^e - \sum_{i=1}^{m} d_i^e \mu_i$$

Figure 4-13 Equivalent failure plane

Taking into consideration the fully correlation occurred amongst some of the variables $X =$ $(X_l,... , X_n)$, there is a reduction in the dimension of X. By doing so, there is negligible of any remaining variables, those are are fully correlated. Accordingly, an elimination of in d corresponding elements are removed and their variables are then eliminated.

With system modelling at level 2, the estimation of the structural system reliability is obtained on the basic of a series system, in which, each of its elements is parallel system with 2 failure elements – what is so-called critical pairs of failure elements. Similarly, with system modelling at level 3, the reliability of a structural system is estimated on the basic of so-called critical triple of failure elements – a set of three failure elements. The β-unzipping method is also used to identify the critical triples of failure elements that will form a parallel system with three failure element and then each of this triple will become a member of a series system. Eventually, the structural system reliability is estimated at level 3 through forming the parallel and series systems.

For a structure with n failure elements, n_1 critical failure element at level 1 and n_2 critical pair of failure elements at level 2, it is assumed that the lowest reliability index $\beta_{e,m}$ of all critical pairs of failure elements is *(e, m)* - the critical pair of failure elements and the failure elements of *(e, m)* is where the failure taken place. Accordingly, the modification of the structure system

142

is to remove the corresponding failure elements *(e, m)* and to add each of them a pair of so-called fictitious loads F_e and F_m (normal forces or moments). The loads $P_1, ... , P_k$ and the fictitious loads F_e and F_m will then formed the modified structure system and being reanalysed. The influence coefficients with respect to $P_1, .. , P_k$ and F_e and F_m are then obtained. With $S_{i,em}$ stands for load effect in failure element *i* given failure in failure elements *e* and *m*, the load effect (either forces or moments) in each of the remaining failure elements is presented through a stochastic variable $S_{i,em}$ is as following:

$$S_{i|\ell,m} = \sum_{j=1}^{k} a_{ij} P_j + a'_{i\ell} F_\ell + a'_{im} F_m$$

Equation 4-51

The corresponding safety margin is then

$$M_{i|\ell,m} = min(R_i^+ - S_{i|\ell,m}, R_i^- + S_{i|\ell,m})$$

Equation 4-52

where R_i+ and R_i- are the stochastic variables describing the (yield) strength capacity in tension and compression for failure element i. In the following $M_{i,em}$ will be approximated by either $R_i+ - S_{je}$ or $R_i- + S_{je}$ depending on the corresponding reliability indices. The reliability index for failure element i, given failure in failure elements e and m, is then given by

$$\beta_{i|\ell,m} = \mu_{M_{i|\ell,m}} / \sigma_{M_{i|\ell,m}}$$

Equation 4-53

In this way new reliability indices are calculated for all failure elements (except e and m) and the smallest β-value is called βmin. These failure elements with β-values in the interval [βmin,

143

βmin + $\Delta\beta_3$] where $\Delta\beta_3$ is a prescribed positive number, are then in tum combined with failure elements e and m to form part of a failure tree and a number of parallel systems. Figure 4-14 illustrates the event, in which three selected failure elements *r, s, t*. This figure clearly shows the parallel systems with three failure elements identified by the above-mentioned procedure
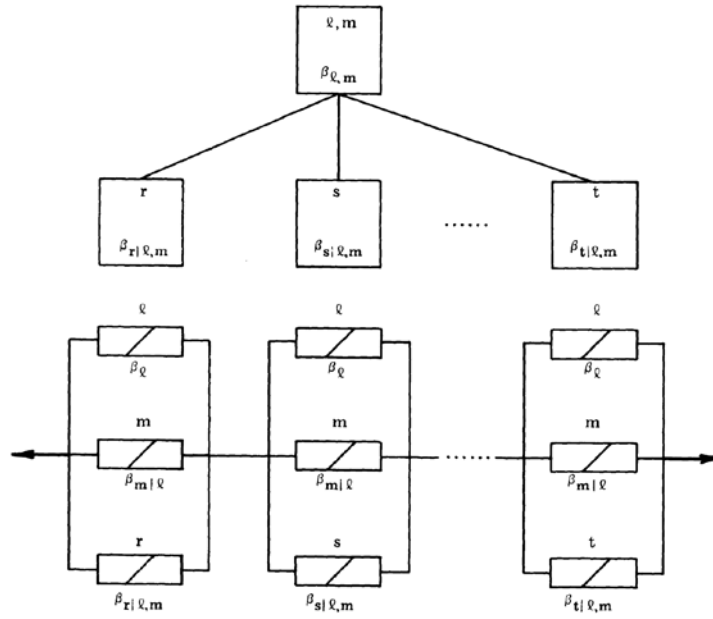

Figure 4-14 Identify of critical triples of failure

The final step in estimating the system reliability is evaluating the failure probability (and the corresponding generalized reliability index) for each of the critical triple of failure elements (the parallel system in Figure 4-14). In consideration of the parallel system with failure elements *e*, *m*, and *r*, the determination of the safety margin M_e for failure element *e* is done by the system modelling at level 1 or the reliability analysis at level 1, while the determination of the safety margin M_{me} for the failure element *m* is done by the system modelling at level 2 or the reliability analysis at level 2. With $M_{r,me}$ stands for the safety margin for safety element *r*, it can be calculated. Accordingly, their corresponding reliability indices can be obtained as β_1 = β_e , $\beta_2 = \beta_{me}$ and $\beta_3 = \beta_{r,me}$. Finally, the correlation matrix ρ can be easily estimated and the probability of failure for the parallel system is then determined as following:

144

$$P_f = \Phi_3(-\beta_1, -\beta_2, -\beta_3; \bar{\bar{\rho}})$$

<div align="right">**Equation 4-54**</div>

An estimate of Φ_3 can be calculated by e.g. the Ditlevsen bounds. If the gap between the lower and upper bounds is too wide a more accurate method to evaluate P_f should be used.

4.3 Design of Learning Function

4.3.1 Importance Sampling Algorithm

Based on a numerical optimization procedure to locate the most probable failure point, the distance from the origin to the probable failure point in the standard Normal space is used to measure the safety margin of a performance function. The utility of the reliability index to quantify the structural failure probability is sufficiently mature and widely accepted. Yet, the numerical accuracy depends largely on the truncation order of the investigated performance function while searching for the probable failure point result. The line sampling method relies on a direction from the origin to the probable failure point for an estimation result of the structural failure probability. A sample moving along the direction will cross the limit-state surface, and the numerical interpolation method was used to determine the reliability index result. Besides, an assembly of several simulation results allows capturing the nonlinearity of the performance function near the probable failure point. To avoid numerical interpolations embedded in the line sampling method, the importance sampling and subset simulation schemes can be alternatively used.

For employing machine learning in the process of analysing the system reliability employed in this study, the CE-based IS algorithm is presented as following in consideration of a numerical integration:

$$I_t = \int H(\mathbf{x}) f(\mathbf{x}; \mathbf{u}) d\mathbf{x}$$

<div align="right">**Equation 4-55**</div>

in which, *H(x)* is a general function of random variables *x*, and *f(x; u)* is the joint probability density function (PDF) of *x* with parameters *u*. For structural reliability analysis, in which the failure event of concern is usually indicated by the negative sign of the limit-state function *g(x)*, one can compute the probability of the failure event using Equation 4-55 by setting H(x) to be the binary indicator function *I{g(x)≤0}*, which gives "*1*" if the limit-state function *g(x)* is negative or zero, and "*0*" otherwise. To compute a statistical moment using Equation 4-55, one can set *H(x)* to be the corresponding polynomial function.

When the integration in Equation 4-55 is performed by a sampling approach, one can improve the efficiency by introducing an alternative sampling density, i.e.

$$I_t = \int \left[\frac{H(\mathbf{x}) f(\mathbf{x}; \mathbf{u})}{h(\mathbf{x}; \mathbf{v})}\right] h(\mathbf{x}; \mathbf{v}) d\mathbf{x}$$

$$= E_v \left[\frac{H(\mathbf{x}) f(\mathbf{x}; \mathbf{u})}{h(\mathbf{x}; \mathbf{v})}\right] \cong \frac{1}{N} \sum_{i=1}^{N} \frac{H(\mathbf{x}_i) f(\mathbf{x}_i; \mathbf{u})}{h(\mathbf{x}_i; \mathbf{v})}$$

<div align="right">**Equation 4-56**</div>

where *h(x; v)* is an alternative sampling density with parameters *v*, *Ev[·]* is the mathematical expectation with respect to the density *h(x; v)*, and *xi* is the *ith* sample generated from *h(x; v)*, *i = 1, ..., N*. The performance of this "importance sampling" (IS) approach is optimal when the variance of the estimate in Equation 4-56 is minimized. The "best" IS density minimizing the variance is derived as Rubinstein and Kroese (2016)

$$p^*(\mathbf{x}) = \frac{|H(\mathbf{x})| f(\mathbf{x}; \mathbf{u})}{\int |H(\mathbf{x})| f(\mathbf{x}; \mathbf{u}) d\mathbf{x}}$$

Equation 4-57

However, one cannot use the best IS density in Equation 4-57 because the denominator is practically equivalent to computing I_t in Equation 4-55 and exactly the same if $H(x)$ is non-negative as in structural reliability problems. Nevertheless, one can still improve the efficiency by choosing a near-optimal IS density whose shape is similar to that of $p^*(x)$ in Equation 4-57.

One can find a near-optimal IS density by minimizing a measure of the difference between $p^*(x)$ and $h(x;v)$, such as the Kullback–Leibler CE

$$D(p^*(\mathbf{x}), h(\mathbf{x}; \mathbf{v})) = \int p^*(\mathbf{x}) \ln p^*(\mathbf{x}) d\mathbf{x} - \int p^*(\mathbf{x}) \ln h(\mathbf{x}; \mathbf{v}) d\mathbf{x}$$

Equation 4-58

Since the IS density parameter v appears in the second term only, one can find a near-optimal IS density $h(x; v)$ by maximizing the second integral in Equation 4-58. For structural reliability analysis, it is noted that $H(x)$ is non-negative, and thus from Equation 4-57, $p^*(x)$ is proportional to $H(x)f(x; u)$. Substituting this to Equation 4-58, one finds

$$\arg \min_{\mathbf{v}} D(p*(\mathbf{x}), h(\mathbf{x}; \mathbf{v})) = \arg \max_{\mathbf{v}} \int H(\mathbf{x}) \ln h(\mathbf{x}; \mathbf{v}) f(\mathbf{x}; \mathbf{u}) d\mathbf{x}$$

$$= \arg \max_{\mathbf{v}} E_{\mathbf{u}}[H(\mathbf{x}) \ln h(\mathbf{x}; \mathbf{v})]$$

Equation 4-59

where $E_u[\cdot]$ denotes the mathematical expectation with respect to the original joint PDF $f(x; u)$. For purposes of evaluating the expectation in Equation 4-59 more efficiently, an alternative sampling density $h(x; w)$ is introduced, i.e.

$$\arg\ \min_{\mathbf{v}} D(p^*(\mathbf{x}), h(\mathbf{x}; \mathbf{v}))$$
$$= \arg\ \max_{\mathbf{v}} \int H(\mathbf{x}) \ln h(\mathbf{x}; \mathbf{v}) \frac{f(\mathbf{x}; \mathbf{u})}{h(\mathbf{x}; \mathbf{w})} h(\mathbf{x}; \mathbf{w}) d\mathbf{x}$$
$$= \arg\ \max_{\mathbf{v}} E_W[H(\mathbf{x}) \ln h(\mathbf{x}; \mathbf{v}) W(\mathbf{x}; \mathbf{u}, \mathbf{w})]$$

Equation 4-60

where *Ew[·]* denotes the mathematical expectation with respect to the density function *h(x; w)*, and *W(x; u, w)* is the likelihood ratio, *f(x; u)/h(x; w)*. By estimating the expectation in Equation 4-60 by IS with h(x; w), one can obtain a near-optimal density approximately by

$$\mathrm{argmin}_{\mathbf{v}} D(p^*(\mathbf{x}), h(\mathbf{x}; \mathbf{v}))$$
$$\cong \mathrm{argmax}_{\mathbf{v}} \frac{1}{N} \sum_{i=1}^{N} H(\mathbf{x}_i) \ln h(\mathbf{x}_i; \mathbf{v}) W(\mathbf{x}_i; \mathbf{u}, \mathbf{w})$$

Equation 4-61

where *xi* is the *ith* sample generated using the density *h(x; w)*, *i = 1, ..., N*. The IS density *h(x; w)* introduced to estimate the expectation in Equation 4-61 employs different parameters w to decouple the parameters of the optimization process, i.e. v from those used for the sampling. In most applications, the function in Equation 4-61 is concave and differentiable with respect to v (Rubinstein and Kroese, 2013); therefore, the values of the parameters v that makes *h(x; v)* a near-optimal density can be obtained by setting the gradient of Equation 4-61 to be zero, i.e.

$$\frac{1}{N} \sum_{i=1}^{N} H(\mathbf{x}_i) W(\mathbf{x}_i; \mathbf{u}, \mathbf{w}) \nabla_{\mathbf{v}} \ln h(\mathbf{x}_i; \mathbf{v}) = 0$$

Equation 4-62

It is noted that if a member of the exponential family of distributions is used for *h(x; v)*, the applied logarithm ensures that each parameter has an explicit updating rule. Rubinstein and

Kroese (2013) derived such explicit updating rules for selected distribution models so that one can find a near-optimal density function by a few rounds of pre-sampling, and then perform the final IS until the target level of convergence is achieved. For example, Figure 4-15 shows the limit-state surface, the two design points and the contour plots of a function proportional to the best IS density. Figure 4-16 shows the limit-state surface, and contour plots of a function proportional to the best IS density
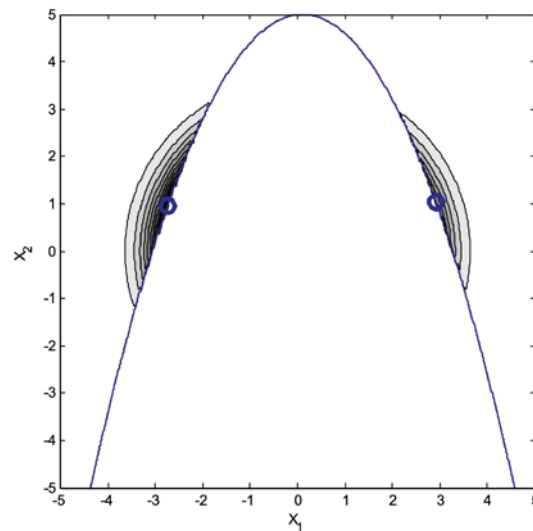
Source: Rubinstein and Kroese (2013)

Figure 4-15 Limit-state surface, design points and contours of a function proportional to the best importance sampling density for parabolic limit-state function with two design points.
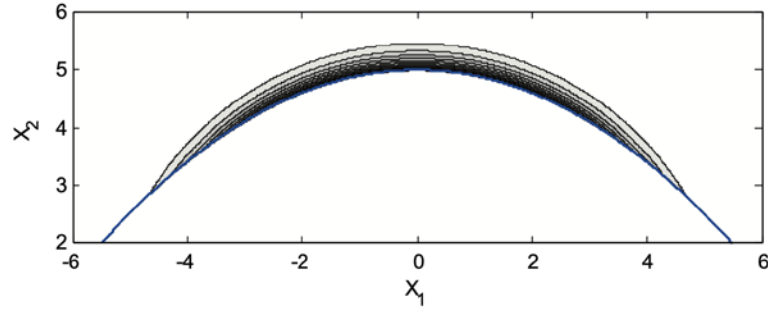
Source: Rubinstein and Kroese (2013)

Figure 4-16 Limit-state surface and contours of a function proportional to the best importance sampling density for parabolic limit-state function with many failure points with similar likelihoods.

4.3.2 Interval Monte Carlo Simulation

Uncertainties in parameter estimates are modeled by interval bounds constructed from confidence intervals. Reliability analysis needs to consider families of distributions whose parameters are within the intervals. Consequently, the probability of failure will vary in an interval itself. To estimate the interval failure probability, an interval Monte Carlo method has been developed which combines simulation process with the interval analysis.

This study adopts the Interval Monte Carlo Simulation to represent the unknown parameters presented by Zhang et al. (2010). In Monte Carlo simulation illustrated by Melchers and Beck (2018), the probability of failure is approximated as

$$p_f \approx \frac{1}{N} \sum_{j=1}^{N} I[G(\hat{\mathbf{x}}_j) \leqslant 0]$$

Equation 4-63

where N is the total number of simulations conducted x_j represents the jth randomly simulated vector of basic variables, and I[ ] is the indicator function, having the value 1 if [ ] is 'true' and the value 0 if [ ] is 'false'.

Let θ represent the unknown parameters. Let Φ denote the confidence intervals, and $\theta \in \Phi$ is a generic (arbitrary) element. The basic Monte Carlo simulation formula can be extended to the case when is a probability box with $f_x(x)$. When θ varies in intervals, the randomly simulated basic variables x_j vary in intervals accordingly. The limit state function $G(x_j)$ becomes a function of θ as well, i.e., $G(x_{j,}\theta)$. If the minimum and the maximum values of $G(x_{j,}\theta)$ can be determined

$$\text{Min}(G(\hat{\mathbf{x}}_j, \theta)) \leqslant G(\hat{\mathbf{x}}_j, \theta) \leqslant \text{Max}(G(\hat{\mathbf{x}}_j, \theta)), \quad \text{for } \theta \in \Theta$$

Equation 4-64

Then

$$I[\text{Max}(G(\hat{\mathbf{x}}_j, \theta)) \leqslant 0] \leqslant I[G(\hat{\mathbf{x}}_j, \theta) \leqslant 0] \leqslant I[\text{Min}(G(\hat{\mathbf{x}}_j, \theta)) \leqslant 0].$$

Equation 4-65

Applying Equation 4-64 and Equation 4-65

$$\frac{1}{N} \sum_{j=1}^{N} I[\text{Max}(G(\hat{\mathbf{x}}_j, \theta)) \leqslant 0] \leqslant \frac{1}{N} \sum_{j=1}^{N} I[G(\hat{\mathbf{x}}_j, \theta) \leqslant 0]$$
$$\leqslant \frac{1}{N} \sum_{j=1}^{N} I[\text{Min}(G(\hat{\mathbf{x}}_j, \theta)) \leqslant 0].$$

Equation 4-66

Thus, Equation 4-66 provides an interval estimate for p_f

$$\underline{p}_f \approx \frac{1}{N}\sum_{j=1}^{N} I[\text{Max}(G(\hat{\mathbf{x}}_j, \theta)) \leqslant 0],$$

$$\bar{p}_f \approx \frac{1}{N}\sum_{j=1}^{N} I[\text{Min}(G(\hat{\mathbf{x}}_j, \theta)) \leqslant 0], \quad \text{for } \theta \in \Theta.$$

Equation 4-67

The first step in the implementation of interval Monte Carlo simulation is the generation of intervals in accordance with the prescribed probability boxes. The inverse transform method is often used to generate random numbers. Consider a random variable X with CDF $F(X)$. If $(u_1, u_2, ..., u_n)$ is a set of values from the standard uniform variate, then the set of values

$$x_i = F_X^{-1}(u_i); \quad i = 1, 2, \ldots, m$$

Equation 4-68

will have the desired CDF $F(X)$. The inverse transform method can be extended to perform random sampling from a probability box. Suppose that an imprecise CDF $F(X)$ is bounded as shown in Figure 4-16. For each u_i in Equation 4-68, two random numbers are generated as

$$\underline{x}_i = \overline{F}^{-1}(u_i), \quad \bar{x}_i = \underline{F}^{-1}(u_i).$$

Equation 4-69

such a pair of x_i form an interval, which contains all possible simulated numbers from the ensemble of distributions for a particular u_i
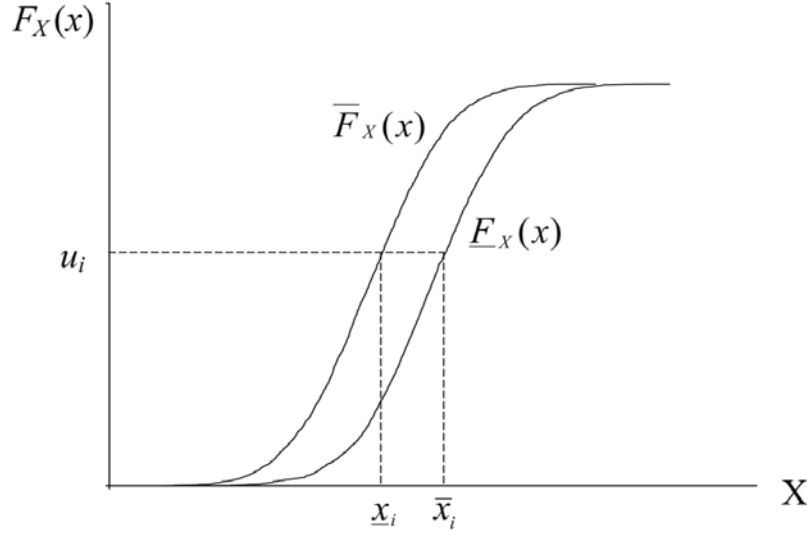
Figure 4-17 Generation of random number from distribution with interval parameters

The computational effort of the interval Monte Carlo simulation is contingent on the efficiency of computing the range (max. and min.) of structural responses through FE analyses when the simulated basic variables vary in intervals. This task can be performed by using the interval FEM. In this study, the interval FE analysis is formulated as an interval analysis problem. The interval analysis and interval FE formulation is briefly introduced as following.

Interval analysis concerns the numerical computations involving interval numbers. The four elementary operations of real arithmetic, namely addition *(+)*, subtraction *(-)*, multiplication *(x)* and division *(:)* can be extended to intervals. Operations $O \in \{+,-,x,:\}$ over interval numbers x and y are defined by the general rule presented by Neumaier and Neumaier (1990); Moore et al. (2009).

$$\boldsymbol{x} \circ \boldsymbol{y} = [\min(x \circ y), \max(x \circ y)] \quad \text{for} \circ \in \{+, -, \times, \div\}$$

Equation 4-70

in which *x* and *y* denote generic elements x and y.

153

For a real-valued function $f(x_1, x_2, ..., x_n)$, the interval extension of $f(\ )$ is obtained by replacing each real variable x_i by an interval variable x_i and each real operation by its corresponding interval arithmetic operation. From the fundamental property of inclusion isotonicity (Moore et al., 2009), the range of the function $f(x_1, x_2, ..., x_n)$ can be rigorously bounded by its interval extension function

$$\{f(x_1,\ldots,x_n) \mid x_1 \in \boldsymbol{x}_1,\ldots,x_n \in \boldsymbol{x}_n\} \subseteq f(\boldsymbol{x}_1,\ldots,\boldsymbol{x}_n).$$

Equation 4-71

Equation 4-71 indicates that $f(x_1, x_2, ..., x_n)$ contains the range of $f(x)$

The system equation in the interval FEM takes the following form

$$(\boldsymbol{K} + Q)\boldsymbol{u} = \boldsymbol{p}$$

Equation 4-72

where K is the interval stiffness matrix, u is the interval displacement vector, p is the interval load vector, and Q is the deterministic penalty matrix. Equation 4-72 can be transformed into a fixed point equation

$$\boldsymbol{R}\boldsymbol{p} - R(\boldsymbol{K} + Q)u_0 + (I - R(\boldsymbol{K} + Q))\boldsymbol{u}^* = \boldsymbol{u}^*$$

Equation 4-73

in which R is a nonsingular preconditioning matrix, and u_o is an approximate deterministic solution. It can be verified that

$$\boldsymbol{u} = \boldsymbol{u}^* + u_0$$

Equation 4-74

154

Based on Equation 4-73, interval fixed point iteration is constructed:

$$Z + Cu^{*(l)} = u^{*(l+1)}$$

$$Z = Rp - R(K + Q)u_0$$

$$C = I - R(K + Q)$$

<div align="right">**Equation 4-75**</div>

The iteration converges when

$$u^{*(l+1)} \subseteq u^{*(l)}$$

$$u^{*(l+1)} + u_0$$

<div align="right">**Equation 4-76**</div>

This guarantees to contain the exact solution set of Equation 4-72. The original interval fixed point iteration implicitly assumes that the coefficients of K vary independently between their bounds. This assumption is not valid for the system equations that arise in the interval FEM. Special formulation has to be developed to remove coefficient-dependence in the algorithm. By using the EBE technique, it is possible to decompose the interval stiffness matrix K into two parts

$$K = SD$$

<div align="right">**Equation 4-77**</div>

in which S is a deterministic matrix and D is an interval diagonal matrix whose diagonal entries are the interval variables associated with each element (e.g., interval modulus of elasticity). The term Z in Equation 4-76 can then be reintroduced as

$$Z = Rp - R(K + Q)u_0 = Rp - RQu_0 - RSDu_0$$
$$= Rp - RQu_0 - RSM\delta.$$

<div align="right">**Equation 4-78**</div>

It must be noted that in Equation 4-78 Du_0 is introduced as $M\delta$ in which M is a deterministic matrix and d is an interval vector. The components of δ are the diagonal entries of D with the difference that every interval variable occurs only once in δ. This treatment eliminates the coefficient-dependence in Z, which is critical for obtaining a tight bound.

The interval fixed point iteration converges if and only if

$$\rho(|C|) < 1$$

<div align="right">**Equation 4-79**</div>

That is the spectral radius of the absolute value of the iterative matrix C. To achieve a small result obtained from Equation 4-79. The choice

$$R = (Q + S)^{-1}$$

<div align="right">**Equation 4-80**</div>

is made such that

$$C = I - R(Q + SD) = I - R(Q + S) - RS(D - I) = -RS(D - I)$$

156

Equation 4-81

Numerical tests have shown that fast convergence (within 10 iterations) generally can be achieved by using the above modified iterative algorithm.

4.3.3   Mean-Interactive Neural Network

Convergence characteristics change if population size changed or an adaptive mutation method was used, but no comparison has been made as to whether their method provides any faster convergence than back propagation or its variants. Training using genetic algorithms was substantially faster than back propagation. However, lack of description on the specific back propagation method and its parameters, and inaccessibility to their task domain. To improve the convergence in the process of training and testing Neural Network, a mean-interactive algorithm is used in this study.

This study employs the Mean-Interactive Neural Network (MINN) proposed by Vu et al. (2010). The general procedure of a new iterative algorithm approaches for parameter model updating loop based on mean-iterative network is shown in Figure 4-18.
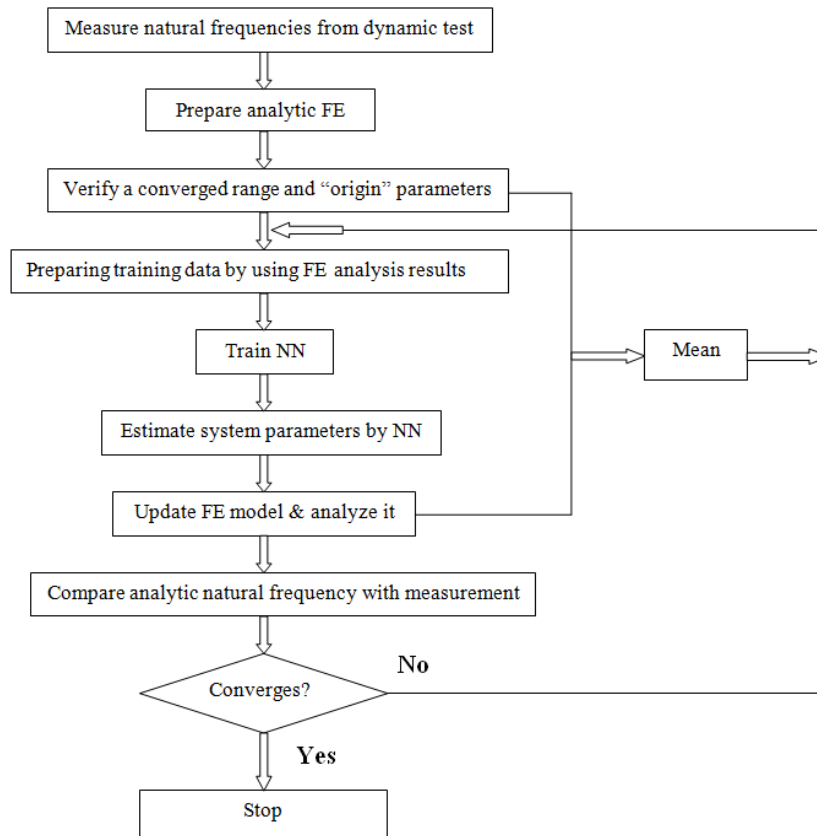
Figure 4-18 Flow chart of mean-iterative neural network

Mean-iterative neural network strategy is divided into two stages: First, the initial defect profile from numerical analysis is trained by neural network in order to identify "origin" structural parameters; the trained neural networks are then used in an iterative algorithm to estimate the parameters given the measurement signals. Mathematically, each of the neural networks approximates the function mapping the input to the output, and as long as the test data is similar to the training data, the network can interpolate between the training set points to obtain a reasonable prediction. Desired parameter estimation can be found by iteratively minimizing an objective function. It is marked that, for the presented method, after each loop getting the estimated values; the mean of "origin" structural parameters is calculated and the given estimated values to be a new training data for the next loop. By doing so, the chosen parameters will jump up and down, but not progressively step up in the course of the iterations, as regular

158

neural network. As a consequence, the identified values for model updating are kept similar during iteration. Better approximation in the solution of the equations is achieved, and therefore the convergence is speeded up. In process, the mean is required after each loop called mean-iterative and thus, the new strategy is named mean-iterative neural network.

In this study Multilayer Perceptron Networks with its simplest processing unit represented by the single neuron as indicated by Figure 4-19 is used.
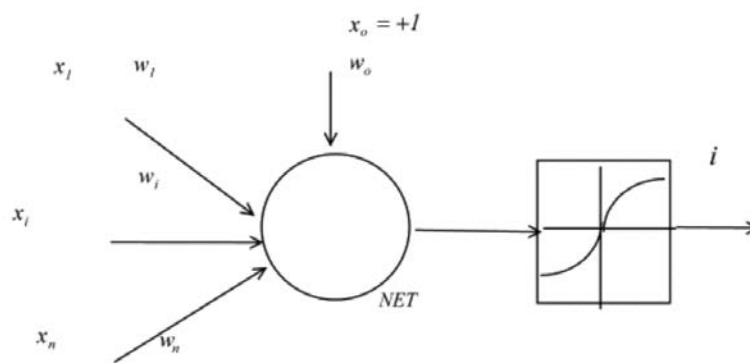

Figure 4-19 Single neuron unit processor

The neuron is the most basic unit of a neural network and, as a processing unit, will receive inputs (x_i) via axons connections. Then, some transformation will be processed to the inputs in order to obtain a desired output. This transformation is carried out in two stages. First, a linear combination of all the inputs to obtain a scalar, called NET, is usually used. The coefficients of the linear transformation are called "weights" and they are denoted by w_i. In a second stage, a linear or non-linear transformation is applied to the scalar NET. The linear or non-linear function is called "activation function" and is denoted by f. As in a natural neuron behaviour, the activation function will decide when, how and whether the neuron output (i) will take place.

As indicated in Figure 6-5, there is an input with constant value $(x_0=+1)$ and its respective weight (w_0), which is related to a parameter in the activation function called "threshold". For convenience, the threshold is considered as an unknown in the equation, which gives the

159

corresponding output. The threshold defines a shift of the original activation function. This process can be written as:

$$i = f\,NET = f \sum_{k=0}^{n} w_k x_k$$

<div align="right">**Equation 4-82**</div>

There are several kinds of activation functions used for the transformation such as linear *[f(x)=x]*, signal *[f(x)=SIGN(x)]*, sigmoid *[f(x)=1/(1+e^{-x})]*, unit step function *[f(x)=H(x–x$_0$)]*, hyperbolic tangent *[f(x)=tanh(x)]*, etc. This single processing units can connect each other to generate the so-called Neural Network. The ways the neurons are connected and the ways they operate are very different originating a great variety of neural networks.

The employed Multilayer Perceptron Network architecture consists on a layered network fully connected, i.e., all neurons belonging to a layer are, each one, connected to the previous and the next layer. The number of input vector followed by the number of neurons on each layer indicates such architecture (e.g. 1:12:1 represents a Neural Network with one input vector followed by one layer with 12 neurons and an output layer with one neuron). Obviously, the input layer and the output layer only "put" or "receive" data from the network. The number of hidden layers and the number of hidden units in each layer needs to be determined. It depends on the complexity of the system being modelled. For a more complex system, a larger number of hidden units are needed. In this study, the optimal number of hidden units is determined by trial and error.

In the training process of neural networks, for an input pattern X_{pi} (where index p means "pattern" and index i means an input neuron), the weights (W_{pi}) adjustment will take place in

the links of the neural network in order to get a desired output or, in the special case of this work, the value of the limit state function for this specific sample, y_{po} (where index p means "pattern", and O means an output neuron). After this first adjustment is achieved, the network will pick up another pair of x_{pi} and y_{po}, will again adjust weights for this new pair. In a similar way, the process will go on till all the input–output pairs are considered. Finally, the network will have a single set of stabilized weights satisfying all the input-output pairs.

5 Validation and Application

This application of the proposed method-based Monte Carlo Simulation and Neural Networks to estimate the structural system reliability index is used in order to validate the results against the study of Hashemolhosseini (2013). The structure is shown in Figure 5-1 with the dimension of the horizontal spans and its height; as well as two applied forces F1 (290kN) and F2 (232kN), respectively. The properties of each sections (steel hollow section) of the ten-bar truss structure is shown in Table 5-1. Considering the fact that only one load effect variable is considered, it is assumed that the internal load of the truss component can be either pure tension or pure compression. It is also noted that in this study, the structure is considered as having two degrees of redundancy or in other words, statically indeterminate to degree of 2. Accordingly, this section will present the resistance and load effect in details as following.
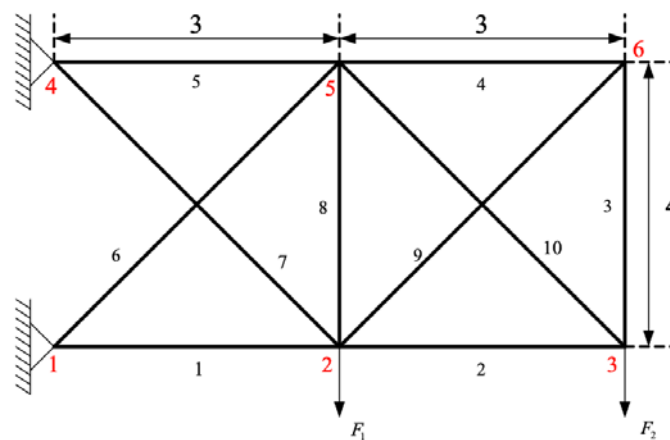

Figure 5-1 10-bar truss structure

Table 5-1 Section properties

Member	Length(m)	Section(Hollow)	Area(mm^2)	r(mm)
1	3	127×5	1916	43.2
2	3	101.6×3	929	34.9
3	4	32×2	188	10.6
4	3	32×2	188	10.6
5	3	101.6×4	1226	34.5
6	5	165.1×4.5	2270	56.8
7	5	114.3×3	1049	39.4
8	4	38×3	331	12.5
9	5	101.6×3	929	34.9
10	5	101.6×2.5	778	35.0

Table 5-2 Internal force and resistance of members

Member	Internal force(kN)	Type	Resistance
1	-379.65	Compression	387.500
2	-145.160	Compression	150.568
3	38.453	Tension	59.370
4	28.840	Tension	59.370
5	369.335	Tension	386.340
6	-325.558	Compression	356.083
7	326.942	Tension	330.428
8	66.889	Tension	104.205
9	-48.066	Compression	71.452
10	241.934	Tension	245.174

Table 5-3 Limit state function for structural component

Member type	Strength performance function
Tension	$G = A \times f_y - E(F)$
Compression	$G = A \times f_y \times \chi - E(F)$

5.1 Reliability Assessment using β-unzipping Method

The member forces together with their resistance are given at Table 5-2 . It is noted that the

following estimation is based on an assumption that no failure is occurred at the truss

connection as well as no failure mode of the fracture of the net section is considered for tension

members. In this context, the limit state function represented the resistance elements illustrates

that a factor χ (that further reducing the capacity of the compression member in purpose of including the buckling effect) is used to differ the tension member from compression member. Table 5-3 demonstrates the limited state functions employed for each element namely tension element and compression element. The structural reliability analysis of the truss structure at component level is estimated using the Finite Difference-Based FORM reliability analysis with the result is shown as following:

Table 5-4 Reliability indices and probability of failure for each component

| Member	β	P_f
1	3.2634	0.00055
2	3.2157	0.00065
3	5.5295	1.61E-08
4	7.3373	1.09E-13
5	3.2639	0.00055
6	3.5298	0.00021
7	3.0797	0.00104
8	5.5759	1.23E-08
9	5.2670	6.93E-08
10	3.0960	0.00098

As presented earlier in Chapter 4, the proposed research approach assumes a normal distribution for all of its input basic variables in the process of estimating the system reliability.

At level zero, the system modelling does not take into account the failure interaction between the failures of the different elements to estimate the system reliability. In other words, each element of the entire structural system is individually considered and the lowest reliability amongst to those of all components is considered as the system reliability at this level. Accordingly, the result needed from the intact structure is only a component-level reliability analysis of the intact structure is required. In regard to Table 5-4, the reliability of the system at level zero is:
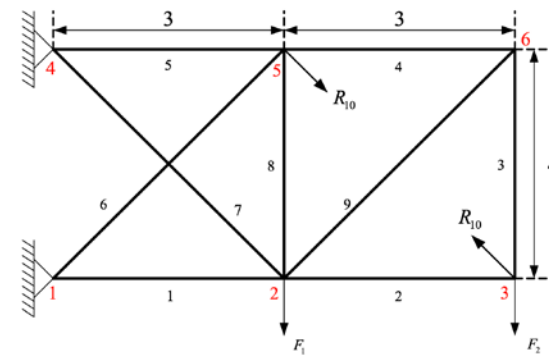
$$\beta^0 = \min \beta_i = \beta_7 = 3.0797$$
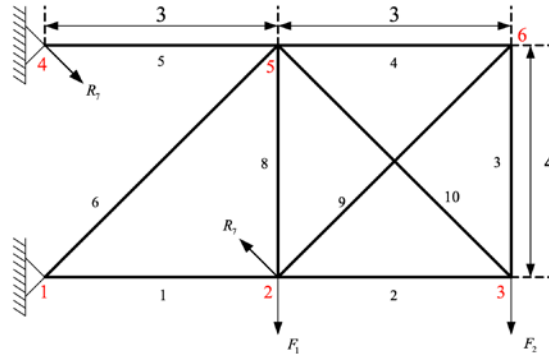
(a) Failure of Element 7 and is replaced by R_7
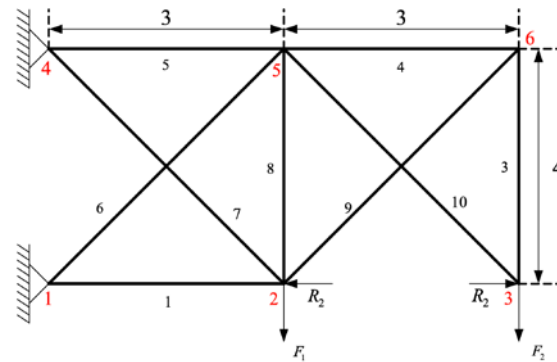
(b) Failure of Element 2 and is replaced by R_2

© Failure of Element 10 and is replaced by R_{10}

Figure 5-2 Scenario 1: Failure of each critical element

However, the system modelling at level 1 obtains the correlation between the probabilities of

failures of any failure elements. The system is modelled with series system where its elements

165

are failure elements. Similar to the probability of failure of the structural system at level 0, at level 1, this probability is also estimated on the basic of the probability of failure of each failure of the individual element; however, it also takes into account the correlation between the safety margins of the failure elements. The critical element is defined by those components with the reliability values in the interval [βmin, βmin + Δβ], that is used in forming a series system, in which, the failure of the structure system is caused by the failure of any of the components – a series system. The first method of Ditlevsen Bounds is used in this study in purpose of calculating the system reliability. The lower bound suggested by Ditlevsen bound is in correspondence with the event in which the full correlations are assumed for all the elements; whereas, the upper bound suggests an event in which the full uncorrelations are assumed for all the elements. The following bounds are defined by Ditlevsen for the structural system:

$$0.001036 < P_f < 0.003969$$

Δβ = 1 is assumed for this study, which defines the lower bound of 3.0797 and the upper bound of 4.0797. Accordingly, the critical elements are obtained as member 1, 2, 5, 6, 7, and 10 as its component reliability index falls between the internal [3.0797, 4.0797]. These elements will be further considered to form a series system. Followed the β-unzipping method, each of these elements will be removed from the ten-bar truss structure and is replaced by fictitious loads in that it is assumed as ductile failure. The whole scenario is shown in Figure 5-2. Following the procedure shown in Section 4.1.2.2 System Reliability Analysis, the reliability indices of each elements in the different scenarios of failure of critical elements is presented in Table 5-5.

Table 5-5 Member reliability indices – failure of critical element

166

Member	Reliability index	Governing Failure Mode
1	3.4673	Compression
2	3.1879	Compression
3	6.8272	Tension
4	11.5364	Compression
5	3.2003	Tension
6	3.3063	Compression
8	3.7373	Tension
9	5.7384	Compression
10	3.0928	Tension
Minimum RI	3.0928	Tension

(a) Failure of element 7

Member	Reliability index	Governing Failure Mode
1	3.2532	Compression
3	3.6370	Tension
4	4.0501	Tension
5	3.2789	Tension
6	3.7099	Compression
7	3.1112	Tension
8	4.2362	Tension
9	3.5850	Compression
10	14.2807	Compression
Minimum RI	3.1112	Tension

(b) Failure of element 2

Member	Reliability index	Governing Failure Mode
1	3.2324	Compression
2	14.2807	Tension
3	3.5406	Tension
4	3.9567	Tension
5	3.3066	Tension
6	3.7735	Compression
7	3.0796	Tension
8	4.1701	Tension
9	3.4877	Compression
Minimum RI	3.0796	Tension

(c) Failure of element 10

If comparison needed, the correlation matrix for the series system is calculated with the requirement of data obtained from the sensitivities analysis (finding the sensitivity factor for each random variable in each individual component's safety margin – limit state function). In consideration the fact that all random variables are normal, the FOSM reliability method is

167

used to perform such computations. With respect to the limit state functions presented in Table 5-3 (the limit state function represented the resistance elements illustrates that a factor χ), the following equations are used to calculated the sensitivity factor and the reliability for each element as well as its corresponding resistance and load effect.

$$\beta = \frac{a\mu_R - b\mu_E}{\sqrt{(a\sigma_R)^2 + (b\sigma_E)^2}}$$

$$\alpha_R = \frac{a\sigma_R}{\sqrt{(a\sigma_R)^2 + (b\sigma_E)^2}}$$

$$\alpha_E = \frac{-b\sigma_E}{\sqrt{(a\sigma_R)^2 + (b\sigma_E)^2}}$$

Equation 5-1

Once the value of the sensitivity factors is calculated for each limit state functions, it is possible to compute the correlation matrix using the following equation:

$$\rho_{ij} = \bar{\alpha}_i^T \bar{\alpha}_j \text{ for all } i \neq j$$

Equation 5-2

where $\bar{\alpha}_i = \{\alpha_1, \alpha_2, ..., \alpha_n\}$ is the vector of directional cosines (sensitivity factors) for each safety margin in the system. Using the aforementioned equation, the sensitivity factors were calculated.

At the next stage – system reliability index at level three, the most critical pairs are identified and removed from the structure replacing by a set of fictious loads represented their post-failure capacity. The whole scenario is shown in Figure 5-3. Following the procedure shown in Section 4.1.2.2 System Reliability Analysis, the reliability indices of each elements in the different scenarios of failure of critical elements is presented in Table 5-5.
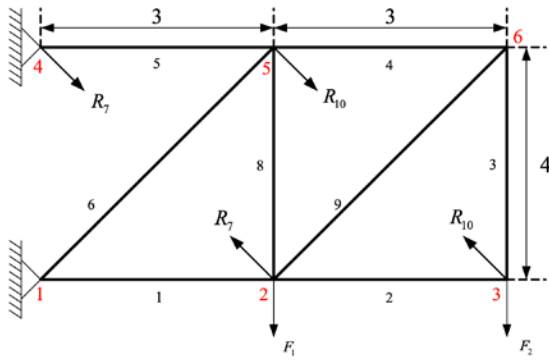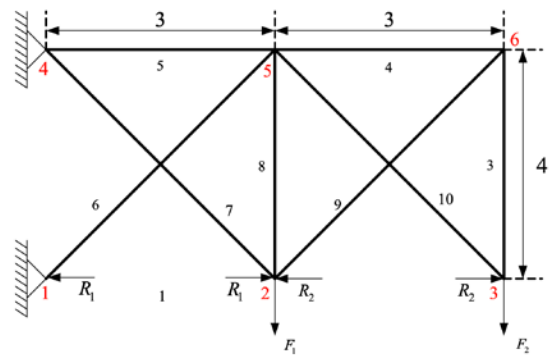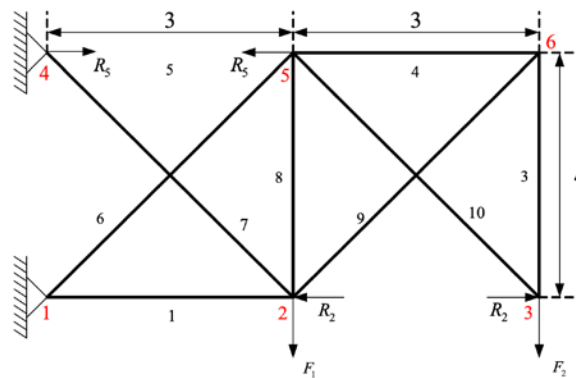
(a) Failure of pair 7 – 10
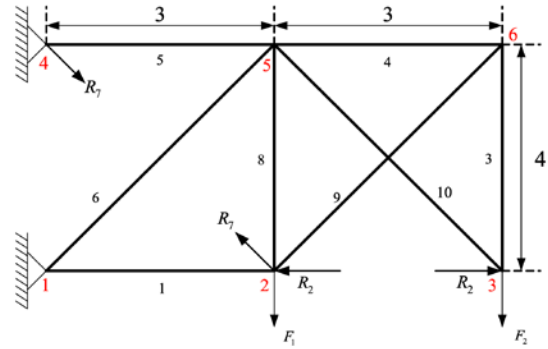
(b) Failure of pair 7 - 2
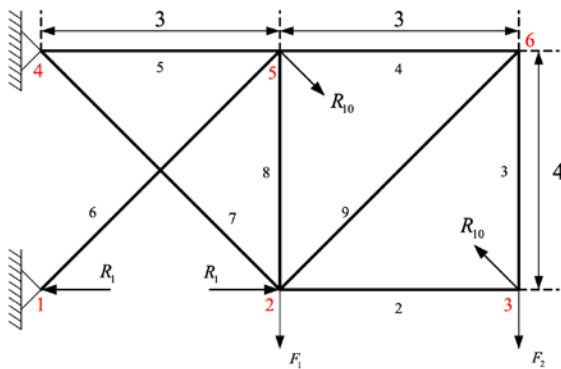
(c) Failure of pair 1 – 10

(d) Failure of pair 1 – 2

(2) Failure of pair 2 – 5

Figure 5-3 Scenario 2: Failure of pair of critical elements

Table 5-6 Member reliability indices – failure of pair of critical elements

Member	Reliability index	Governing Failure Mode
1	3.4673	Compression
2	14.2807	Tension
3	3.5406	Compression
4	3.9567	Compression
5	3.2003	Compression
6	3.3063	Tension
8	3.4402	Compression
9	3.4877	Tension
Minimum RI	3.2003	Compression

(a) Failure of pair 7 – 10

Member	Reliability index	Governing Failure Mode
1	3.4673	Compression
3	3.6375	Tension
4	4.0501	Tension
5	3.2003	Tension
6	3.3063	Compression
8	3.4838	Tension
9	3.5850	Compression
10	14.2807	Compression
Minimum RI	3.2003	Compression

(b) Failure of pair 7 – 2

Member	Reliability index	Governing Failure Mode
2	14.2807	Tension
3	3.5406	Tension
4	3.9567	Tension
5	3.2636	Tension
6	3.3101	Compression
7	8.6704	Compression
8	3.4485	Tension
9	3.4877	Compression
Minimum RI	3.2636	Tension

(c) Failure of pair 1 – 10

170

Member	Reliability index	Governing Failure Mode
3	3.6375	Tension
4	4.0501	Tension
5	3.2636	Tension
6	3.3560	Compression
7	8.6704	Compression
8	3.4786	Tension
9	3.5850	Compression
10	14.2807	Compression
Minimum RI	3.2636	Tension

(d) Failure of pair 1 – 2

Member	Reliability index	Governing Failure Mode
1	3.2637	Compression
3	3.6375	Tension
4	4.0501	Tension
6	11.5292	Tension
7	3.2004	Tension
8	4.8397	Compression
9	3.5850	Compression
10	14.2807	Compression
Minimum RI	3.2004	Tension

(e) Failure of pair 2 – 5

5.2 Machine Learning

In summary, there are nine cases of the two-scenario mentioned that the reliability index of each element for each scenario showed previously is shown as following, of which 0 stands for element failure and 1 stands for elements working in its full capacity. This data will be used as primary data for training using Neural Networks, of which, the working capability of each elements (either in full or failure) is selected to be inputs; accordingly, there are 10 inputs of the deep learning machine. Whereas, the reliability index of ten elements in each case is selected to be outputs along with the estimated reliability index of the whole structural system in each case; accordingly, there are 11 outputs in totals towards the training process. It is well

171

known that the success of a NN design often depends on a fortunate set of random initial weights and a reasonable value for the number of hidden nodes.

In this study, the data set contains only nine cases is considered as relatively lack of efficiency. In order to address the problem regarding convergence and consistency, application of iterative NN based on Vu et al. (2012) model is performed. The key of this technique is to update the model during iteration in a faster and more accurate way. At the beginning, as usual, the analysis results (origin values) are used to train NN. Then mean solution starts from the second outer iteration until convergence occurs. That is, the parameter values are created by taking mean of previous estimated and origin ones. For example, at iteration i, training data is made by taking mean of identified parameters at iteration $(i-1)$ and origin values. Accordingly, estimated parameters fluctuate to some values different from zero, not from the value used in the first outer iteration but the origin parameters instead. In this way, the identified parameters are moved up and down relative to one determined value. As a consequence, the updated parameters for model updating are kept similar during iteration. Furthermore, it is performed a better approximation for model updating as well as a faster achievement in convergence.

Table 5-7 Data set for deep learning machine

	Comp.	7 Fail	2 Fail	10 Fail	7-10 Fail	7-2 Fail	10-1 Fail	2-1 Fail	2-5 Fail
E1	1	1	1	1	1	1	0	0	1
E2	1	1	0	1	1	0	1	0	0
E3	1	1	1	1	1	1	1	1	1
E4	1	1	1	1	1	1	1	1	1
E5	1	1	1	1	1	1	1	1	0
E6	1	1	1	1	1	1	1	1	1
E7	1	0	1	1	0	0	1	1	1
E8	1	1	1	1	1	1	1	1	1
E9	1	1	1	1	1	1	1	1	1
E10	1	1	1	0	0	1	0	1	1
Beta 1	3.2634	3.4673	3.2532	3.2324	3.4673	3.4673	3.2634	3.2634	3.2637
Beta 2	3.2157	3.1879	3.2157	14.2807	14.2807	3.2157	14.2807	3.2157	3.2157
Beta 3	5.5295	6.8272	3.6370	3.5406	3.5406	3.6375	3.5406	3.6375	3.6376
Beta 4	7.3373	11.5364	4.0501	3.9567	3.9567	4.0501	3.9567	4.0501	4.0501
Beta 5	3.2639	3.2003	3.2789	3.3066	3.2003	3.2003	3.2636	3.2636	3.2639
Beta 6	3.5298	3.3063	3.7099	3.7735	3.3063	3.3063	3.3101	3.3560	11.5292
Beta 7	3.0797	3.0797	3.1112	3.0796	3.0797	3.0797	8.6704	8.6704	3.2004
Beta 8	5.5759	3.7373	4.2362	4.1701	3.4402	3.4838	3.4485	3.4786	4.8397
Beta 9	5.2670	5.7384	3.5850	3.4877	3.4877	3.5850	3.4877	3.5850	3.5850
Beta 10	3.0960	3.0928	14.2807	3.0960	3.0960	14.2807	3.0960	14.2807	14.2807
Beta	3.0797	3.0928	3.1112	3.0796	3.2003	3.2003	3.2636	3.2636	3.2004

In which, Ei represents for scenario i of failure investigated earlier in Section 5.1 when critical element fails. For example. E1 is scenario 1 of failure when critical element 1 removed and replaced by fiction loads as well as elements 10 and element 2 fail. Similarly, E10 is scenario 10 of failure when critical element 10 removed and replaced by fiction loads as well as elements 7 and element 1 fail. Betaj represents the reliability indexes of either element or critical pairs in Ei scenario.

The back-propagation algorithm (Figure 2-12) is designed with the following information and the process was coded in Neural Networks as following:

- S_i - size of ith layer, for N_l layers contains of two layers, of which, the input layer contains 20 notes and the output layer contains 11 notes.

173

- TFi - transfer function of ith layer – is set as default,

- BTF - backprop network training function – is Levenberg – Marquardt

- BLF - backprop weight/bias learning function, is set as default

- PF - performance function, is set Mean Squared Error

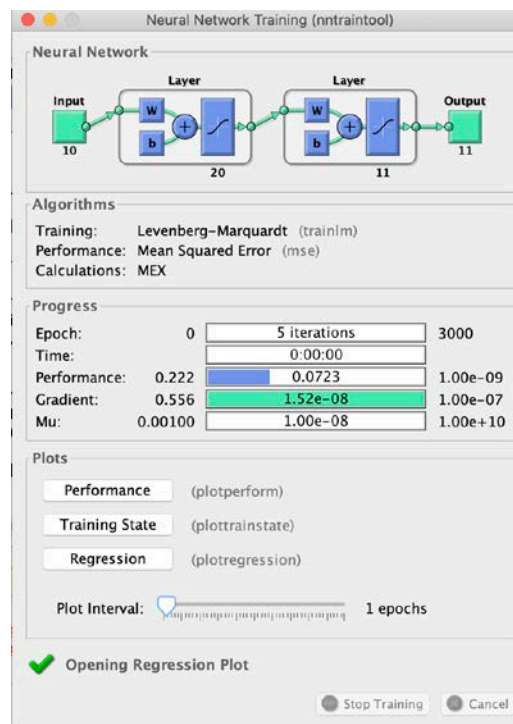The typical performance is shown in Figure 5-4.

Figure 5-4 Typical performance of machine learning

Iterations are calculated based on the values of MiniBatchSize, epochs mentioned in the trainingOptions and the number of training samples. An iteration is one step taken in the gradient descent algorithm towards minimizing the loss function using a mini-batch. An epoch is the full pass of the training algorithm over the entire training set. Gradient means the rate of inclination or declination of a slope.

Iterations per epoch = Number of training samples ÷ MiniBatchSize i.e.,

174

In how many iterations in an epoch the forward and backward pass takes place during training the network.

Iterations = Iterations per epoch * Number of epochs

If number of epochs is = n then it means that the network is trained with same data n times.

5.3   Validation

The estimated results from the deep machine learning Neural Networks is compared against the expected values of the outputs as shown in Figure 5-6 with the mapping results demonstrated in Figure 5-6. After only four interaction, the convergence is achieved with the reliability indices for each case presented in Figure 5-7, which reflects that the proposed method is promising of a better result in convergence by being faster, more accurate as well as more stable. In addition, to verify the effectiveness and accuracy of the proposed method, the comparison between estimated reliability indices obtained from β-unzipping method and deep machine learning can be found in Table 5-8.

It is observed that the errors between simulated and estimated reliability indices for each different element in different cases of two scenarios are mostly less than 3% with some are event achieved at almost no differences, the proposed method is validated against the β-unzipping method presented in Hashemolhosseini (2013). It is noted the relatively high training error for the Element 2 with 6.62% and Element 10 with 5.82%. The reason is given due to the lack of primary data set that possibly cause some error in mapping the population and thus giving the testing output of Neural Networks not accurate. However, considering the fact that they are all less then 10%, which is relatively accepted in deep machine learning with small input data, the proposed method proved their competences and operatives in practice.
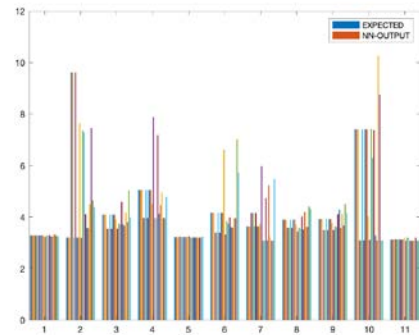
175
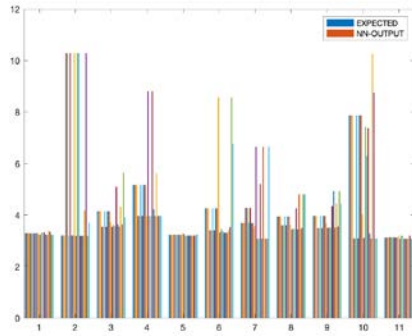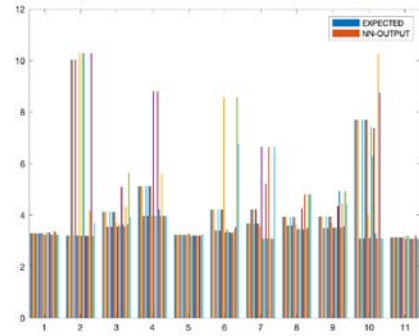
(a) Interaction 1
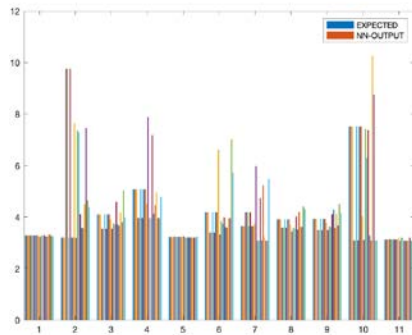
(b) Interaction 2

(c) Interaction 1
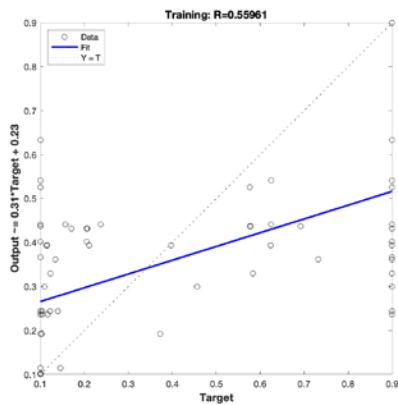

(d) Interaction 2

Number 1 to 11 represents reliability indexes of represents the reliability indexes of either element or critical pairs in Ei scenario. Each column in Number i represents the results obtained from interaction j until there is a converge in training process.

Figure 5-5 Comparison of Predicted and Calculated Outputs

Gradient descent is an iterative optimization algorithm used in machine learning to find the best results (minima of a curve). The algorithm is iterative means that we need to get the results multiple times to get the most optimal result. The iterative quality of the gradient descent helps under-fitted graph to make the graph fit optimally to the data. The Gradient descent has a parameter called learning rate. Initially the steps are bigger that means the learning rate is higher and as the point goes down the learning rate becomes more smaller by the shorter size

176

of steps. Also, the Cost Function is decreasing, or the cost is decreasing. One Epoch is when an entire dataset is passed forward and backward through the neural network only once. As the number of epochs increases, more number of times the weight are changed in the neural network and the curve goes from underfitting to optimal to overfitting curve.
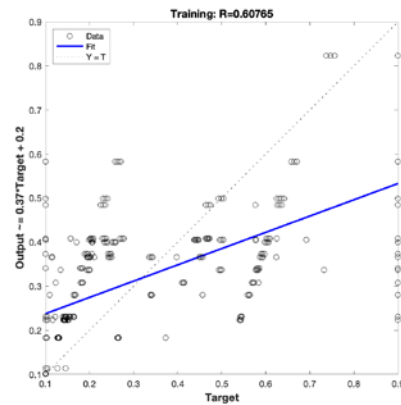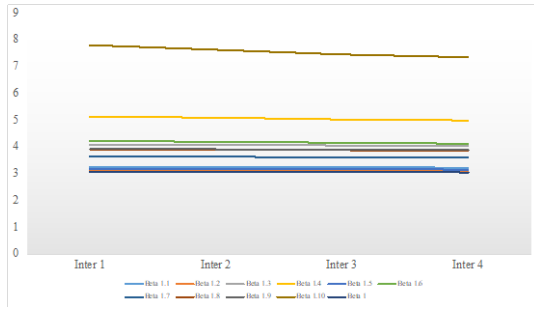

(a) Interaction 1
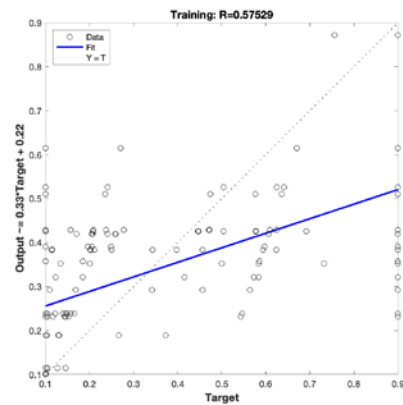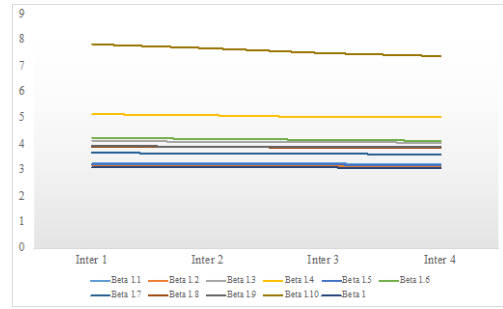
(b) Interaction 2
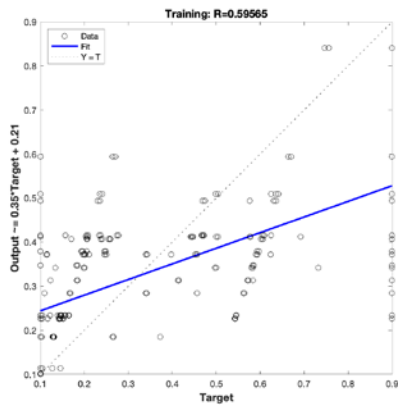
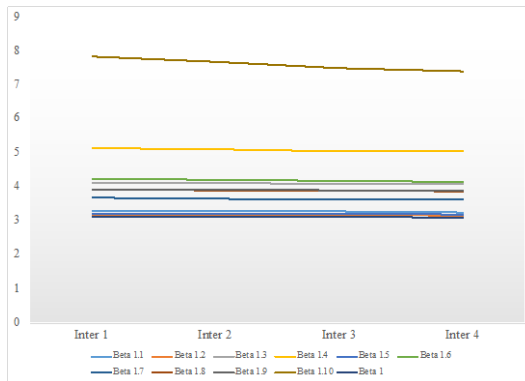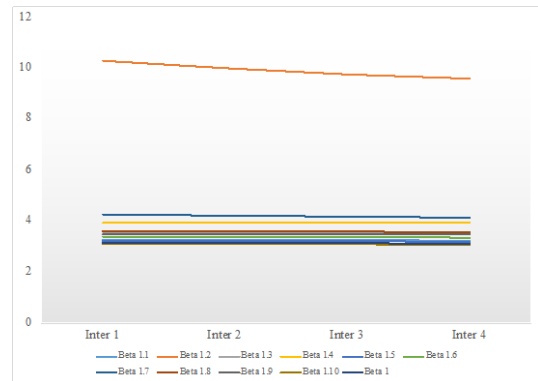(c) Interaction 3

(d) Interaction 4
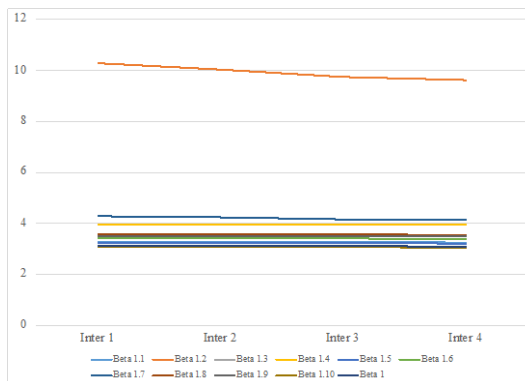
Figure 5-6 Data Mapping of 1ˢᵗ Epoch

(a) Case 1

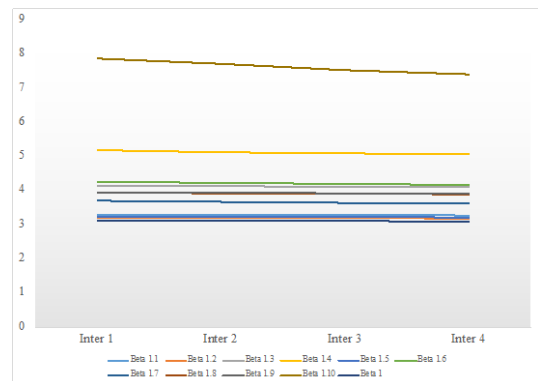
(b) Case 2

(c) Case 3

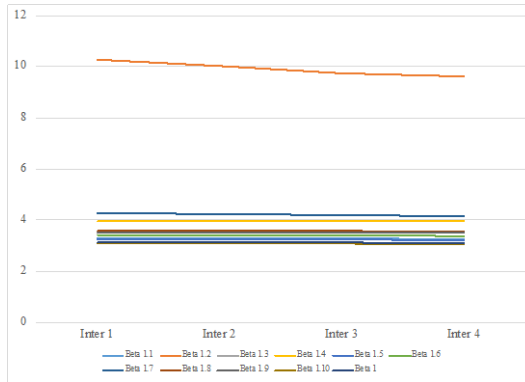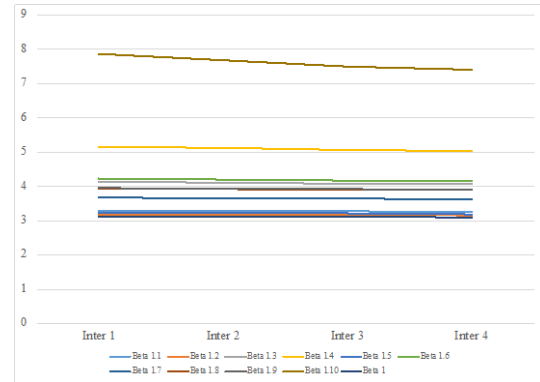(d) Case 4

(e) Case 5

(f) Case 6

(g) Case 7   (h) Case 8
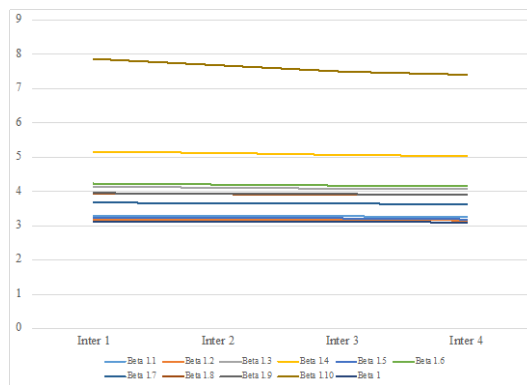
(i)   Case 9

Figure 5-7 Fluctuation of NN-outputs

Table 5-8 Differences between NN-outputs and β-unzipping estimation (%)

	Beta 1	Beta 2	Beta 3	Beta 4	Beta 5	Beta 6	Beta 7	Beta 8	Beta 9	Beta 10	Beta
7 Fail	0.18	0.04	1.40	2.24	0.09	2.14	1.59	1.22	1.14	5.82	0.15
2 Fail	0.18	0.04	1.40	2.24	0.09	2.14	1.59	1.22	1.14	5.82	0.15
10 Fail	0.17	6.62	0.00	0.00	0.11	0.28	2.68	0.42	0.00	0.01	0.20
7-10 Fail	0.17	6.62	0.00	0.00	0.11	0.28	2.68	0.42	0.00	0.01	0.20
7-2 Fail	0.18	0.04	1.40	2.24	0.09	2.14	1.59	1.22	1.14	5.82	0.15
10-1 Fail	0.17	6.62	0.00	0.00	0.11	0.28	2.68	0.42	0.00	0.01	0.20
2-1 Fail	0.18	0.04	1.40	2.24	0.09	2.14	1.59	1.22	1.14	5.82	0.15
2-5 Fail	0.18	0.04	1.40	2.24	0.09	2.14	1.59	1.22	1.14	5.82	0.15

The final estimation of reliability index for each element of convergence is presented below.

According to this estimation, the structural system reliability analysis is Min (β_i) = 3.2013.

Comparing against the structural system reliability analysis of Hashemolhosseini (2013), the

difference is only 3.46% – 3.95% at level 0 to level 2, respectively. It is interesting that the

179

error is only 0.03% at Level 3, which is relatively excellent. For this reason, this study rejected the claim of Thoft-Christensen and Murotsu (2012) that "the total number of mechanisms for a real structure is usually too high to include all possible mechanism". Accordingly, rather than including only most dominant mechanisms as what has been currently done in literature, the propose method allows the system modelling at mechanism level as thus, it is possible to estimate the structural system reliability at mechanism level.

Table 5-9 Predicted reliability indices

Beta 1	Beta 2	Beta 3	Beta 4	Beta 5	Beta 6	Beta 7	Beta 8	Beta 9	Beta 10	Beta
3.2887	3.2013	4.0867	5.0497	3.2263	4.1646	3.6335	3.8945	3.9139	7.4089	3.1250

Table 5-10 Compared predicted results against Hashemolhosseini (2013)

Hashemolhosseini (2013)				Predicted results	
Level 0	Level 1	Level 2	Level 3	B Min	B predicted
3.0797	3.0797	3.0942	3.2003		
Error for B Min (%)				3.2013	3.1250
3.95	3.95	3.46	0.03		
Error for B predicted (%)					
1.47	1.47	0.99	-2.35		

6 System Reliability for CFTA Girder under Blast Loading

Buildings have typically been the focus of blast damage analysis, but it is valuable to extend these analyses to bridge structures for several reasons (Wei et al., 2007; Quintero et al., 2007). The social and economic impact of removing bridges from service in the event of damage is significant (Rodrigue and Notteboom, 2013). In accordance to Thomas et al. (2018), bridges are also in most cases easily accessible, relatively unsecured, and subject to limited surveillance. Vehicular impact is the third leading cause of bridge damage or failure; and damage in vehicle-bridge impact events occurs simultaneously to the vehicle and the bridge element as a result of the compliance of the vehicle (Yi et al., 2014). Though short in duration, blast loadings are particularly catastrophic due to their high intensity. An explosive blast results in a very high-velocity shock wave, which is the primary cause of damage; if the charge weight and standoff distance are known, then it is possible to estimate the resulting damage to a structure. Taking interest into the field, the study employed the proposed system reliability assessment employed Monte Carlo Simulation and Neural Networks to examine the effects of blast loading on the structural reliability of a steel tubular filled concrete CFTA) girder. To that end, this section will discuss:

- The structural modelling of the CFTA including its FE model and Blast Loading
- The structural response of the CFTA girder under the investigated blast loading
- The probability of failure for the CFTA as a structural system subjected to blast loading

6.1 Structural Model

6.1.1 CFTA Model

The FE model has been developed using ABAQUS software for the CFTA comprised of four main components: tubular steel frame, concrete arch, PS tendon and concrete slab (Figure 6-1) with properties shown in Table 6-1. The shape and concept of CFTA girder are shown in Figure

181

6-2. The arch shape is constructed by concrete blocks in order to transfer the self-weight load to the arch rib. These blocks are filled by pumping concrete into the tubular steel frame. The steel frame protects the concrete blocks as well as forms the shape of CFTA girder. Inside each block, there is a hollow space holding the concrete creating a very efficient composite section. Pre-stressing force is applied on tendons in two construction stages: two inner PS tendons are tensioned in the first stage after constructing the arch girder and the two outer ones are tensioned in the next stage after pouring concrete of the slab. The second pre-stressing force is active after the girder is mounted on the abutment.

Thicknesses of the steel frame were 10, 12, and 22 (mm) and modeled as shell element and homogeneous steel section. Pre-stressing forces for the tendons (two inside and two outside) were 844.57 and 441.16 (MPa), respectively. The slab was modeled as solid elements and the reinforcing bars were embedded as the two-node linear 3-D truss elements. The nonlinear mechanical properties of steel and tendon used in the simulation are presented in Table 6-2. For slab and arch blocks, a conventional type of concrete (Table 6-3) is considered. The Poisson's ratios are 0.167 and 0.3 for steel, tendon and for concrete, respectively. The density values are 78.5, 80 and 25(kN/m^3) for the steel, tendon and concrete, respectively. The applied load causes approximately the same bending moment and axial force as that caused by the design truckload in the experiment (at the middle of the girder). Additionally, the FE model accounts for the construction steps by reflecting the net displacements of three stages (two tensioning stages and slab casting stage), which are 37.9, 23.9 and 65.0 (mm), respectively.

(a) Slab   (b) Filled concrete

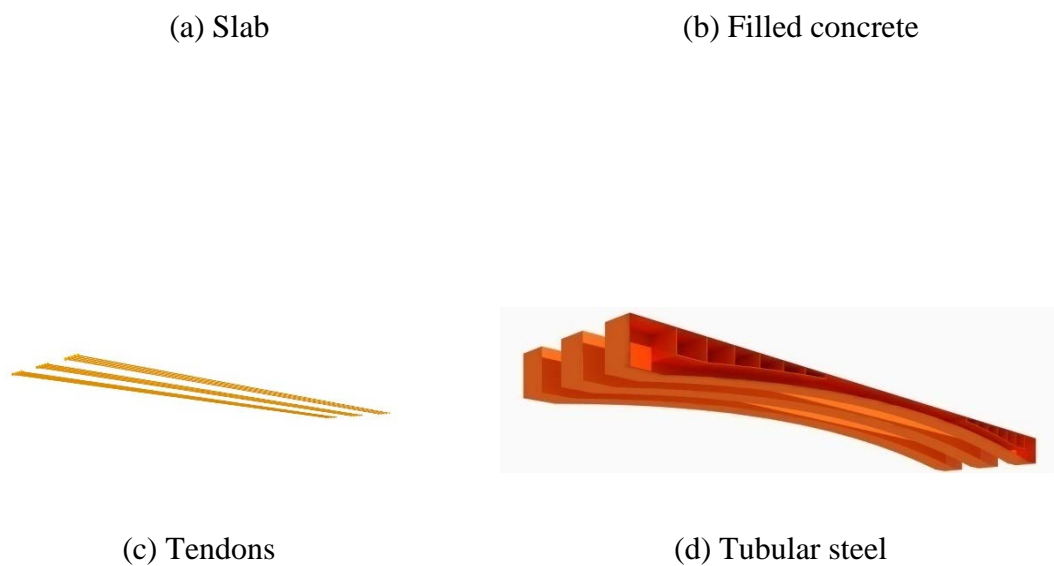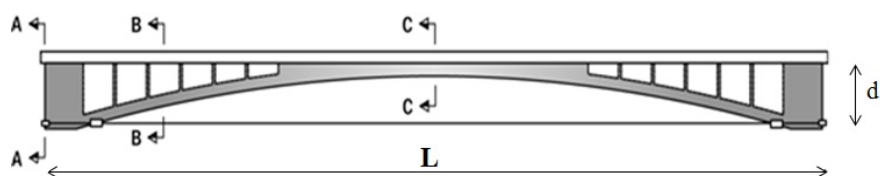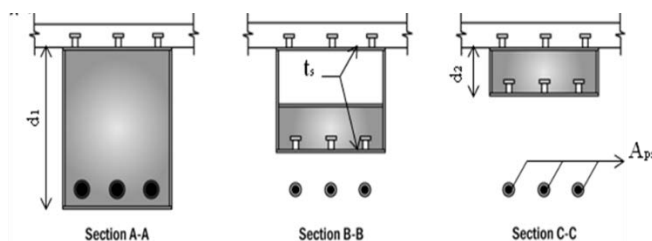(c) Tendons   (d) Tubular steel
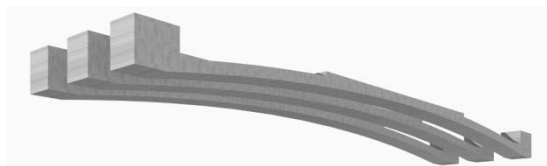
Figure 6-1 Components of CFTA girder bridge

(a) Longitudinal section

(b) Cross section

Figure 6-2 Concept diagram of CFTA

Table 6-1 Properties of CFTA components

Component	Element code	Dimension	Element type	Note

Concrete slab	C3D8R		Solid	Reduced integration with hourglass control
Rebar	T3D2	8 in radius	2-node linear 3D Truss	Total 30 reinforcing bars
Concrete block	C3D8R		Solid	Created by pumping and confining into steel frame
Steel block	S4R		Shell	Homogenous steel sections with 10, 12 and 22 mm thickness
Pre-stressed Tendon	T3D2	46 in radius	Beam/truss	Pre-stress for 2 inners and 2 outers are 844.57 and 441.16 (MPa)

Note:

- *Due to the fact that the clearance – distance separating two surfaces – between the concrete and steel must be zero, constraint contact is applied to simulate the simultaneous working between steel frame and filled concrete. This constrain section uses tie constrains (type 07) to tie together two surfaces for the duration of a simulation. This is the surface-to-surface constraints enforcement method in which steel plates will be the master surface while concrete will be the slave surfaces.*

- *The two ends of all 4 tendons are constrained in the composite CFTA surfaces by the kinematic coupling type, with constrained U1, U2 and U3 degrees of freedom.*

Table 6-2 Properties of steel and tendon

Material	Yield stress	Plastic strain
	MPa	mm

	392.4	0.000
Steel	392.4	0.018
	539.6	0.167
	1700	0.000
	1920	0.002
Tendons	2050	0.010
	2100	0.019
	2150	0.039

Table 6-3 Properties of slab and arch block

Compressive Behaviour (MPa)			
Concrete on slab		Concrete on arch block	
Yield stress	Inelastic strain	Yield stress	Inelastic strain
15.3404	0.00000	22.5850	0.00000
26.4416	0.00022	38.0605	0.00016
29.5620	0.00045	43.1281	0.00034
30.6807	0.00076	45.1701	0.00006
29.8659	0.00109	44.2443	0.00009

27.2497	0.00150	40.9871	0.00124
15.3404	0.00262	22.5850	0.00237
2.2704	0.00521	2.1342	0.00514
0.4023	0.01029	0.3498	0.01021

Table 6-4 PS Tendon specification (mm)

Girder		Width	2000
	Depth	End of span	1750
		Middle of span	580
Slab		Effective width	3500
		Thickness	240
Steel Plate	Thickness at the middle of span	Top flange	18
		Bottom flange	18
		Web	10
PS Tendon		Inners	SWPC 7B Φ15.2 19 strands × 2 ducts
		Outers	SWPC 7B Φ15.2 12 stands × 2 ducts

In this study, a FE model using ABAQUS software has been developed and validated against an experimental test presented by Vu et al. (2012) towards a real-scale specimen with a single span bridge of 30.6 m-length has been constructed at Korea Institute of Construction Technology (KICT), South Korea.

6.1.2 Blast Loading

This study uses CONWEB model that applies curve-fitting techniques to represent the data with high-order polynomial equations to define the blast loading applied to the structure. It is well accepted in literature that comparing to other methods, CONWEP takes a realistic approach, assuming an exponential decay of the pressure with time:

$$P(t) = P_{inc} \left[1 - \frac{t - t_a}{t_+} \right] exp \left[- \frac{a(t - t_a)}{t_+} \right]$$

The objective of this algorithm is to produce an appropriate pressure history given an equivalent TNT explosive weight. The quantities to be determined by the algorithm are:

- P_{inc} : maximum incident pressure

- P_{ref} : maximum reflected pressure

- t_a : time of arrival of the shock wave

- $-t_+$: positive phase duration

- a, b : exponential decay factors (wave form numbers) for incident and reflects waves, respectively

- R : range from charge location to the centroid of loaded surface,

- $cos\theta$: cosine of the incident angle; angle between surface normal and range unit vector.

6.2 Structural reliability analysis

The framework to assess the structure system reliability employed for the CFTA girder using the proposed method presented earlier in Chapter 4 is a combination of the Monte Carlo Simulation - Neural Network, structural system reliability and progressive collapse assessment approach. The Monte Carlo Simulation and Neural Network is intended to predict the failure probability of the uncertain structural system while the progressive collapse assessment is employed as a deterministic analysis to check if the sample point falls into the failure region.

One of the intrinsic characteristics of the blast loads is its high magnitude and short duration. For these reasons, the responses of the structural buildings under blast loads can be divided in two stages:

- The direct response of structure against blast loads is mainly associated with structural components. Due to the large mass of floor slabs, which provide large inertia resistant to blast, the responses at the floor level are small.

- If the structural member loses its load-carrying capacity, structural progressive collapse might be triggered due to the insufficient of structural integrity.

Therefore, the analysis of structural system reliability under blast load involves the following three steps: (1) determine the blast load (2) calculate the structural member response against blast loads (3) post- assessment of the damaged structure; and (4) employing the proposed system reliability analyse using MCS and NNs.

Terrorist scenarios of Vehicle Borne Improvised Explosive Device (VBIED) are considered to reflect the reality of current terrorist threat (Sapir and Giangrande, 2009). Since the main objective of this study is concentrated on risk of structural collapse, the blast scenarios considered herein is truck-size home-made Ammonium Nitrate Fuel Oil (ANFO), detonated at various stand-off distances from the bridge. Not only a surface but also an air blast explosion

is considered in this study. If any components of the CFTA girder loses its load-carrying capacity under the blast loads, a post-blast assessment is carried out to investigate the collapse behaviour of the damaged structure.

6.2.1 Structural Response

The applied actions are defined in accordance to the Eurocode that includes:

- Self-weight
- Blast load

Blast load is employed following the CONWEP model described in Section 0 through a selection of an explosive charge mass (m) and/or standoff distance (r) enable the CFTA girder to be subjected to a range of blast load intensities as shown in Figure 6-3 and Figure 6-4. There are two main scenarios employed for the variation of the blast load exposed on the structure: (1) with the fixed standoff distance (r); and vary the intensity of loading by varying the explosive charge weight (m); and (2) with the fixed charge mass (m) and vary the distance from the explosion to the structure (r). For the former case, three analyses are carried out with centre detonated, TNT cylindrical charges of 100, 500 and 900 kg. For the latter cases, three more analyses are carried out with the standoff distance from the detonation to the slab are 1, 2 and 3 meters. The identical set of explosions is shown in Table 6-5.

Table 6-5 Loading scenario

Case (No.)	TNT (kg)	Distance
1	100	1000
2	500	1000
3	900	1000

4	100	2000
5	500	2000
6	900	2000
7	100	3000
8	500	3000
9	900	3000
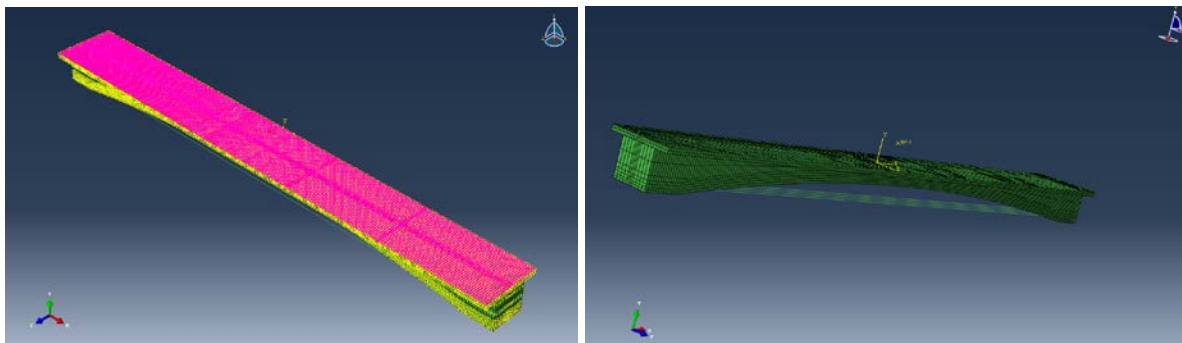
Figure 6-3 Response surface and standoff distance of explosion

Figure 6-4 Property of explosion

In this research, the main objective is to investigate the ability of the Neural Network either to perform the deterministic and probabilistic constraints check or to predict the structural collapse loads. To achieve such purpose, it is essential to first design the appropriate Neural

Network to effectively and efficiently estimate the probability of failure of the targeted structures.
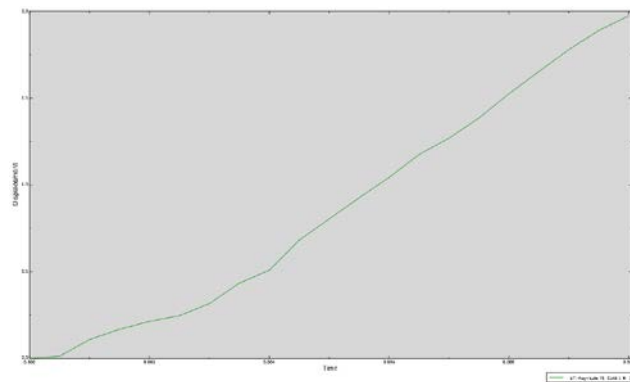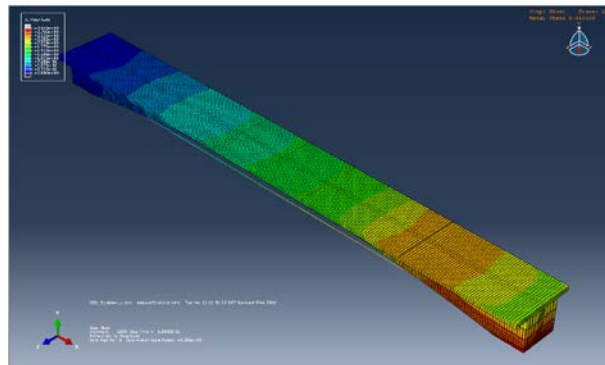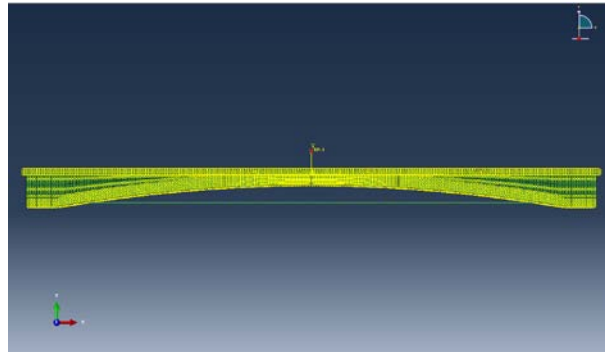
6.2.2 Reliability Assessment

This study uses the probability of structural collapse presented by Ellingwood et al. (2009), P(C), due to different damage scenarios, L, caused by multiple hazards, E, be expressed as:

191

$$P(C) = \sum_E \sum_L P(C|LE)P(L|E)P(E)$$

Equation 6-1

Where

- P(E) is the probability of occurrence of hazard E;

- P(L |E) is probability of local failure,

- L is the occurrence of E

- $P(C|LE)$ is the probability of structural collapse given the occurrence of a damage scenario L resulting from hazard, E.

The probability of collapse will be obtained by summing over all possible hazards and all possible load failure scenarios. The conditional probability of collapse term $P(C|LE)$ is related to the analysis of the response of the structure to a given damage scenario independently of what hazards have led to the damage.

In according to Starossek and Haberland (2009), the probability of progressive collapse can be minimised in three ways, namely by: controlling abnormal events, controlling local element behaviour and/or controlling global system behaviour. Controlling abnormal events by structural engineers is normally very difficult. However, engineers can influence the local and global system behaviour e.i. P(D|H) and P(C|DH).

The proposed method has the following process:

- *Step 1 - Training set selection step*

- *Step 2 - Deterministic constraints check*

- *Step 3 – Monte Carlo Simulation step*

- *Step 4 - Probabilistic constraints check*

- *Step 5 - Training step*

- *Step 6 - Testing step*

In accordance to the probabilistic model – Probabilistic model, the training set is built upon the results exported from the structural analysis by the FE model. After the selection of the appropriate Neural Network architecture towards the training procedure, the training process coded in MATLAB (shown in Appendix) is used to utilise information generated from this data set that consists of a number of property selected design vectors. This process includes both the deterministic and probabilistic constraints check through the optimization process in purpose of mapping the Input/Output function needed to predict the response of the structure upon the different set of design variables.

Particularly, in *training step – Step 5*, a trained Neural Network utilise information obtained from a number of random variables, which are computed through the FE model of the structural member through the deterministic and probabilistic constraints checks during the optimization process. The information generated from this step is needed in purpose of obtaining the necessary Input/Output pairs that should be subsequently employed for predict the output of the testing data set generated through Monte Carlo Simulation.

In *testing step – Step 6*, the Input/Output mapping function determined through Step 5 is employed in predict the responses of the structure through the deterministic and probabilistic constraints checks due to different sets of design variables. With the assigned limit state function, the training process is considered as successful if the estimated values resample

closely to the corresponding values, which are considered as "exact value". Otherwise, as the function of back-propagation algorithm, the network will go back to the *Step 5 – Training step* to repeat the entire loop until the criterion are met.

An estimation of the systems reliability at mechanism level is made from the application of Neural Networks Monte Carlo Simulation.

In regard to Hurtado and Alvarez (2001), multi-layer back-propagation algorithm is used in this study.

Literature has been indicated that the efficiency of a Neural Network training and learning process is much depended on the correct design of its learning rate, momentum and network architecture. However, there is a very limited number of researches and investigations guided on how to select these parameters. For this reason, the selection of a Neural Network used in this study is based on a trial and error procedure. This process comprises the following tasks:

- Select proper training set
- Find suitable network architecture
- Determine appropriate values of characteristic parameters, such as learning rate and momentum term

In order to achieve a good approximation of the probability of structural failure, it is a must to have a proper training set that consist of information covered the entire range of the Input/Output space. For this reason, selecting the appropriate Input/Output training data is considered as the important task that should take into account not only the training patterns but also the distribution of samples. In the present study the sample space for each random variable generated by Monte Carlo Simulation is divided into equally spaced distances for the application of the Neural Network simulation and for the selection of the suitable training pairs.

194

Moreover, the number of samples generated by Monte Carlo Simulation should be also selected through a trial-and-error procedure.

It is noted that Monte Carlo Simulation requires a number of limit elasto-plastic analyses (Zio, 2013), which are dealt independently and concurrently from the FE model under the different blast scenario. This process is considered as the nature of implementing Monte Carlo in simulation in regard to a parallel computing environment. In this study, it is done through the straightforward parallel implementation from assigning one limit-elasto-plastic analyses to a processor without any need of inter-processor communication during the analysis phase. The application of the properly selected and trained Neural Network in the approximate concepts is believed to possibly eliminate any limitation on the sample size presented in terms of Monte Carlo Simulation as well as on the dimensionality of the problem due to the drastic reduction of the needed computational cost (Cardoso et al., 2008).

In regard to Hurtado and Alvarez (2001), the basic NN configuration employed in this study is selected to have two hidden layers. In term of finding suitable network architecture, the number of neurons in the hidden layers are also be selected through a trial and error process. This can be done by first starting with an increased number of the hidden layer 1 and then, after the desired convergence is achieved, an increased number of the hidden layer 2 will be then performed until it also converged. This optimization process helps to find the minimal size of network that is able to perform the assigned task (Hirose et al., 1991).

6.2.3   System Reliability Estimation

The method for reliability estimation described in the previous sections is now applied in the case study of CFTA girder under blast loading based on a nonlinear finite element structural model. As it is quite difficult to compute the probability of failure for CFTA girder using the conventional procedure of reliability analysis, the convergence of the training process is rather

195

controlled by the prediction error between two trials by mean of the root mean square (RMS) given by:

$$e_{\text{RMS}} = \sqrt{\frac{1}{N_P N_{\text{out}}} \sum_{N_P} \sum_{i=1}^{N_{\text{out}}} (\text{tar}_i - \text{out}_i)^2},$$

Equation 6-2

in which, N_P denotes for the total number of Input/Output pairs in the training set, N_{out} denotes for the number of output units. e_{RMS} gives a measure of the difference between predicted value at each Neural Network cycle against value predicted in previous Neural Network cycle. After the selection procedure is completed and the appropriate architecture is designed for Neural Network training and learning process, this network is employed in producing approximation of the deterministic and probabilistic check in correspondence to the different set of Input/Output variables. Eventually, it is used to process the reliability assessment for the target structures by mean of Monte Carlo Simulation in calculating the probability of failure p_f and the reliability index β_f

The networks are trained with a training set representative of the structural response. More relevance is given to values situated in the upper extreme of the distribution, because it is important to obtain a precise approximation for those values as they influence greatly the probability of failure. Accordingly, the variation of nine possible values for applied blast load, related to the mean and the standard deviation of the probabilistic distribution of the lead is shown in Table 6-6.

Table 6-6 Variables of blast code and maximum displacement of slab

Case	TNT (kg)	Distance	Displacement

| (No.)			
1	100	1000	19.2874
2	500	1000	158.049
3	900	1000	407.045
4	100	2000	15.806
5	500	2000	78.3769
6	900	2000	139.016
7	100	3000	12.0571
8	500	3000	42.4978
9	900	3000	75.1271

The ultimate compressive strength reliability of a deck under a loading set is assed. The allowable deflection under Eurocode is between L/300 to L/500, for simple analysis, this study assumed this number as L/500. Accordingly, the maximum displaces employed is 30,000/500 = 60 (mm)

In order to design the architecture of the fully connected feed-forward learning process of the Neural Network described in Figure 2-10, several variables of the networks were trained, each with a different number of neurons in the hidden layers. As for this case study, there is only one output layer, the number of neurons for the hidden layer 2 (S_2) is one; while the number of neurons for the hidden layer 1 (S_1) is defined through the sensitivity process starting by number two until when the convergence is achieved. Figure 6-5 demonstrates the performance of the Neural Network configuration using different numbers of hidden neurons for the hidden layer 1 – S_1. It can be seen that the convergence is reaching after a certain number of hidden units without any further improvements. The depicted results indicate that the selection of the best Neural Network is based upon the minimum error between two trials by mean of the root mean

square (RMS) given by Equation 6-2. Accordingly, the number of neutrons selected for the hidden layer 1 is eight.
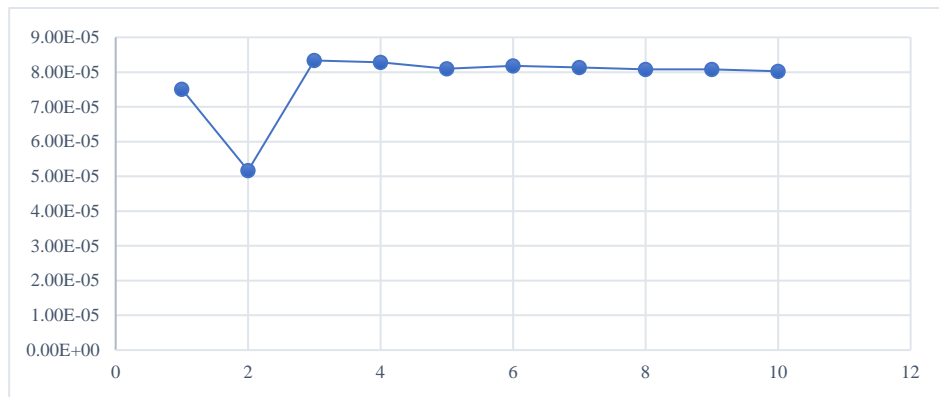
(a) Probability of failure
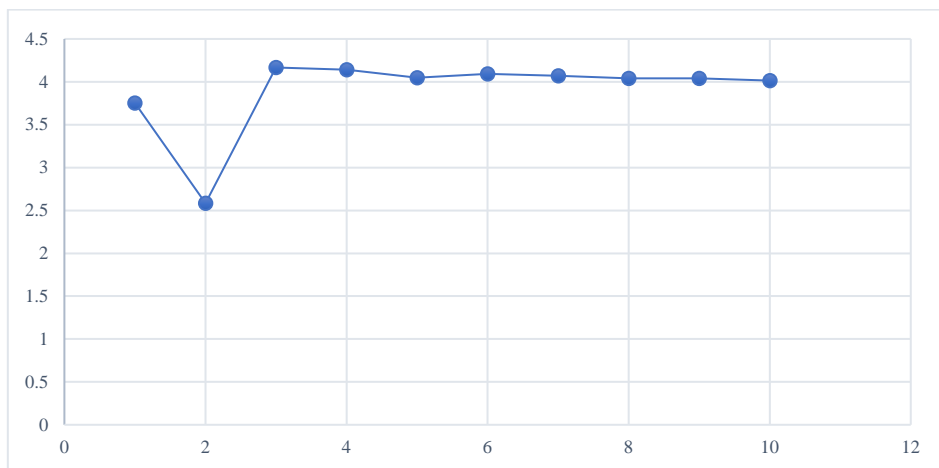
(b) Safety index

Figure 6-5 Performance of NN configuration with different hidden neurons

Using Neural Network with $S_1=8$, several Monte Carlo simulations are performed considering the probabilistic model – Case 1 presented in Section **Error! Reference source not found.**. The corresponding values of the probability of failure are shown in Table 6-7. In a similar procedure and criteria to select the number of neutrons in the hidden layer, the sample size depicted from the obtained results is $5x10^5$.

Table 6-7 Probability of failure computed with different sample size

Sample size	Probability of failure	Safety Index
5×10^2	8.60E-05	4.30
5×10^3	8.04E-05	4.02
5×10^4	8.08E-05	4.04
5×10^5	*8.01E-05*	*4.00*
5×10^6	8.01E-05	4.00

6.3 Summary

Once the acceptable trained Neural Network in predicting the critical load factors is obtained, the probability of failure for the slab of the CFTA girder is estimated by means of Neural Network based Monte Carlo Simulation. It is observed that the probability of failure of the structure, p_f, is found to be 8.01×10^{-5}, and the corresponding reliability index β is equal to 4.00. It is therefore clear that the level 1 methodology prescribed in the Eurocodes produces, in this case, a design safer than the limit $\beta = 3.8$ recommended for common structures. It has proved that the application of the proposed method allows a more rigorous design approach comparing to other methods presented in the Eurocode.

7 Conclusion

To estimate the structural system reliability, the existing researches have faced the challenges in the two most critical issues: firstly on the evaluation of the current employed numerical methods in assessing the probabilities of the second or higher order joint failure events with high efficiency and accuracy that are in demand to evaluate system reliability; secondly, there is no unique system reliability approximation formula, which can be evaluated efficiently with commonly used reliability methods. Added to this, in consideration of complex system, there is the challenges in identifying the component failure events characterized in terms of physical members, failure modes, failure locations, and time points of failure occurrences. For these reasons, the problem of system reliability for the complex structure has been negligible in literature with little or no progress up to recent. Accordingly, this thesis proposed an approach employing Monte Carlo Simulation and Neural Network (MCS-NN SSR) to effectively calculate the system reliability of the structural system, which is considered as the first approach ever proposed to solve the problem of structural system reliability at higher level than component-based approach. The proposed MCS-NN SSR used the mechanism modelling of the structure to simplify the structure system behaviour. In design of the deep learning algorithm used to test and train, several techniques are employed namely importance sampling, interval Monte Carlo Simulation and Mean-Interactive Neural Network. In order to determine the structural system reliability, the proposed method contains several stages from developing a computerised method for the system reliability analysis; estimating the structural system reliability at different level – demonstrated in this study level 0 (focusing on single structural element), level 1 (considering the structural system comprises of serial structural members), level 2 (on the basic of a system where the elements are parallel to each other- with critical pairs of failure elements) and level 3 (on the basic of a system where the elements are parallel systems each - with critical triples of failure elements) using the β-unzipping method

(introduced by Thoft-Christensen and Murotsu, 1986). Using such data, it is to generate the sample population by Monte Carlo Simulation with the response surface of the reliability indexes obtained that is then trained and tested the population using Neural Networks.

7.1 Key Findings

The proposed MCS-NN SSR was applied to estimate the structural system reliability for the 10-bar truss structure to validate its application against the convential β-unzipping method. The sensitivity analysis was also performed to observe the computing power in analysing the system reliability. After only four interactions, the convergence is achieved, which reflects that the proposed method is promising of a better result in convergence by being faster, more accurate as well as more stable. In addition, to verify the effectiveness and accuracy of the proposed method, the comparison between estimated reliability indices obtained from β-unzipping method and deep machine learning are also obtained. It is observed that the errors between simulated and estimated reliability indices for each different element in different cases of two scenarios are mostly less than 3% with some are event achieved at almost no differences, the proposed method is validated against the β-unzipping method.

After the validation, the proposed MCS-NN SSR was employed to assess the structure system reliability employed for the CFTA girder under the blast loading (explosion), such problem is also highlighted in the literature review as very challenging and up-to-recent, there has been no research investigated into the field. The Monte Carlo Simulation and Neural Network is intended to predict the failure probability of the uncertain structural system while the progressive collapse assessment is employed as a deterministic analysis to check if the sample point falls into the failure region. The analysis of structural system reliability under blast load involves the following three steps: (1) determine the blast load (2) calculate the structural

member response against blast loads (3) post-assessment of the damaged structure; and (4) employing the proposed system reliability analyse using MCS and NNs.

It is observed that the probability of failure of the structure, p_f is found to be 8.01×10^{-5}, and the corresponding reliability index β is equal to 4.00. It is therefore clear that the level 1 methodology prescribed in the Eurocodes produces, in this case, a design safer than the limit β $=3.8$ recommended for common structures. It has proved that the application of the proposed method allows a more rigorous design approach comparing to other methods presented in the Eurocode. Therefore, it is further recommended a modification in the current codes and standards to take into consideration of structure reliability not only as component-based assessment but also as mechanics-based system.

7.2   Recommendation for Future Work

In reliability assessment of structures, there are two levels of reliability analysis required to consider including (1) structural members reliability and (2) system reliability. This research has put an effort to solve the later problem by proposing the new method that involved Monte Carlo Simulation with the Importance Sampling Techniques and Neural Network with Back-Propagation Algorithm. Although the obtained results have shown a very promising application of the proposed method comparing to other methods presented in the Eurocode, there are more investigations needed to take a closer look at its employment to estimate the structural system reliability, specifically, when the blast loading involved. Accordingly, future works are recommended to stay focus on the blast responses of structures against blast loading at both component and system levels, in which, progressive collapse should be taken into account.

Reference

1. AASHTO, L., 2002. Standard specifications for highway bridges. *Officials, Seventeenth Edition, American Association of State Highway and Transportation Washington, DC*.

2. Abdelwahed, B., 2019. A review on building progressive collapse, survey and discussion. *Case Studies in Construction Materials*, *11*, p.e00264.

3. Acito, M., Stochino, F. and Tattoni, S., 2011. Structural response and reliability analysis of RC beam subjected to explosive loading. In *Applied Mechanics and Materials* (Vol. 82, pp. 434-439). Trans Tech Publications Ltd.

4. Adam, J.M., Parisi, F., Sagaseta, J. and Lu, X., 2018. Research and practice on progressive collapse and robustness of building structures in the 21st century. *Engineering Structures*, *173*, pp.122-149.

5. Adrees, A., 2017. Power System Modelling and SSR Analysis Methods. In *Risk Based Assessment of Subsynchronous Resonance in AC/DC Systems* (pp. 39-66). Springer, Cham.

6. Ang, G.L., Ang, A.H.S. and Tang, W.H., 1991, June. Multi-dimensional kernel method in importance sampling. In *Proc. 6th Int. Conf. on Applications of Statistics and Probability in Civil Engineering* (pp. 289-296).

7. Anthony, M. and Bartlett, P.L., 2009. *Neural network learning: Theoretical foundations*. cambridge university press.

8. ASCE (American Society of Civil Engineers), 2010. Minimum design loads for buildings and other structures. *Standard ASCE/SEI 7-10*.

9. ASCE-EWRI, 2005. The ASCE standardized reference evapotranspiration equation. *ASCE–EWRI Standardization of Reference Evapotranspiration Task Committe Rep.*

10. Ash, R.B., 2012. *Basic probability theory*. Courier Corporation.

11. Baker, W.E., 1973. *Explosions in air*. University of Texas press.

12. Barkhori, M., Shayanfar, M.A., Barkhordari, M.A. and Bakhshpoori, T., 2019. Kriging-Aided Cross-Entropy-Based Adaptive Importance Sampling Using Gaussian Mixture. *Iranian Journal of Science and Technology, Transactions of Civil Engineering*, *43*(1), pp.81-88.

13. Basler, E., 1960. *Analysis of Structural Safety*. ASCE Annual Convention, Boston, MA

14. Biggs, J.M. and Biggs, J.M., 1964. *Introduction to structural dynamics*. McGraw-Hill College.

15. Binder, K., Ceperley, D.M., Hansen, J.P., Kalos, M.H., Landau, D.P., Levesque, D., Mueller-Krumbhaar, H., Stauffer, D. and Weis, J.J., 2012. *Monte Carlo methods in statistical physics*(Vol. 7). Springer Science & Business Media.

16. Birolini, A., 2017. Reliability engineering: theory and practice. Springer.

17. BIS (2002). Eurocode — Basis of structural design. [Online]. Available at: https://www.unirc.it/documentazione/materiale_didattico/599_2010_260_7481.pdf Accessed 10 July 2017

18. Bogosian, D., Ferritto, J. and Shi, Y., 2002. *Measuring uncertainty and conservatism in simplified blast models*. Karagozian and Case Glendale CA. [Online]. Available at: http://www.dtic.mil/get-tr-doc/pdf?AD=ADA526954 Accessed 30 June 2017

19. Bucher, C.G., 1988. Adaptive sampling—an iterative fast Monte Carlo procedure. *Structural safety*, *5*(2), pp.119-126.

20. Byfield, M., Mudalige, W., Morison, C. and Stoddart, E., 2014. A review of progressive collapse research and regulations. *Proceedings of the Institution of Civil Engineers-Structures and Buildings*, *167*(8), pp.447-456.

21. Byun, J. and Song, J., 2017. Structural System Reliability, Reloaded. In *Risk and Reliability Analysis: Theory and Applications* (pp. 27-46). Springer International Publishing.

22. Byun, J.E., Noh, H.M. and Song, J., 2017. Reliability growth analysis of k-out-of-N systems using matrix-based system reliability method. *Reliability Engineering & System Safety*, *165*, pp.410-421.

23. Cabello, B., 2011. Dynamic stress analysis of the effect of an air blast wave on a stainless steel plate. *Rensselaer Polytechnic Institute Hartford, Connecticut*. [Online]. Available at: http://www.ewp.rpi.edu/hartford/~ernesto/SPR/Cabello-FinalReport.pdf

24. Cai, J.G., Xu, Y.X., Zhuang, L.P., Feng, J. and Zhang, J., 2012. Comparison of various procedures for progressive collapse analysis of cable-stayed bridges. *Journal of Zhejiang University SCIENCE A*, *13*(5), pp.323-334.

25. Campidelli, M., Razaqpur, A.G. and Foo, S., 2013. Reliability-based load factors for blast design. *canadian Journal of civil Engineering*, *40*(5), pp.461-474.

26. Cardoso, J.B., de Almeida, J.R., Dias, J.M. and Coelho, P.G., 2008. Structural reliability analysis using Monte Carlo simulation and neural networks. *Advances in Engineering Software*, *39*(6), pp.505-513.

27. Chang, F.K. and Kopsaftopoulos, F. eds., 2015. *Structural Health Monitoring 2015: System Reliability for Verification and Implementation*. DEStech Publications, Inc.

28. Chang, Y. and Mori, Y., 2013. A study on the relaxed linear programming bounds method for system reliability. *Structural Safety*, *41*, pp.64-72.

29. Chang, Y. and Mori, Y., 2014. A study of system reliability analysis using linear programming. *Journal of Asian Architecture and Building Engineering*, *13*(1), pp.179-186.

30. Charitha, M., Maiti, P.R. and Sashidhar, C., 2018. Experimental and Numerical Analysis of Structures Under Blast Loading-A Review. *i-Manager's Journal on Structural Engineering*, *7*(2), p.27.

31. Chassiakos, A.G. and Masri, S.F., 1996. Modelling unknown structural systems through the use of neural networks. *Earthquake engineering & structural dynamics*, *25*(2), pp.117-128.

32. Ching, J. and Hsieh, Y.H., 2007. Local estimation of failure probability function and its confidence interval with maximum entropy principle. *Probabilistic Engineering Mechanics*, *22*(1), pp.39-49.

33. Choi, B.S. and Song, J., 2017. Cross-entropy-based adaptive importance sampling for probabilistic seismic risk assessment of lifeline networks considering spatial correlation. *Procedia engineering*, *198*, pp.999-1006.

34. Chojaczyk, A.A., Teixeira, A.P., Neves, L.C., Cardoso, J.B. and Soares, C.G., 2015. Review and application of artificial neural networks models in reliability analysis of steel structures. *Structural Safety*, *52*, pp.78-89.

35. Chun, J., Song, J. and Paulino, G.H., 2015. Parameter sensitivity of system reliability using sequential compounding method. *Structural safety*, *55*, pp.26-36.

36. Chun, J., Song, J. and Paulino, G.H., 2019. System-reliability-based design and topology optimization of structures under constraints on first-passage probability. *Structural Safety*, *76*, pp.81-94.

37. Coccon, M.N., Song, J., Ok, S.Y. and Galvanetto, U., 2017. A new approach to system reliability analysis of offshore structures using dominant failure modes identified by selective searching technique. *KSCE Journal of Civil Engineering*, *21*(6), pp.2360-2372.

38. Coit, D.W. and Zio, E., 2019. The evolution of system reliability optimization. *Reliability Engineering & System Safety*, *192*, p.106259.

39. COMREL-TI Users Manual, *www.strurel.de*, RCP GmbH, Munich, 1992

40. ConWep blast simulation software, US Army Corps of Engineers, Vicksburg, MS

41. Cooper, P.W., 1996. *Explosives engineering*. Vch Pub.

42. Cornell, C.A., 1976. Requirements for probabilistic approach. *J. Amer. Concrete Inst.*

43. Corotis, R.B. and Nafday, A.M., 1989. Structural system reliability using linear programming and simulation. *Journal of Structural Engineering*, *115*(10), pp.2435-2447.

44. Der Kiureghian A (2006) Structural system reliability, revisited. Proceedings, 3rd ASRANet International Colloquium, Glasgow, UK, July 10–12, 2006 (CD-ROM)

45. Der Kiureghian, A. and Dakessian, T., 1998. Multiple design points in first and second-order reliability. *Structural Safety*, *20*(1), pp.37-49.

46. Der Kiureghian, A. and Song, J., 2008. Multi-scale reliability analysis and updating of complex systems by use of linear programming. *Reliability Engineering & System Safety*, *93*(2), pp.288-297.

47. Dharmasena, K.P., Wadley, H.N., Xue, Z. and Hutchinson, J.W., 2008. Mechanical response of metallic honeycomb sandwich panel structures to high-intensity dynamic loading. *International Journal of Impact Engineering*, *35*(9), pp.1063-1074.

48. Ding, H., Cai, Q., Zhang, Y. and Jiang, L., 2017, July. Passive System Reliability Analysis Based on Improved Support Vector Machine. In *International Conference on Nuclear Engineering*(Vol. 57823, p. V004T06A037). American Society of Mechanical Engineers.

49. Ditlevsen, O., 1979. Narrow reliability bounds for structural systems. *Journal of structural mechanics*, *7*(4), pp.453-472.

50. DOE/TIC-11268. A Manual for the Prediction of Blast and Fragment Loadings on Structures. [Online]. Available at: http://www.dtic.mil/dtic/tr/fulltext/u2/a476207.pdf Accessed 10 July 2017

51. Du, H. and Li, Z., 2009. Numerical analysis of dynamic behavior of RC slabs under blast loading. *Transactions of Tianjin University*, *15*(1), pp.61-64.

52. Dubourg, V. and Deheeger, F., 2011. Metamodel-based importance sampling for the simulation. *Applications of Statistics and Probability in Civil Engineering*, *26*, p.192.

53. Dueňas-Osorio, D.O., Craig, J.I. and Goodno, B.J., 2006. Tolerance of interdependent infrastructures to natural hazards and intentional disruptions. *Mid-America Earthquake Center Report*.

54. Durrett, R., 2010. *Probability: theory and examples*. Cambridge university press.

55. Dusenberry, D.O. ed., 2010. *Handbook for blast resistant design of buildings*. John Wiley & Sons.

56. Ellingwood, B., Marjanishvili, S., Mlakar, P., Sasani, M. and Williamson, E., 2009. Disproportionate collapse research needs. In *Structures Congress 2009: Don't Mess with Structural Engineers: Expanding Our Role* (pp. 1-12).

57. Ellingwood, B.R., 2006. Mitigating risk from abnormal loads and progressive collapse. *Journal of Performance of Constructed Facilities*, *20*(4), pp.315-323.

58. Engelund, S. and Rackwitz, R., 1993. A benchmark study on importance sampling techniques in structural reliability. *Structural safety*, *12*(4), pp.255-276.

59. Eurocode 1 (1994). Basis of design and actions on structures. European Committee for Standardization, Brussels

60. Eurocode 3 (1992). Design of Steel Structures. European Committee for Standardization, Brussels

61. Faber, M.H., 2009. *Basics of structural reliability*. Swiss Federal Institute of Technology ETH, Zürich, Switzerland.

62. Faber, M.H., 2012. Basic Probability Theory. *Statistics and Probability Theory*, pp.9-20.

63. Fu, F., 2013. Dynamic response and robustness of tall buildings under blast loading. *Journal of Constructional steel research*, *80*, pp.299-307.

64. Fu, G. and Moses, F., 1988, May. Importance sampling in structural system reliability. In *Probabilistic Methods in Civil Engineering* (pp. 340-343). ASCE.

65. Gao, X. and Li, S., 2017. Dominant failure modes identification and structural system reliability analysis for a long-span arch bridge. *Structural Engineering and Mechanics*, *63*(6), pp.799-808.

66. Gaspar, B., Naess, A., Leira, B.J. and Guedes Soares, C., 2011, January. Efficient system reliability analysis by finite element structural models. In *International Conference on Offshore Mechanics and Arctic Engineering* (Vol. 44342, pp. 693-702).

67. Gaspar, B., Naess, A., Leira, B.J. and Soares, C.G., 2014. System reliability analysis by Monte Carlo based method and finite element structural models. *Journal of offshore mechanics and Arctic engineering*, *136*(3).

68. Geyer, S., Papaioannou, I. and Straub, D., 2019. Cross entropy-based importance sampling using Gaussian densities revisited. *Structural Safety*, *76*, pp.15-27.

69. Ghosn, M. and Moses, F., 1998. NCHRP report 406: Redundancy in highway bridge superstructures. *Transportation Research Board, National Research Council, Washington, DC*.

70. Gilbert, R.I., 2011. The serviceability limit states in reinforced concrete design. *Procedia Engineering*, *14*, pp.385-395.

71. Goel, M.D. and Matsagar, V.A., 2013. Blast-resistant design of structures. *Practice Periodical on Structural Design and Construction*, *19*(2), p.04014007.

72. Goel, M.D., 2015. Blast: Characteristics, Loading and Computation—An Overview. In *Advances in Structural Engineering* (pp. 417-434). Springer, New Delhi.

73. Graves, T.L., Anderson-Cook, C.M. and Hamada, M.S., 2010. Reliability models for almost-series and almost-parallel systems. *Technometrics*, *52*(2), pp.160-171.

74. Greig, G.L., 1992. An assessment of high-order bounds for structural reliability. *Structural Safety*, *11*(3-4), pp.213-225.

75. Grierson, D.E., Safi, M., Xu, L. and Liu, Y., 2005a. Simplified methods for progressive-collapse analysis of buildings. In *Structures Congress 2005: Metropolis and Beyond* (pp. 1-8).

76. Grierson, D.E., Xu, L. and Liu, Y., 2005b. Progressive-failure analysis of buildings subjected to abnormal loading. *Computer-Aided Civil and Infrastructure Engineering*, *20*(3), pp.155-171.

77. Grooteman, F., 2011. An adaptive directional importance sampling method for structural reliability. *Probabilistic Engineering Mechanics*, *26*(2), pp.134-141.

78. GSA. (2000). Progressive Collapse analysis and design guidelines for new federal office buildings and major modernization projects, Office of Chief Architect, Washington, D.C.

79. GuhaRay, A., Mondal, S. and Mohiuddin, H.H., 2018. Reliability analysis of retaining walls subjected to blast loading by finite element approach. *Journal of The Institution of Engineers (India): Series A*, *99*(1), pp.95-102.

80. Haberland, M. and Starossek, U., 2009. Progressive collapse nomenclature. In *Structures Congress 2009: Don't Mess with Structural Engineers: Expanding Our Role* (pp. 1-10).

81. Hasofer, A.M. and Lind, N.C., 1974. Exact and invariant second-moment code format. *Journal of the Engineering Mechanics division*, *100*(1), pp.111-121.

82. Henchie, T.F., Yuen, S.C.K., Nurick, G.N., Ranwaha, N. and Balden, V.H., 2014. The response of circular plates to repeated uniform blast loads: An experimental and numerical study. *International Journal of Impact Engineering*, *74*, pp.36-45.

83. Hirose, Y., Yamashita, K. and Hijiya, S., 1991. Back-propagation algorithm which varies the number of hidden units. *Neural Networks*, *4*(1), pp.61-66.

84. Hu, Z. and Mahadevan, S., 2016. Resilience assessment based on time-dependent system reliability analysis. *Journal of Mechanical Design*, *138*(11).

85. Hurtado, J.E. and Alvarez, D.A., 2001. Neural-network-based reliability analysis: a comparative study. *Computer methods in applied mechanics and engineering*, *191*(1), pp.113-132.

86. Jimenez-Rodriguez, R. and Sitar, N., 2007. Rock wedge stability analysis using system reliability methods. *Rock Mechanics and Rock Engineering*, *40*(4), pp.419-427.

87. Johari, A. and Lari, A.M., 2016. System reliability analysis of rock wedge stability considering correlated failure modes using sequential compounding method. *International Journal of Rock Mechanics and Mining Sciences*, *82*, pp.61-70.

88. Johari, A. and Rahmati, H., 2019. System reliability analysis of slopes based on the method of slices using sequential compounding method. *Computers and Geotechnics*, *114*, p.103116.

89. Kang, W.H. and Kliese, A., 2014. A rapid reliability estimation method for directed acyclic lifeline networks with statistically dependent components. *Reliability Engineering & System Safety*, *124*, pp.81-91.

90. Kang, W.H., Lee, Y.J., Song, J. and Gencturk, B., 2012. Further development of matrix-based system reliability method and applications to structural systems. *Structure and Infrastructure Engineering*, *8*(5), pp.441-457.

91. Kang, W.H., Song, J. and Gardoni, P., 2008. Matrix-based system reliability method and applications to bridge networks. *Reliability Engineering & System Safety*, *93*(11), pp.1584-1593.

92. Kapur, K.C. and Pecht, M., 2014. *Reliability engineering*. John Wiley & Sons

93. Karayiannis, N. and Venetsanopoulos, A.N., 2013. *Artificial neural networks: learning algorithms, performance evaluation, and applications* (Vol. 209). Springer Science & Business Media.

94. Kim, D.S., Ok, S.Y., Song, J. and Koh, H.M., 2013. System reliability analysis using dominant failure modes identified by selective searching technique. *Reliability Engineering & System Safety*, *119*, pp.316-331.

95. Kim, D.S., Ok, S.Y., Song, J. and Koh, H.M., 2013. System reliability analysis using dominant failure modes identified by selective searching technique. *Reliability Engineering & System Safety*, *119*, pp.316-331.

96. Kim, J. and Kim, T., 2009. Assessment of progressive collapse-resisting capacity of steel moment frames. *Journal of Constructional Steel Research*, *65*(1), pp.169-179.

97. Kim, J.P., Vlahopoulos, N. and Zhang, G., 2012. Development of a blast event simulation process for multi-scale modelling of composite armour for lightweight vehicles. *International Journal of Vehicle Design*, *61*(1-4), pp.157-176.

98. Kingery, C.N. and Bulmash, G., 1984. *Airblast parameters from TNT spherical air burst and hemispherical surface burst*. US Army Armament and Development Center, Ballistic Research Laboratory.

99. Kounias, E.G., 1968. Bounds for the probability of a union, with applications. *The Annals of Mathematical Statistics*, *39*(6), pp.2154-2158.

100. Kurtz, N. and Song, J., 2013. Cross-entropy-based adaptive importance sampling using Gaussian mixture. *Structural Safety*, *42*, pp.35-44.

101. Kurtz, N.S., 2011. System reliability analysis of structures subjected to fatigue induced sequential failures using evolutionary algorithms.

102. Lahiri, S.K. and Ho, L., 2011, May. Simulation of rapid structural failure due to blast loads from conventional weapons (CONWEP). In *Proceedings of the NAFEMS World Congress*.

103. Lemaire, M., 2013. *Structural reliability*. John Wiley & Sons.

104. Li, Z., Xu, T., Gu, J., Dong, Q. and Fu, L., 2018. Reliability modelling and analysis of a multi-state element based on a dynamic Bayesian network. *Royal Society open science*, *5*(4), p.171438.

105. Liu, H., 2011. Soil-structure interaction and failure of cast-iron subway tunnels subjected to medium internal blast loading. *Journal of Performance of Constructed Facilities*, *26*(5), pp.691-701.

106. Low, H.Y. and Hao, H., 2002. Reliability analysis of direct shear and flexural failure modes of RC slabs under explosive loading. *Engineering Structures*, *24*(2), pp.189-198.

107. Madsen, H.O., Krenk, S. and Lind, N.C., 1986. Methods of structural safety. Englewood Cliffs, NJ: Prentice-Hall

108. Marjanishvili, S. and Agnew, E., 2006. Comparison of various procedures for progressive collapse analysis. *Journal of Performance of Constructed Facilities*, *20*(4), pp.365-374.

109. Marjanishvili, S.M., 2004. Progressive analysis procedure for progressive collapse. *Journal of Performance of Constructed Facilities*, *18*(2), pp.79-85.

110. Markose, A. and Rao, C.L., 2017. Mechanical response of V shaped plates under blast loading. *Thin-Walled Structures*, *115*, pp.12-20.

111. Markova, J. and Holicky, M., 2017. Probabilistic Analysis of Combination Rules in Eurocodes. In *14th International Probabilistic Workshop* (pp. 461-469). Springer International Publishing.

112. Melchers, R.E. and Beck, A.T., 2018. *Structural reliability analysis and prediction*. John wiley & sons.

113. Miao, F. and Ghosn, M., 2016. Reliability-based progressive collapse analysis of highway bridges. *Structural safety*, *63*, pp.33-46.

114. Miller, D., Pan, H., Nance, R., Shirley, A. and Cogar, J., 2010. A coupled Eulerian/Lagrangian simulation of blast dynamics. In *Proceedings of the IMPLAST 2010 conference October* (pp. 12-14).

115. Modarres, M., Kaminskiy, M.P. and Krivtsov, V., 2016. *Reliability engineering and risk analysis: a practical guide*. CRC press.

116. Moore, R.E., Kearfott, R.B. and Cloud, M.J., 2009. *Introduction to interval analysis*. Society for Industrial and Applied Mathematics.

117. Mougeotte, C., Carlucci, P., Recchia, S. and Ji, H., 2010. *Novel approach to conducting blast load analyses using Abaqus/Explicit-CEL*. Army Armament Research Development and Engineering Center Picatinny Arsenal NJ. [Online]. Available at: http://www.dtic.mil/get-tr-doc/pdf?AD=ADA558175 Accessed 30 June 2017

118. Müller, B., Reinhardt, J. and Strickland, M.T., 2012. *Neural networks: an introduction*. Springer Science & Business Media.

119. Naess, A., Leira, B.J. and Batsevych, O., 2009. System reliability analysis by enhanced Monte Carlo simulation. *Structural safety*, *31*(5), pp.349-355.

120. Naess, A., Leira, B.J. and Batsevych, O., 2012. Reliability analysis of large structural systems. *Probabilistic Engineering Mechanics*, *28*, pp.164-168.

121. Nafday, A.M., Corotis, R.B. and Cohort, J.L., 1987. Failure mode identification for structural frames. *Journal of Structural Engineering*, *113*(7), pp.1415-1432.

122. Nale, M., Chiozzi, A. and Tralli, A., 2019, September. Stochastic Seismic Assessment of Bridge Networks by Matrix Based System Reliability Method. In *Conference of the Italian Association of Theoretical and Applied Mechanics* (pp. 1559-1566). Springer, Cham.

123. Netherton, M.D. and Stewart, M.G., 2016. Risk-based blast-load modelling: Techniques, models and benefits. *International Journal of Protective Structures*, *7*(3), pp.430-451.

124. Neumaier, A. and Neumaier, A., 1990. *Interval methods for systems of equations* (Vol. 37). Cambridge university press.

125. Ngo, T., Mendis, P., Gupta, A. and Ramsay, J., 2007. Blast loading and blast effects on structures–an overview. *Electronic Journal of Structural Engineering*, *7*(S1), pp.76-91.

126. Nguyen, T.H., Song, J. and Paulino, G.H., 2010. Single-loop system reliability-based design optimization using matrix-based system reliability method: theory and applications. *Journal of Mechanical Design*, *132*(1).

127. Nikhil, G. and Narayanan, N.I., 2017. Interaction of Blast Load on AASHTO Girder Bridge. In *Applied Mechanics and Materials* (Vol. 857, pp. 131-135). Trans Tech Publications.

128. Okasha, N.M., 2016. System Reliability Based Multi-Objective Design Optimization of Bridges. *Structural Engineering International*, *26*(4), pp.324-332.

129. Papadrakakis, M. and Lagaros, N.D., 2002. Reliability-based structural optimization using neural networks and Monte Carlo simulation. *Computer methods in applied mechanics and engineering*, *191*(32), pp.3491-3507.

130. Papadrakakis, M., Papadopoulos, V. and Lagaros, N.D., 1996. Structural reliability analyis of elastic-plastic structures using neural networks and Monte Carlo simulation. *Computer methods in applied mechanics and engineering*, *136*(1-2), pp.145-163.

131. Paschenko, A.E., Pavlov, A.N., Pavlov, A.A., Slin'ko, A.A. and Masalkin, A.A., 2016. Research into Structural Reliability and Survivability of Complex Objects. In *Automation Control Theory Perspectives in Intelligent Systems*(pp. 463-473). Springer, Cham.

132. Protective Design Center, U. S. Army Corps of Engineers. ConWep, Conventional Weapons Effect. 2010. https://pdc.usace.army.mil/software/conwep/.

133. Quintero, R., Wei, J., Galati, N. and Nanni, A., 2007. Failure Modeling of Bridge Components Subjected to Blast Loading: Part II: Estimation of the Capacity and Critical Charge. *International Journal of Concrete Structures and Materials*, *1*(1), pp.29-36.

134. Rahimi, A., 2015. Evaluation of explosion loading effects on concrete infrastructures using ABAQUS software. *International Journal of Engineering & Technology*, *4*(1), pp.161-168.

135. Rajkumar, D., Senthil, R., Bala Murali Kumar, B., AkshayaGomathi, K. and Mahesh Velan, S., 2020. Numerical Study on Parametric Analysis of Reinforced Concrete

Column under Blast Loading. *Journal of Performance of Constructed Facilities*, *34*(1), p.04019102.

136. Ramachandran, K., 1990. Best ordering for system bounds. *Computers & structures*, *37*(3), pp.303-308.

137. Ramachandran, K., 2004. System reliability bounds: a new look with improvements. *Civil Engineering and Environmental Systems*, *21*(4), pp.265-278.

138. Rausand, M., 2014. Reliability of safety-critical systems: theory and applications. John Wiley & Sons.

139. Remennikov, A.M. and Rose, T.A., 2005. Modelling blast loads on buildings in complex city geometries. *Computers & Structures*, *83*(27), pp.2197-2205.

140. Rigby, S.E., Tyas, A. and Bennett, T., 2012. Single-degree-of-freedom response of finite targets subjected to blast loading–the influence of clearing. *Engineering Structures*, *45*, pp.396-404.

141. Rodrigue, J.P. and Notteboom, T., 2013. Transportation and economic development. *The Journal of Geography of Transportation*, pp.1-29.

142. Rojas, R., 2013. *Neural networks: a systematic introduction*. Springer Science & Business Media.

143. Rubinstein, R.Y. and Kroese, D.P., 2013. *The cross-entropy method: a unified approach to combinatorial optimization, Monte-Carlo simulation and machine learning*. Springer Science & Business Media.

144. Rubinstein, R.Y. and Kroese, D.P., 2016. *Simulation and the Monte Carlo method* (Vol. 10). John Wiley & Sons.

145. Sapir, G.I. and Giangrande, M.G., 2009. Explosives and Dangerous Chemicals: Constitutional Aspects of Search and Seizure. In *Aspects of Explosives Detection* (pp. 245-282). Elsevier.

146. Shallan, O., Eraky, A., Sakr, T. and Emad, S., 2014. Response of building structures to blast effects. *International journal of engineering and innovative technology ISSN*, pp.2277-3754.

147. Shi, Y. and Stewart, M.G., 2015. Spatial reliability analysis of explosive blast load damage to reinforced concrete columns. *Structural safety*, *53*, pp.13-25.

148. Shooman, M.L. (1968) Probabilistic reliability: An engineering approach, McGraw-Hill

149. Smith, P.D. and Hetherington, J.G., 1994. *Blast and ballistic loading of structures*. Digital Press.

150. Song, J. and Der Kiureghian, A., 2003. Bounds on system reliability by linear programming. *Journal of Engineering Mechanics*, *129*(6), pp.627-636.

151. Song, J. and Der Kiureghian, A., 2005, June. Component importance measures by linear programming bounds on system reliability. In *Proceedings of the 9th International Conference on Structural Safety and Reliability* (pp. 19-23).

152. Song, J. and Kang, W.H., 2009. System reliability and sensitivity under statistical dependence by matrix-based system reliability method. *Structural Safety*, *31*(2), pp.148-156.

153. Stern, R.E., Song, J. and Work, D.B., 2017. Accelerated Monte Carlo system reliability analysis through machine-learning-based surrogate models of network connectivity. *Reliability Engineering & System Safety*, *164*, pp.1-9.

154. Stevens, D., Crowder, B., Sunshine, D., Marchand, K., Smilowitz, R., Williamson, E. and Waggoner, M., 2011. DoD research and criteria for the design of buildings to resist progressive collapse. *Journal of Structural Engineering*, *137*(9), pp.870-880.

155. Stewart, M. and Melchers, R.E., 1997. Probabilistic risk assessment of engineering systems. Springer.

156. Stewart, M.G. and Netherton, M.D., 2014. Reliability-based design load factors for explosive blast loading. *Journal of Performance of constructed Facilities*, *29*(5), p.B4014010.

157. Stochino, F., 2016. RC beams under blast load: Reliability and sensitivity analysis. *Engineering Failure Analysis*, *66*, pp.544-565.

158. Suykens, J.A., Vandewalle, J.P. and de Moor, B.L., 2012. *Artificial neural networks for modelling and control of non-linear systems*. Springer Science & Business Media.

159. Syngellakis, S., 2013. Design Against Blast: Load Definition & Structural Response (Vol. 11). WIT Press.

160. Taranath, B.S., 2016. *Structural analysis and design of tall buildings: Steel and composite construction*. CRC press.

161. Thakkar, J.J., 2020. Introduction to Structural Equation Modelling. In *Structural Equation Modelling* (pp. 1-11). Springer, Singapore.

162. Thoft-Christensen, P. and Murotsu, Y., 2012. *Application of structural systems reliability theory*. Springer Science & Business Media.

163. Thomas, R.J., Steel, K. and Sorensen, A.D., 2018. Reliability analysis of circular reinforced concrete columns subject to sequential vehicular impact and blast loading. *Engineering Structures*, *168*, pp.838-851.

164. Tiwari, R., Chakraborty, T. and Matsagar, V., 2015. Dynamic Analysis of Curved Tunnels Subjected to Internal Blast Loading. In *Advances in Structural Engineering* (pp. 405-415). Springer, New Delhi.

165. Tomasson, E. and Söder, L., 2016. Improved importance sampling for reliability evaluation of composite power systems. *IEEE Transactions on Power Systems*, *32*(3), pp.2426-2434.

166.   Truong, V.H. and Kim, S.E., 2017. An efficient method of system reliability analysis of steel cable-stayed bridges. *Advances in Engineering Software*, *114*, pp.295-311.

167. UFC 3-340-02 (2008). Structure to resist the effects of accidental explosions. [Online]. Available at: ftp://ftp.analysischamp.com/books/ufc_3_340_02_pdf.

168.   Vu, T. D., 2019. Application of Neural Networks and Monte Carlo Simulation in Structural System Reliability Analysis. *The Sixteenth International Conference on Civil, Structural & Environmental Engineering Computing.* Italy

169.   Vu, T.D., Kim, D. and Cho, S.G., 2013. Updating of Analytical Model to Consider Aging Effects of Lead-Rubber Bearings for the Seismic Design of Base-Isolated Nuclear Power Plants. *Nuclear Technology*, *182*(1), pp.75-83.

170. Vu, T.D., Lee, S.Y., Chaudhary, S. and Kim, D., 2013. Effects of tendon damage on static and dynamic behavior of CFTA girder. *Steel and Composite Structures*, *15*(5), pp.567-583.

171.   Wang, H., Duan, F. and Ma, J., 2019. Reliability analysis of complex uncertainty multi-state system based on Bayesian network. *Eksploatacja i Niezawodność*, *21*.

172. Wang, Y., 2017. An enhanced Markov Chain Monte Carlo-integrated cross-entropy method with a partially collapsed Gibbs sampler for probabilistic spinning reserve adequacy evaluation of generating systems. *Electric Power Components and Systems*, *45*(15), pp.1617-1628.

173. Wang, Z. and Song, J., 2016. Cross-entropy-based adaptive importance sampling using von Mises-Fisher mixture for high dimensional reliability analysis. *Structural Safety*, *59*, pp.42-52.

174. Wei, J., Quintero, R., Galati, N. and Nanni, A., 2007. Failure modeling of bridge components subjected to blast loading part I: strain rate-dependent damage model for concrete. *International Journal of Concrete Structures and Materials*, *1*(1), pp.19-28.

175. Wei, P., Liu, F. and Tang, C., 2018. Reliability and reliability-based importance analysis of structural systems using multiple response Gaussian process model. *Reliability Engineering & System Safety*, *175*, pp.183-195.

176. Wei, P., Lu, Z. and Tian, L., 2013. Addition laws of failure probability and their applications in reliability analysis of structural system with multiple failure modes. *Proceedings of the Institution of Mechanical Engineers, Part C: Journal of Mechanical Engineering Science*, *227*(1), pp.120-136.

177. Wu, M., Jin, L. and Du, X., 2020. Dynamic responses and reliability analysis of bridge double-column under vehicle collision. *Engineering structures*, *221*, p.111035.

178. Xiao, N.C., Zhan, H. and Yuan, K., 2020. A new reliability method for small failure probability problems by combining the adaptive importance sampling and surrogate models. *Computer Methods in Applied Mechanics and Engineering*, *372*, p.113336.

179. Xu, J., Zhang, W. and Sun, R., 2016. Efficient reliability assessment of structural dynamic systems with unequal weighted quasi-Monte Carlo Simulation. *Computers & Structures*, *175*, pp.37-51.

180. Yalaoui, A., Chu, C. and Chatelet, E., 2005. Reliability allocation problem in a series–parallel system. *Reliability engineering & system safety*, *90*(1), pp.55-61.

181. Yang, D.Y., Teng, J.G. and Frangopol, D.M., 2015. Efficient adaptive importance sampling for time-dependent reliability analysis of structures.

182. Yi, Z., Agrawal, A.K., Ettouney, M. and Alampalli, S., 2014. Blast load effects on highway bridges. I: Modeling and blast load effects. *Journal of Bridge Engineering*, *19*(4), p.04013023.

183. Youn, B.D. and Wang, P., 2009. Complementary intersection method for system reliability analysis. *Journal of Mechanical Design*, *131*(4).

184. Zhang, H., Mullen, R.L. and Muhanna, R.L., 2010. Interval Monte Carlo methods for structural reliability. *Structural Safety*, *32*(3), pp.183-190.

185. Zhang, X., Gao, H., Huang, H.Z., Li, Y.F. and Mi, J., 2018. Dynamic reliability modeling for system analysis under complex load. *Reliability Engineering & System Safety*, *180*, pp.345-351.

186. Zhang, X., Wang, L. and Sørensen, J.D., 2020. AKOIS: an adaptive Kriging oriented importance sampling method for structural system reliability analysis. *Structural Safety*, *82*, p.101876.

187. Zio, E., 2013. System reliability and risk analysis. In *The Monte Carlo simulation method for system reliability and risk analysis* (pp. 7-17). Springer, London.

188. Zio, E., 2013. *The Monte Carlo simulation method for system reliability and risk analysis*. London: Springer.

Appendix 1

Blast Loading and Blast Impacts on Structure

Explosions caused by conventional weapons can cause severe damage to structures such as buildings, pipelines, bridges, vehicles etc., leading to significant loss of life and property. Engineers from military, automobile industry, oil and gas industry, nuclear industry, and several other organisations need to develop designs for blast mitigation. These designs must be validated either experimentally or using simulations. Experiments are expensive as they involve cost of material and instrumentations. Information from previous experiments is often not publicly available, because such tests are conducted by defence organisations or affiliated agencies and remain as classified information. Hence, simulations play an important role in validating structural designs against blast loads. Most of the simulations have been conducted using empirical models for blast phenomena, since detailed computational fluid dynamics (CFD) simulations become computationally expensive. One of the most commonly used models is the CONWEP model, initially developed by Kingery and Bulmash (1984). Simulations have been conducted using the Abaqus/Explicit software, where the blast loads were externally defined. Recently, this feature has been implemented as a built-in functionality in Abaqus/Explicit software (in version 6.10) making it convenient to subject models to diverse blast loads. Such simulations have been performed by several researchers such as Mougeotte et al. (2010); Cabello (2011); Henchie et al. (2014); Liu (2011); Kim, Vlahopoulos and Zhang (2012); Nikhil and Narayanan (2017); Rahimi (2015); Markose and Rao (2017); Tiwari, Chakraborty and Matsagar (2015).

Conventional Weapons and Blast Phenomena

Nuclear weapons, chemical weapons, and biological weapons are notorious for causing large scale mass destruction. Those weapons which do not cause large scale mass destruction and

223

yet are capable of causing significant damage to life and property are generically referred to as conventional weapons. In general, such explosions caused by land mine, non-nuclear bomb, shell, rocket, missile etc are listed as typical conventional weapons of which their threats are defined by Goel (2015) through two equally important factors – (1) W: the size of bombs and the charging weight of bombs; and (2) R: the standoff distances between the targeted subjects and the blast sources as demonstrated in Figure 0-1. Typical examples are explained by Ngo et al. (2007) that the blast occurred at the basement of World Trade Centre in 1993 has the charge weight of 816.5 kg TNT; Shallan et al. (2004) that the Oklahoma bomb in 1995 has a charge weight of 1814 kg at a standoff of 4.5m. Or the nuclear bomb deployed in the city of Nagasaki, Japan on August 9th of 1945 had an explosive power approximately equivalent to 21 kilotons of TNT (Lahiri and Ho, 2011).
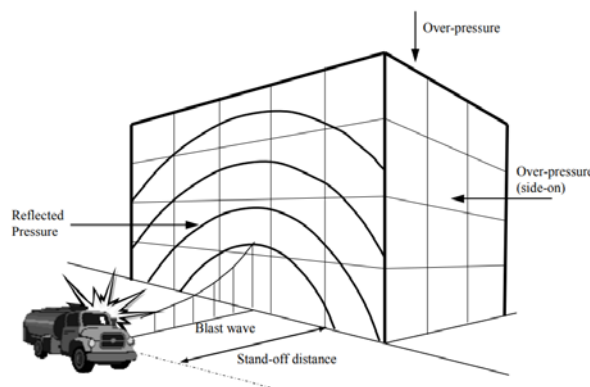
Source: Shallan et al. (2004)

Figure 0-1 Blast loads on a building

Detonation of an explosive involves chemical reactions which causes rapid heating and expansion of the detonated products. This rapid expansion causes abrupt compression of the surrounding medium, leading to a strong shock wave, commonly known as a blast wave, which propagates away from the source with high velocity. The state of the medium, described by its pressure, density, temperature, and velocity are discontinuous across the shock front. The states

224

before and after the shock are related by the conservation of mass, momentum, and energy, which are collectively expressed as the well-known Rankine-Hugoniot jump condition. The blast waves are typically supersonic (moving with a speed faster than the fastest-speed of propagation of any perturbation in the medium). Hence the medium remains unperturbed until the advent of the shock front, with the pressure just ahead of the shock (away from the source) remaining close to ambient pressure. The pressure just behind the shock, often referred to as the over pressure, propels the shock away from the source, as shown qualitatively in Figure 0-2.
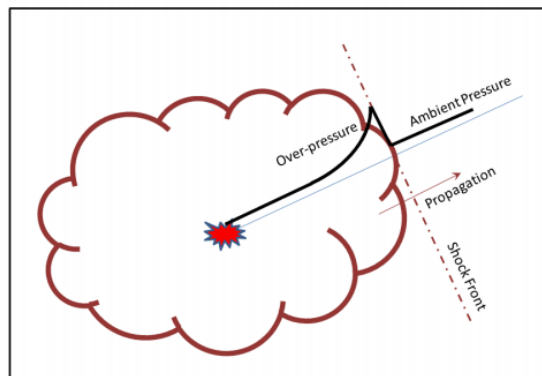
Source: Lahiri and Ho (2011)

Figure 0-2 A schematic of pressure distribution across a blast wave
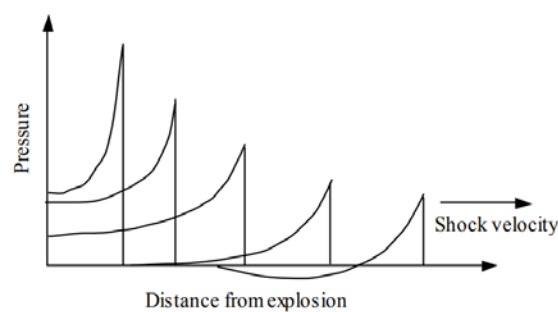
Source: Lahiri and Ho (2011)

Figure 0-3 Pressure distribution at different time levels

As the shock propagates away from the source, this over pressure reduces, causing the pressure of a region, behind the shock, to drop below ambient pressure, which causes transport of debris far away from the explosion source. The pressure distribution at different time levels is qualitatively shown in Figure 0-3. A typical time history of the pressure inflicted by a blast wave at a fixed distance from the source is shown in Figure 0-4.
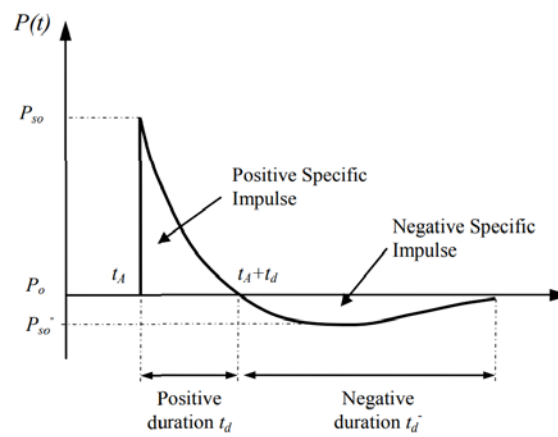
Figure 0-4 Time history of pressure due to a blast wave at a given location

This qualitative model has been known and developed by several researchers directly or indirectly working for defence organisations. Much of their work has remained classified information and is not available for public access (Shallan et al., 2004). Later the model developed by Kingery and Bulmash (1984), more commonly known as the CONWEP model, has been widely used for free explosions in air.

In accordance to the CONWEP model, the shock wave caused by blast loading travel through (time, pressure) dimensions that highly compressed air particles exert pressures on all surfaces encountered. As shown in Figure 0-5, a discontinuous ''jump'' of the shock front pressure is occurred with the pressure rising from ambient (p_a) to (p_s) that is generally referencing as the blast overpressure – the pressure differences between (p_a) and (p_s). In the space is considered

as a fixed location, the pressure exponentially decays in regards of time and is followed by a negative (i.e. suction) phases. It is general observation that the blast wave pressure pulse has a very short time period that its typical measurement is fractions of milliseconds. For this reason, Shallan et al. (2004) described the free-field pressure-time response with a modified Friedlander equation,

$$p(t) = (p_\text{s} - p_\text{a}) \left[1 - \frac{t - t_\text{a}}{t_\text{d}} \right] e^{-(t - t_\text{a})/\theta},$$

<div align="right">**Equation 0-1**</div>

where t_a is the arrival time, t_d the time duration of the positive phase and θ the time decay constant.

There are two determinants of the air blast load intensity on a targeted surface namely (1) the materials and the weight of the explosive devices denoted as (m); and (2) the standoff distance (r) between the targeted surface and the explosive devices. In regards to the CONWEP model, there is an approximation for the free-field peak pressure of the blast wave (P) for a given explosion as expressed in the equation below.

$$P = K \left[\frac{m}{r^3} \right],$$

<div align="right">**Equation 0-2**</div>

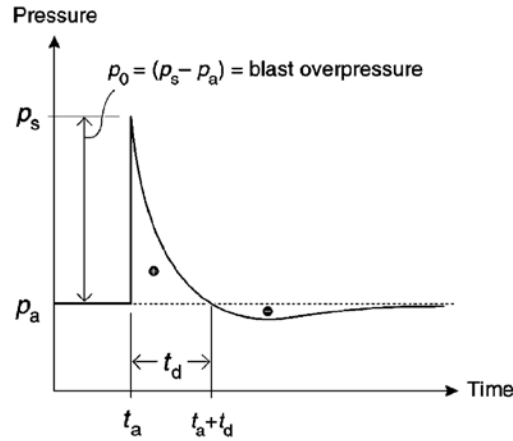where K is an explosive material parameter defined by Cooper (1996).

Figure 0-5 Characteristic air blast pressure response

when the shock wave encounters a surface, the incident overpressure is thus reflected with the possible magnification of highly non-linear that much depended on the incident shock strengths and the angles of incidences. Of which, the resultant blast loads are doubled on reflection of the shock wave in the event of a weak shock; while that for a strong shock is reported to have reflection coefficients of 8 assumed ideal gas condition and even up to 20 with real gas effect in consideration of dissociations and ionizations of air molecules (Baker, 1973).

Equation 0-3 is used to calculate the impulse load (*I*) delivering to the structures through the time integration of the employed pressure-time response within duration of the positive phase. In general, most researches employed the pressure and impulse loads applied to the surface of the structures estimated using CONWEP through a blast simulation code developed by the US Army Corps of Engineers (2010).

$$ I = \int_{t_a}^{t_a + t_d} p \, \mathrm{d}t, $$

Equation 0-3

In which *p* denotes the incident pressure multiplied by the pressure reflection coefficient.

228

When an incident blast wave impinges on a surface, it creates a secondary wave that reflects from the surface, often called the reflected wave. The pressure felt by the surface is the combined effect of the incident wave and the reflected wave. It can be interpreted as the reaction force (applied by the medium on the surface) per unit area, due to the rate of change of momentum of the particles of the medium. To calculate the pressure felt by the surface, the pressure from the incident and the reflected waves are calculated separately. The combined pressure $p(t)$ depends on the angle at which the shock impinges on the surface. If the angle of incidence (say θ) is the angle between the outward facing normal and the ray that joins the point on the surface to the source, then the pressure felt by the surface is related to the incident pressure $p_i(t)$ and the reflected pressure $p_r(t)$ as follows:

$$\text{For } \cos\theta \geq 0$$
$$p(t) = p_i(t)[1 + \cos\theta - 2\cos^2\theta] + p_r(t)\cos^2\theta$$

$$\text{For } \cos\theta < 0$$
$$p(t) = p_i(t)$$

Equation 0-4

This relation has been developed by curve fitting pressure measurements from experiments. A detailed study on blast wave reflection can be found in the book by Smith and Hetherington (2003).

In evaluation of the practical application of the CONWEP model, Bogosian, Ferritto and Shi (2002) compared the predictions of blast loading with this method against a number of other popular simplified models such as BlastX and SHOCK. This study took into account both reflected and incident loads from not only pressure but also impulse for both phrases – positive and negative, respectively. Using the data collected from literature upon a wide range of test spanning over the last three decades that comprised of nearly 300 individual measurements in total, this research has plotted such comparisons of performing blast loading analysis using

229

CONWEP against BlastX and SHOCK as shown in Figure 0-6, Figure 0-7, Figure 0-8 and Figure 0-9. It is noted that all of these data sets were taken at low heights above the ground that some on small cubicles and most of them on larger buildings. With the restricted data to a scaled range of 3–100 ft/lb1/3, the findings from this research indicated that the implementation of CONWEP towards the K-B model is accurate and verified. Further research was done by Remennikov and Rose (2005), in which, the CONWEP model is based on data from free-air explosions; hence it does not include effects of reflections due to confinement and shadow effects from one body on another.
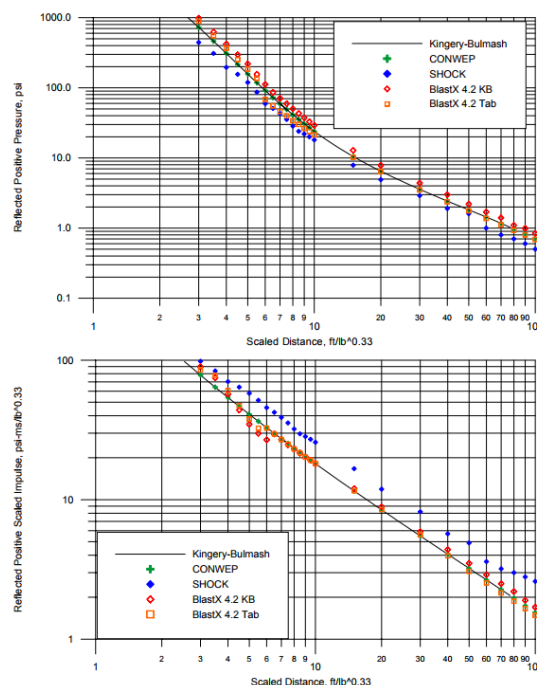
Source: Bogosian, Ferritto and Shi (2002)

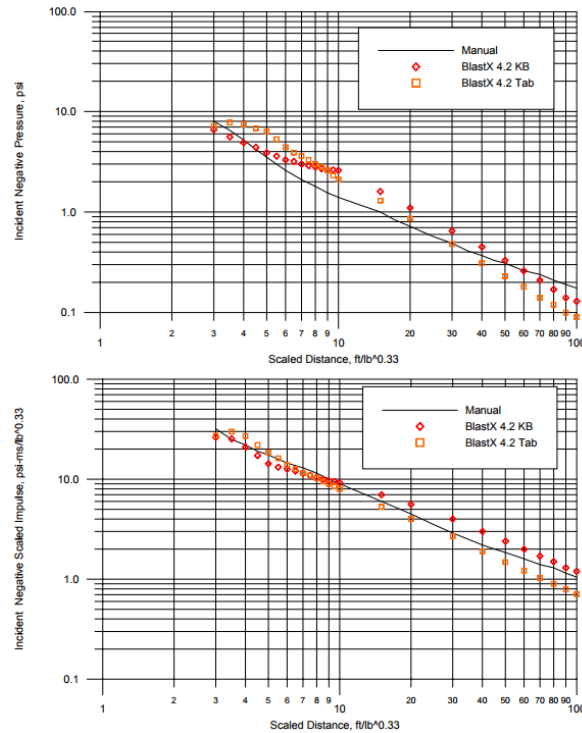**Figure 0-6 Reflected positive pressure and impulse comparison among models**
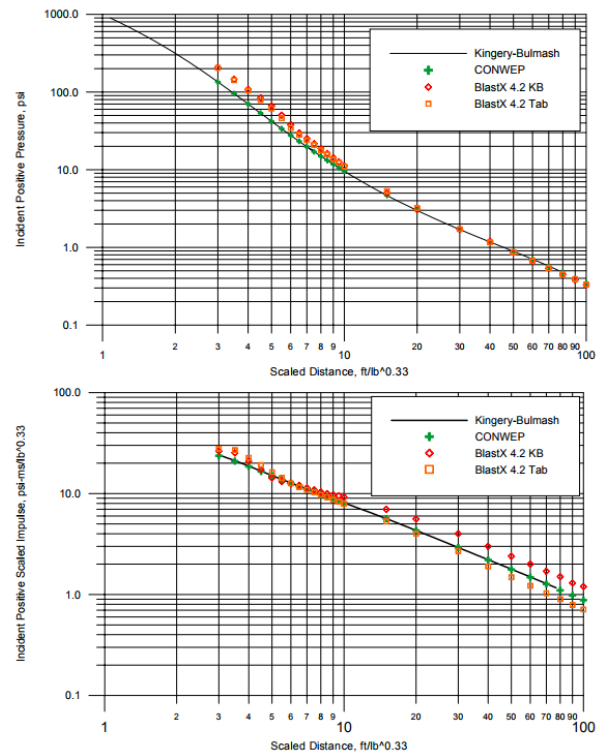
Source: Bogosian, Ferritto and Shi (2002)

Figure 0-7 Incident positive pressure and impulse comparison among models
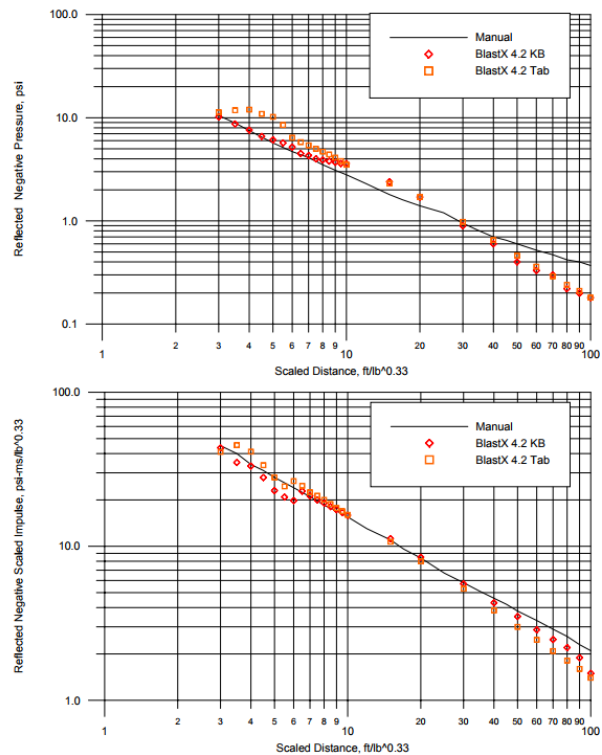
Figure 0-8 Reflected negative pressure and impulse comparison among models

Figure 0-9 Incident negative pressure and impulse comparison among models

Moreover, a recent research of Miller et al. (2010) comparing the CONWEP model to a coupled Eulerian-Lagrangian (CEL) analysis towards a simple test case was developed involving three metallic plates with a 10lb spherical TNT charge centered between them (Figure 0-10). Figure 0-11 illustrate the change in velocity at the center of mass of the lower and upper plates, respectively. The results indicate that since the CONWEP algorithm only considers the initial expansion of the shockwave, any secondary effects are lost and will not affect the system dynamics.
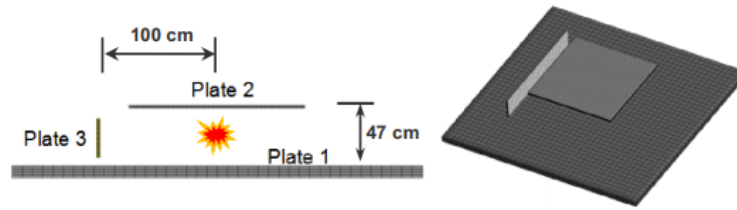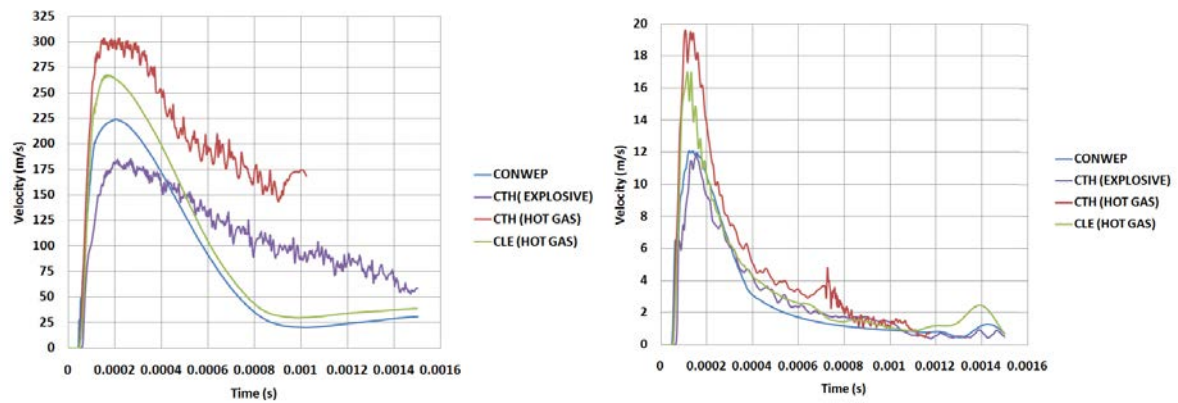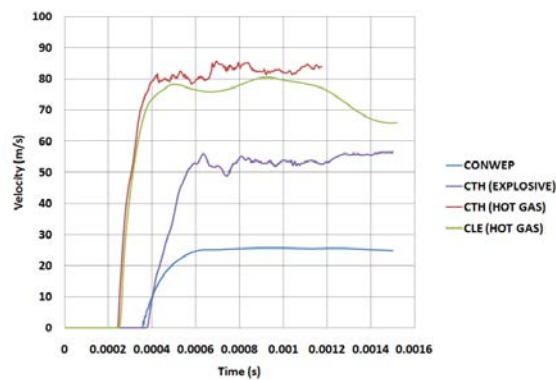
232

Figure 0-10 Test case of Miller et al. (2010)



Upper plate

Lower plate

Side plate

Figure 0-11 Velocity response for test case of Miller et al. (2010)

Structural Response to Blast Loading

233

In literature, the dynamic response of blast-loaded structures has been identified as a complex and complicated analysis due to the high involvement of the effects of high strain rates, the uncertainties of blast loading calculation, the time-dependent deformation and the non-linear inelastic material behaviour (Dusenberry, 2010; Syngellakis, 2013; Goel and Matsagar, 2013). Due to this matter, there has been a number of assumptions made in prior researches in purpose of simplifying such analysis in practices in regards of not only the structural responses but also the blast load definition. Although many research models and approaches have been proposed and widely accepted, the principles of such analyses are established through the two main assumptions: (1) the structure is converted to an equivalent single degree of freedom (SDOF); and (2) the blast load is idealised through an established link between the positive duration of the blast load and the natural period of vibration of the structure that also simplified the classification of the blast loading regimes.

Elastic SDOF Systems

The elastic SDOF approach is considered as the simplest discretization of transient problems (Rigby, Tyas and Bennett, 2012). In regards to this assumption, the actual structure being investigated is replaced by an equivalent system defined through: (1) a concentrated mass; and (2) a weightless spring represented the structural resistance towards its structural deformation. Figure 0-12 (a) demonstrates the idealized system of the elastic SDOF approach in analysis the structural responses under blast loading; while Figure 0-12 (b) demonstrates the idealized blast load as a triangular pulse and positive phase duration.
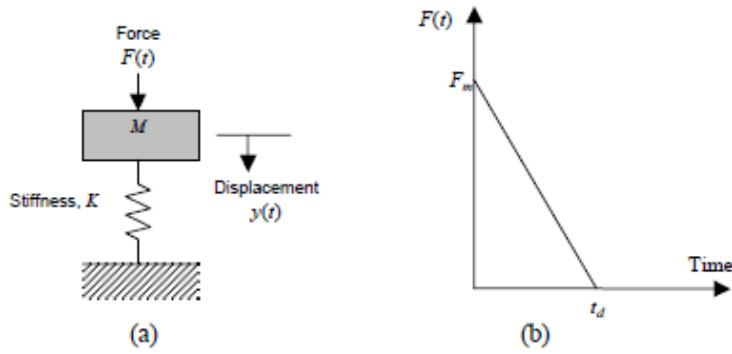
Source: Ngo et al. (2007)

Figure 0-12 (a) SDOF system and (b) blast loading

With the structural mass, M, and the external force, $F(t)$, the structural resistance, R, expressed in reflected to the vertical displacement, $y(t)$, and the spring constant, K as well as the blast load expressed with a peak force, F_m, and positive phase duration, t_d, the forcing function is given in **Equation 0-5**; while the blast impulse is given in **Equation 0-6**.

$$F(t) = F_m\left(1 - \frac{t}{t_d}\right)$$

Equation 0-5

$$I = \frac{1}{2}F_m t_d$$

Equation 0-6

In regards to Biggs and Biggs (1964), for a time ranged from 0 to t_d within the positive phase duration, the motion of the un-damped elastic SDOF system is expressed in **Equation 0-7** and its general solution can be solved through **Equation 0-8**.

$$M\ddot{y} + Ky = F_m\left(1 - \frac{t}{t_d}\right)$$

Equation 0-7

Displacement
$$y(t) = \frac{F_m}{K}(1 - \cos\omega t) + \frac{F_m}{Kt_d}\left(\frac{\sin\omega t}{\omega} - t\right)$$
Velocity
$$\dot{y}(t) = \frac{dy}{dt} = \frac{F_m}{K}\left[\omega\sin\omega t + \frac{1}{t_d}(\cos\omega t - 1)\right]$$

Equation 0-8

in which, ω denotes for the natural circular frequency; while T denotes for the natural period

of the structural vibration that are reflected in **Equation 0-9**.

$$\omega = \frac{2\pi}{T} = \sqrt{\frac{K}{M}}$$

Equation 0-9

In Equation 2-8, the dynamic deflection y_m of the structure under the blast load occurred at time

t_m is achived by setting $dy/dt = 0$ that in case, the velocity of the structure is equal to zero. In

this regards, the DLF, dynamic load factor, is defined as the ratio of the maximum dynamic

deflection y_m to the static deflection y_{st} that possible result from the static application of the

peak load F_m. Accordingly, the DLF is expressed in **Equation 0-10**.

$$DLF = \frac{y_{max}}{y_{st}} = \frac{y_{max}}{F_m/K} = \psi(\omega t_d) = \Psi\left(\frac{t_d}{T}\right)$$

Equation 0-10

As can be seen from **Equation 0-10**, the ratio t_d/T or ωt_d ($t_d/T = \omega t_d /2\pi$) is the significant factor determining the structural response to under blast loading that in this regards, Ngo et al. (2007) categorized three regimes of loading system:

- ωt_d <0.4: impulsive loading regime.

- ωt_d >40: quasi-static loading regime.

- 0.4< ωt_d <0.4: dynamic loading regime

Elasto-Plastic SDOF Systems

Although the structural response to blast can be simply analysed by mean of the elastic SDOF approach, under the event of blast load or high velocity impacts, its structural components are expected to undergoing the large inelastic deformation. For this reason, the elastic SDOF system might not be possible to solve the transient problems. Rather, it is only possible to conduct exact analysis of dynamic structural response through step-by-step numerical solutions required a non-linear dynamic finite-element modelling. Nevertheless, Ngo et al. (2007) indicated that such problem can possibly be solved through the ideal elasto-plastic SDOF system proposed by Biggs and Biggs (1964). This model expresses the degree of uncertainties in both the determination of the loading and the interpretation of acceptability of the resulting deformation in a postulated equivalent ideal elasto-plastic SDOF system by the solution of the required ductility factor $\mu = y_m/y_e$ as demonstrated in Figure 0-13. The triangular load pulse is also defined to comprise rapid rise and linear decay with maximum value F_m and duration t_d. Accordingly, the maximum response of the structure expressed through the maximum displacement of the ideal bilinear elasto-plastic system presented in chart form (TM 5-1300) (Figure 0-14) demonstrating through a selected of R_u/F_m value and corresponding t_d/T value

237

(shows the required ductility μ) with R_u (the structural resistance of the beam) and T (the natural period).
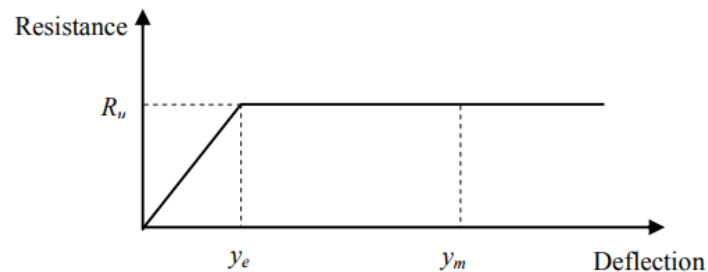

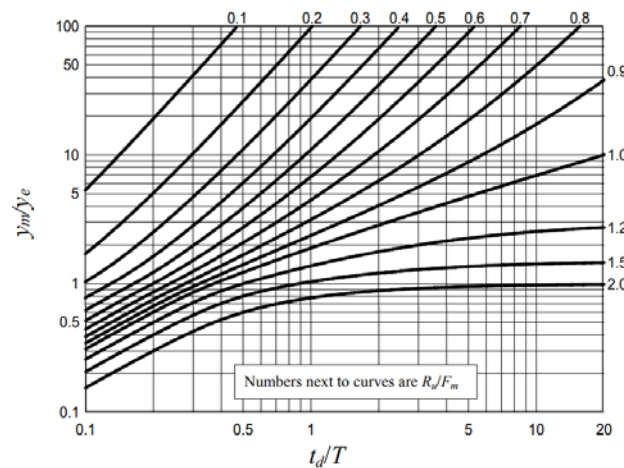**Figure 0-13 Simplified resistance function of an elasto-plastic SDOF system**

Figure 0-14 Maximum response of elasto-plastic SDF system to a triangular load

Design Guidelines for Blast-Resistant Design

This section summarizes applicable military design manuals and computational approaches to predicting blast loads and the responses of structural systems. Although the majority of these design guidelines were focused on military applications this knowledge are relevant for civil design practice.

Structures to Resist the Effects of Accidental Explosions (TM 5-1300. NAFVAC P-397, AFM 88-22 and updated version UFC 3-340-02). This manual appears to be the most widely

used publication by both military and civilian organizations for designing structures to prevent the propagation of explosion and to provide protection for personnel and valuable equipment. It includes step-by-step analysis and design procedures, including information on such items as (1) blast, fragment, and shock-loading; (2) principles of dynamic analysis; (3) reinforced and structural steel design; and (4) a number of special design considerations, including information on tolerances and fragility, as well as shock isolation. Guidance is provided for selection and design of security windows, doors, utility openings, and other components that must resist blast and forced-entry effects.

A Manual for the Prediction of Blast and Fragment Loadings on Structures, DOE/TIC-11268 (U.S. Department of Energy, 1992). This manual provides guidance to the designers of facilities subject to accidental explosions and aids in the assessment of the explosion-resistant capabilities of existing buildings.

Protective Construction Design Manual, ESLTR-87-57 (Air Force Engineering and Services Center, 1989). This manual provides procedures for the analysis and design of protective structures exposed to the effects of conventional (non-nuclear) weapons and is intended for use by engineers with basic knowledge of weapons effects, structural dynamics, and hardened protective structures.

Fundamentals of Protective Design for Conventional Weapons, TM 5-855-1 (U.S. Department of the Army, 1986). This manual provides procedures for the design and analysis of protective structures subjected to the effects of conventional weapons. It is intended for use by engineers involved in designing hardened facilities.

The Design and Analysis of Hardened Structures to Conventional Weapons Effects (DAHSCWE, 1998). This new Joint Services manual, written by a team of more than 200 experts in conventional weapons and protective structures engineering, supersedes U.S.

239

Department of the Army TM 5-855-1, Fundamentals of Protective Design for Conventional Weapons (1986), and Air Force Engineering and Services Centre ESL-TR-87-57, Protective Construction Design Manual (1989).

Structural Design for Physical Security—State of the Practice Report (ASCE, 1995). This report is intended to be a comprehensive guide for civilian designers and planners who wish to incorporate physical security considerations into their designs or building retrofit efforts.